A rapid and accessible method to profile and identify antibiotic resistance genes in bacteria using multiplex amplicon panels and Oxford Nanopore Technology.

A thesis presented in partial fulfilment of the

requirements for the degree of

Master of Science

in

Biological Sciences

at Massey University, Albany

New Zealand

Nick McGrath, supervised by Olin Silander (2023).

Abstract

The spread of antibiotic resistance is severely burdening agriculture and healthcare industries. Bacteria have readily gained resistance to nearly all commercially available antibiotics through the use and overuse of antibiotics in both industries. Current methods to detect resistance genes in bacteria are either outdated and slow or too expensive and inaccessible. A method that is rapid and accessible is necessary to help lessen the burden of antibiotic resistance.

Our research aimed to develop a method to rapidly detect antibiotic resistance genes in single-strain bacteria and metagenomic samples. To achieve this, we developed a nested PCR protocol that could enrich a panel of target resistance genes and provide each a genomic context through degenerate primers and Nanopore sequencing. In single-strain bacteria, we can enrich all target antibiotic-resistance genes; an average of 38% reads will provide a genomic context to each gene. Using our novel nested-PCR protocol, we can also enrich all target resistance genes up to 1000-fold in faecal samples compared to metagenomic sequencing. With this nested PCR protocol and Oxford Nanopore as a sequencing platform, we can detect target resistance genes in single-strain bacteria and faecal samples in under 6 hours, making this method rapid, inexpensive, and accessible. Further, we can provide a genomic context to each resistance gene, allowing us to determine whether genes are chromosomal or plasmid-bound.

Acknowledgments

First, a huge thank you to my supervisor, Dr. Olin Silander. His support, guidance and patience during undergraduate and postgraduate studies and research taught me invaluable techniques and knowledge, and I will continue utilising and developing them throughout my scientific career. A special thanks to Dr. Tim Cooper, who has continually provided encouragement and wisdom during undergraduate and postgraduate studies.

Thank you to my parents, who have never doubted my path and have continually supported me throughout my years of study. Without their support throughout this journey, I would have never thought I could reach this level.

Thank you to Emily and Bhargava, who helped me when I first entered the lab, making the transition from undergraduate to research easy. Thank you to Razvan, who has been on the same path as me during my studies. Having someone at the same level to talk about similar challenges has been helpful. Thank you to Jamie, who is always willing to chat about projects or anything to do with science and for proofreading my work.

Special mention and thank you to Lauren Brebner-Fox, who was heavily involved with the initial testing.

Table of Contents

Abstract **2**
Acknowledgments **3**
Table of Contents **4**
List of Figures **8**
List of Tables **9**
Abbreviations **11**
Chapter 1: Introduction **12**
1.1 What is antibiotic resistance? Moreover, why is it occurring? 12
1.2 How are ARGs spread: 13
1.2.1 Mobile genetic elements (MGE) 13
1.2.2 Horizontal gene transfer (HGT) 13
Figure 1.1 Mechanisms for horizontal gene transfer. 14
1.2.3 Plasmid-mediated ARG spread 15
1.3 Resistance Mechanisms 15
1.7.1 Aminoglycosides 15
1.7.2 Beta-lactams 16
1.7.3 Trimethoprim 16
1.7.4 Macrolide, lincosamide, and streptogramin B (MLS) 16
1.7.5 Sulfonamide 17
1.7.6 Tetracycline 17
Figure 1.2. Resistance mechanisms of common antibiotics. 18
1.3 The burden of antibiotic resistance 18
1.3.1 Antibiotic Resistance in Healthcare 19
1.3.2 Antibiotic Resistance in Agriculture and the Food Processing Industry 19
1.3 What are we doing about resistance? How can we slow the spread? 20
1.5 Culture-based methods for ARG detection 20
1.6 Molecular Methods 21
1.6.1 Metagenomics versus targeted approaches 21
1.6.1 Oxford nanopore sequencing as a platform to profile ARGs 21
1.8 Research hypothesis and objectives 23
Chapter 2: Materials and Methods **24**
2.1 E. coli L3Cip3 24
2.1.1 DNA extraction 24
2.1.2 Selecting Target ARGs 24

Table 2.1. Target ARGs for E. coli L3Cip3. 25
2.2 Metagenomic samples. 27
Table 2.2. Metagenomic faecal samples. 27
2.2.1 Metagenomic DNA extraction 27
2.3 Nested PCR 27
Table 2.3. ARG primer pool containing all target ARGs. 28
Table 2.4. Description of degenerate primers and constant primers. 29
Figure 2.1. Degenerate primers paired with ARG primers produce sequences that can provide a genomic context to an ARG. 30
2.3.1 First round PCR 31
2.3.2 PCR Cleanup 31
2.3.3 Second-round nested PCR 31
2.4 Oxford Nanopore Sequencing 32
2.4.1 Rapid barcoding - R9.4.1 32
2.4.2 Rapid barcoding - R10.4.1 32
Figure 2.2. Principle of Oxford Nanopore sequencing. 33
2.5 Bioinformatic Workflow 33
2.5.1 Basecalling and quality control 33
2.5.2 Mapping 34
Figure 2.3. Nested PCR with ONT sequencing can be completed within 5-6 hours. 34
Figure 2.4. Strategy to develop functional primer pools with degenerate primers and ARG primers. 35
Chapter 3: Single Strain Results **37**
3.1 Primer Optimisation 37
3.1.1 Testing Degenerate Primers 37
Table 3.1. ONT sequencing reports for each run. 38
Figure 3.1. 46℃+62℃ is the best annealing temperature condition for all degenerate primers during N-PCR. 39
3.2 Testing individual ARG primers with pooled degenerate primers 39
Figure 3.2. The *aph(6)* and *sul2* primers working with the degenerate primer pool produced the highest percentage of reads providing a genomic context. 40
3.3 Improving tetracycline genomic context frequency 42
Table 3.2. The degenerate primer F-TAA produced reads that provide a genomic context for *tet(A)* at high frequencies. 42
3.4 Developing an ARG primer pool 43
3.4.1 Testing individual degenerate primers with pooled ARG primers 43
Table 3.3. Testing individual degenerate primers with an ARG primer pool. 44

3.4.2 Pooling of ARG primers results in amplification bias toward specific ARGs 44
3.4.3 Amplification of specific ARGs is more likely to yield genomic context 45
Figure 3.4. *bla-$_{CTX}$* is consistently enriched the most regardless of the degenerate primer set. 46
Figure 3.5. Reads mapping to *rmtB* consistently provide genomic context at higher percentages than other ARGs. 47
3.4.2 Combining the ARG primer pool with the degenerate primer pool 48
Table 3.4. Percentage of reads mapping to target ARGs while providing a genomic context. 49
Chapter 4: Metagenomic Results 50
4.1 Metagenomic sequencing 50
Table 4.1. Sequence statistics for unfiltered reads from each faecal sample and prep method. 51
4.2 Difference between extraction methods 53
Figure 4.2. Tetracycline resistance is the most abundant within metagenomic samples.. 54
4.3 Application of the N-PCR protocol on faecal samples (L3Cip3 enriched) 55
Table 4.2. Percentage of reads mapping to target ARGs that provide a genomic context. 55
4.4 Application of N-PCR protocol on pure faecal samples 56
Table 4.3.Comparison of metagenomic sequencing and PCR-targeted sequencing. 57
Figure 4.3. Comparison of PCR-enriched samples to metagenomic sequencing. 58
4.5 Genomic context in metagenomic samples 59
Table 4.4. Genomic context of PCR-enriched metagenomic samples. 59
Figure 4.4. Genomic context for *aph(6)* is consistently high across all samples. 61
Chapter 5: Discussion 61
5.1 Genomic context 62
5.2 Rapidly detecting ARGs in single colonies 62
5.3 Rapid detection of ARGs in metagenomic samples 63
5.4 An active tool to profile ARGs in bacteria 63
5.5 Oxford nanopore as a cheap and reliable sequencing platform 64
5.6 Limitations 64
5.7 Conclusion and Future perspectives. 65
References 66
Chapter 6: Appendices 79
Supplementary Table 6.1. Panel of primers capable of multiplex qPCR. 79
Supplementary Table 6.2. Testing of Freed degenerate primers at differing annealing temperatures. 81
Supplementary Table 6.3. Testing of Freed and Manoil degenerate primers at differing annealing temperatures. 82
Supplementary Table 6.4. Testing of Freed and Manoil degenerate primers at differing annealing temperatures. 83

Supplementary Table 6.5. Testing of Freed and Manoil degenerate primers at differing annealing temperatures. 84

Supplementary Table 6.6. Testing of Freed and Manoil degenerate primers at differing annealing temperatures. 85

Supplementary Table 6.7. Testing of Freed and Manoil degenerate primers at differing annealing temperatures. 86

Supplementary Table 6.8. Testing of Freed and manoil degenerate primers at differing annealing temperatures and a 0.7 bead clean. 86

Supplementary Table 6.9. Statistics of testing the degenerate primer pool containing M-TAA, M-TGA, and F-TGA with individual ARG primers to provide genomic context to target ARGs. 87

Supplementary Table 6.10. Testing individual degenerate primers with pooled ARG primers. 88

Supplementary Table 6.11. Testing the degenerate primer pool containing M-TAA, M-TGA, and F-TGA with individual ARG primers to provide genomic context to target ARGs. 88

Supplementary Table 6.12. Testing the degenerate primer pool containing M-TAA, M-TGA, and F-TGA with individual ARG primers to provide genomic context to target ARGs. 89

Supplementary Table 6.13. Testing individual degenerate primers with primers targeting *aph(3)* and t*et(A)*. 90

Supplementary Table 6.14. Testing individual degenerate primers with primers targeting *aph(4)* and *tet(A)*. 91

Supplementary Table 6.15. Testing the degenerate primer pool containing M-TAA, M-TGA, F-TGA and F-TAA with individual ARG primers to provide genomic context to target ARGs. 92

Supplementary Table 6.16. Testing the degenerate and ARG primer pools on faecal samples. 92

Supplementary Table 6.17. Testing the developed degenerate and ARG primer pools on faecal samples. 93

Supplementary Table 6.18. Testing the degenerate and ARGprimer pools on faecal samples using two DNA extraction methods. 93

Supplementary Table 6.19. Testing the degenerate and ARG primer pools on faecal samples using two DNA extraction methods with new ONT chemistry. 94

Supplementary Table 6.20. Testing the degenerate and ARG primer pools on metagenomic faecal samples using two DNA extraction methods with new ONT chemistry (Repeat). 95

List of Figures

Figure 1.1. Mechanisms for horizontal gene transfer
Figure 1.2. Resistance mechanisms of common antibiotics
Figure 2.1. Degenerate primers paired with ARG primers produce sequences that can provide a genomic context to an ARG.
Figure 2.2. Principle of Oxford Nanopore sequencing.
Figure 2.3. Nested PCR with ONT sequencing can be completed within 5-6 hours.
Figure 2.4. Strategy to develop functional primer pools with degenerate primers and ARG primers.
Figure 3.1. 46°C+62°C is the best annealing temperature condition for all degenerate primers during N-PCR.
Figure 3.2. The *aph(6)* and *sul2* primers working with the degenerate primer pool produced the highest percentage of reads providing a genomic context.
Figure 3.3. The primer for *tet(A)* working with the degenerate primer pool does not produce reads that provide a genomic context at high percentages.
Figure 3.4. Beta-lactamase gene bla_{CTX} is consistently enriched the most with every degenerate primer.
Figure 3.5. *rmtB* provides a genomic context at higher percentages than all other ARGs.
Figure 3.6. A high percentage of reads mapping to beta-lactamase genes $bla\text{-}_{CTX}$ and $bla\text{-}_{TEM}$ provide a genomic context.
Figure 4.1. High abundance of ARGs encoding resistance to tetracycline across all metagenomic samples.
Figure 4.2. Tetracycline resistance is the most abundant within metagenomic samples.
Figure 4.3. Comparison of PCR-enriched samples to metagenomic sequencing.
Figure 4.4. Genomic context for *aph(6)* is consistently high across all samples.

List of Tables

Table 2.1. Target ARGs for *E. coli* L3Cip3.

Table 2.2. Metagenomic faecal samples.

Table 2.3. ARG primer pool containing all target ARGs.

Table 2.4. Description of degenerate primers and constant primers.

Table 3.1. ONT sequencing reports for each run.

Table 3.2. The degenerate primer F-TAA produced reads that provide a genomic context for tet(A) at high frequencies.

Table 3.3. Testing individual degenerate primers with an ARG primer pool.

Table 3.4. Percentage of reads mapping to target ARGs while providing a genomic context.

Table 4.1. Sequence statistics from each sample.

Table 4.2. Percentage of reads mapping to target ARGs that provide a genomic context.

Table 4.3. Comparison of metagenomic sequencing and PCR-targeted sequencing.

Table 4.4. Genomic context of PCR-enriched metagenomic samples.

Supplementary Table 6.1. Panel of primers capable of multiplex qPCR.

Supplementary Table 6.2. Testing of Freed degenerate primers at differing annealing temperatures 42℃+58℃ and 44℃+58℃.

Supplementary Table 6.3. Testing of Freed and Manoil degenerate primers at differing annealing temperatures 44℃+60℃, 46℃+60℃ and 42℃+60℃.

Supplementary Table 6.4. Testing of Freed and Manoil degenerate primers at differing annealing temperatures 44℃+58℃ and 46℃+58℃.

Supplementary Table 6.5. Testing of Freed and Manoil degenerate primers at differing annealing temperatures 44℃+62℃.

Supplementary Table 6.6. Testing of Freed and Manoil degenerate primers at differing annealing temperatures 44℃+60℃ and 46℃+62℃.

Supplementary Table 6.7. Testing of Freed and Manoil degenerate primers at differing annealing temperatures 46℃+60℃.

Supplementary Table 6.8. Testing of Freed and manoil degenerate primers at differing annealing temperatures 46℃+60℃ and a 0.7 bead clean.

Supplementary Table 6.9. Statistics of testing the degenerate primer pool containing M-TAA, M-TGA, and F-TGA with individual ARG primers to provide genomic context to target ARGs.

Supplementary Table 6.10. Testing individual degenerate primers with pooled ARG primers.

Supplementary Table 6.11. Testing the degenerate primer pool containing M-TAA, M-TGA, and F-TGA with individual ARG primers to provide genomic context to target ARGs.

Supplementary Table 6.12. Testing the degenerate primer pool containing M-TAA, M-TGA, and F-TGA with individual ARG primers to provide genomic context to target ARGs.

Supplementary Table 6.13. Testing individual degenerate primers with primers targeting aph(3) and tet(A).

Supplementary Table 6.14. Testing individual degenerate primers with primers targeting aph(4) and tet(A).

Supplementary Table 6.15. Testing the degenerate primer pool containing M-TAA, M-TGA, F-TGA and F-TAA with individual ARG primers to provide genomic context to target ARGs.

Supplementary Table 6.16. Testing the degenerate and ARG primer pools on faecal samples.

Supplementary Table 6.17. Testing the developed degenerate and ARG primer pools on faecal samples.

Supplementary Table 6.18. Testing the degenerate and ARGprimer pools on faecal samples using two DNA extraction methods.

Supplementary Table 6.19. Testing the degenerate and ARG primer pools on faecal samples using two DNA extraction methods with new ONT chemistry.

Supplementary Table 6.20. Testing the degenerate and ARG primer pools on metagenomic faecal samples using two DNA extraction methods with new ONT chemistry (Repeat).

Abbreviations

AMR - Antimicrobial resistance
ARGs - Antibiotic resistance genes
HGT - Horizontal gene transfer
ICEs - Integrated conjugative elements
MGE - Mobile genetic elements
N-PCR - Nested polymerase chain reaction
ONT - Oxford Nanopore Technology
PCR - Polymerase chain reaction

Chapter 1: Introduction

1.1 What is antibiotic resistance? Moreover, why is it occurring?

Antimicrobials were widely used before the term ‘antibiotic’ was coined. However, they were first deemed as chemotherapy, which then became antimicrobials. Antimicrobials from chemical dyes were used as they could be selective in the cells they killed, according to the discoverer Paul Ehrlich. These were known as the earliest antibiotics, and since their first applications, microbes have been evolving resistance to them.

Microbes adapting to their environment through selective pressure is nothing new. Microbes have been found to be resistant to antibiotics even before the first antibiotic was isolated (Aminov, 2010). However, after the development of chemotherapy drugs, microbes rapidly developed resistance to chemotherapeutics and antimicrobials, such as disinfectants, through chemotherapy-induced selective pressures. For the most part, the modern era of antibiotic use resistance started with Alexander Fleming, who discovered penicillin in 1928. Since penicillin's discovery, antibiotics have been used to treat millions of humans and animals, vastly reducing morbidity and mortality. Resistance against penicillin rapidly evolved (Lobanovska & Pilla, 2017). Since the first use of penicillin, many different antibiotics have been developed, and these could be applied in conjunction with each other for especially persistent infections. However, in 1955, a strain of *Shigella* was discovered that was resistant to sulphonamides, streptomycin, chloramphenicol, and tetracycline (Klemm et al., 2018). A methicillin-resistant *Staphylococcus aureus* was discovered soon after, in 1962 (Sengupta et al., 2013 & Tenover et al., 2006). Since then, and despite the discovery and development of many new antibiotics, resistance to most new antibiotics has evolved quickly in many species (Spellberg & Gilbert, 2014).

The dissemination of antibiotic resistance combined with the rapid and worldwide travel of humans and animals, antibiotic discharge (improper disposal of antibiotics), and wastewater treatment has led us to a situation where microbes easily spread antibiotic resistance genes (ARGs) across international borders (Antimicrobial Resistance Collaborators, 2022). Any localised outbreak of resistant microbes can rapidly become global.

The overuse of antibiotics within clinical settings is a massive factor when considering what has driven the development and widespread resistance (Read & Woods, 2014 & zur Wiesch et al., 2011). Currently, antibiotics are prescribed for prolonged and often imprecise durations (Dellinger et al., 2013 & Masterton et al., 2008), increasing recurrent infections of antibiotic-resistant bacteria. It should be mentioned that any antibiotic use, either short-term or prolonged, will result in selective pressure on microbes. Antibiotic use in agriculture is also a significant driver of resistance. It has been estimated that 70% of antibiotics are used for

agricultural purposes (Aslam et al., 2021); however, this is hard to quantify (Ventola, 2015). Furthermore, 70% of those applied in agricultural settings are medically relevant to human health (Manyi-Loh et al., 2018). To understand how microbes resist chemotherapy drugs and antibiotics, we must first understand the mechanisms microbes use to gain and spread antimicrobial resistance.

1.2 How are antibiotic resistance genes spread?

ARGs can be spread from agricultural settings to humans and the environment through interconnected pathways involved in food production, livestock, waste disposal, and human-to-human contact (Aslam et al., 2021). Understanding how ARGs are spread throughout the mentioned environments is essential to profiling and detecting ARGs. Underlying this spread are molecular mechanisms that bacteria use to transfer ARGs.

1.2.1 Mobile genetic elements (MGE)

Mobile genetic element (MGE) is a broad term that encompasses plasmids, transposons, insertion sequences, and pathogenicity islands. In simple terms, MGEs are pieces of DNA that encode proteins that regulate the frequency of DNA movement between genomes (intercellular mobility) and within genomes (intracellular mobility). MGEs can be transferred vertically from parent to offspring (or mother cell to daughter cell in the case of bacteria) or through horizontal gene transfer to neighbouring cells and organisms within their vicinity (Vale et al., 2022 & Frost et al., 2005). The presence of MGEs allows genomes to change content rapidly, increasing the rate of adaptation to the current environment. This can occur through MGEs changing their genomic location, altering chromosomal gene expression, or providing new gene functions.

1.2.2 Horizontal gene transfer (HGT)

Bacteria can quickly adapt to particular environments through natural selection. Compared to mammals, bacteria have a fast generation-to-generation turnaround, making the time scale of bacterial adaptation very short. Bacteria and other organisms can also horizontally transfer genes between cells that are unrelated by descent. This is distinct from vertical gene transfer, in which genes transfer from parent to offspring. Horizontal gene transfer (HGT) can be subcategorised into three specific forms: (1) Transformation occurs when free DNA is taken up from the environment. However, conditions must be met for bacteria to take up this DNA. The bacterial cell must be in a state of competence. Once in this state, the cell can bind to and integrate the free DNA into its chromosome through homologous recombination (Frost et al., 2005 & Ochman et al., 2000). (2) Conjugation is mediated by independently replicating genetic elements called conjugative plasmids or chromosomally integrated conjugative elements (ICEs). These elements facilitate the direct transfer of genetic material between bacteria through

physical contact (Ochman et al., 2000). (3) Transduction can be broken down into generalised and specialised transduction. Generalised transduction introduces new genetic information into a bacterium by a bacteriophage replicating within the host bacteria and packaging random DNA fragments. In contrast, in specialised transduction, the bacteriophage packages the DNA directly adjacent to the phage's attachment site. Via these three HGT mechanisms, bacteria have gained antimicrobial resistance readily, allowing particular bacteria to thrive in environments that contain noxious compounds (**Figure 1.1**) (Frost et al., 2005; Ochman et al., 2000 & Smillie et al., 2011).

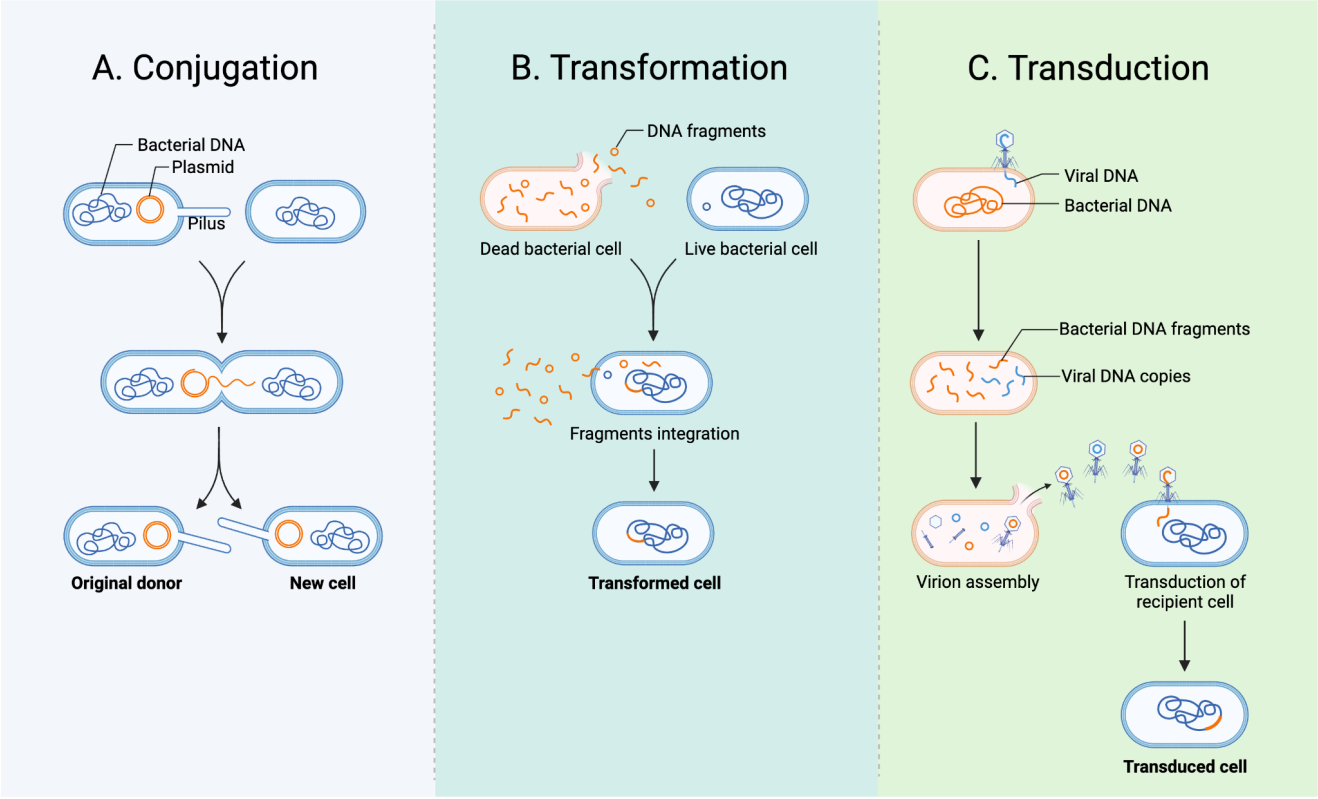

Figure 1.1 Mechanisms for horizontal gene transfer. A. Conjugation is the direct transfer of genetic material from one cell to another, either the same or different species. B. Transformation can occur when a cell is in a state of competence. In this state, the live cell can take up free DNA from the environment and integrate free DNA fragments into its genome, creating a transformed cell. C. Transduction is the process of a cell acquiring DNA through a bacteriophage transmitting DNA from one cell to another. This new DNA is taken up in the new and integrated into that cell's genome. Created with BioRender.com.

1.2.3 Plasmid-mediated antibiotic resistance gene spread

Plasmids are extra-chromosomal pieces of DNA capable of replicating independently of the genome. Plasmids are a crucial driver and important in spreading antibiotic resistance (Furuya & Lowy, 2006; Svara & Rankin, 2011 & Ramirez et al., 2014). Conjugative plasmids are extra-chromosomal DNA MGEs capable of HGT. Plasmids are the primary holders of antibiotic resistance genes (ARGs). Plasmids can carry genes with a range of functions that are relevant to cell survival. (Carattoli, 2013). Many plasmids encode resistance to more than one antibiotic, and this is often the case with methicillin-resistant *Staphylococcus aureus,* which is usually resistant not only to methicillin, which in this case is located on the chromosome but also aminoglycosides, macrolides, tetracycline and lincosamides which are plasmid bound (Nikaido, 2009). MDR is defined as non-susceptibility to at least one agent across at least three antimicrobial classes (Magiorakos et al., 2012), with some MDR strains being Resistant to all known antibiotic classes (Nikaido, 2009). MDR bacteria have become highly prevalent, causing clinical and environmental issues worldwide (Bassetti & Garau, 2021).

1.3 Resistance Mechanisms

While there are a wide range of antibiotic classes, here I focus on the most relevant for this study. The most common types of mechanisms are described in **Figure 1.2**.

1.7.1 Aminoglycosides

The first aminoglycoside, streptomycin, was isolated from *Streptomyces grieus* and used to treat infections with gram-negative bacteria and *Mycobacterium tuberculosis*. Aminoglycosides have been a valuable asset in combating bacterial infections. However, over the last ten years, antibiotic resistance has spread through many different genera and species of bacteria, with many different genes being identified to confer resistance to aminoglycosides.

Aminoglycosides bind to the aminoacyl-tRNA A-site of the 16S rRNA, which leads to the ribosome's inability to synthesise polypeptides and eventual cell death (Doi et al., 2016). As bacteria evolve through the mechanisms mentioned above, they have become resistant to aminoglycosides in several different ways: (1) Direct modification of the 30S ribosomal subunit, this modification through methylation functions to inhibit the binding of the aminoglycoside antibiotic to the subunit, rendering the antibiotic non-functional (adaptive resistance); (2) decreased permeability due to cell wall and membrane-bound protein modifications (intrinsic and adaptive resistance). Intrinsic resistance in a mechanical sense involves inherited characteristics of the microbial species, whereas adaptive resistance arises from gene mutations and HGT (Motta et al., 2015); and (3) modification and inactivation of the

aminoglycoside in action by enzymatic activity (adaptive resistance) (Garneau-Tsodikova & Labby, 2016).

1.7.2 Beta-lactams

Beta-lactams have been used since the discovery and development of penicillin and are currently the most widely used antibacterial worldwide (WHO, 2020). Beta-lactams are a class of antibiotics characterised by a reactive four-membered beta-lactam ring; this ring and its activity are essential to their bactericidal function (Mora-Ochomogo & Lohans, 2021). Beta-lactams are a diverse group of antibiotics, including penicillins, cephalosporins, and carbapenems. Their diversity is due to many different modifications that can be made to the beta-lactam ring. Beta-lactams function by interfering with the synthesis of a component of the bacterial cell wall. Because of this, there is a loss in the integrity of the cell wall, leading to eventual autolysis (Worthington & Melander, 2013).

Bacteria, particularly gram-negative bacteria, have genes that encode an enzyme that degrades beta-lactams, called beta-lactamases. These enzymes, of which there are two different classes, catalyse the opening of the beta-lactam ring, rendering the antibiotic unable to target the site of the cell wall component (Mora-Ochomogo & Lohans, 2021). This is the most common mechanism of resistance. A second resistance mechanism is through altering penicillin-binding proteins to decrease affinity to the antibiotic (Worthington & Melander, 2013 & Rice, 2012).

1.7.3 Macrolide, lincosamide, and streptogramin B (MLS)

The primary mechanism by which the MLS group of antibiotics acts is binding the peptidyltransferase centre of the 50S ribosomal subunit in bacteria; binding to this region causes a block in the formation of a peptide bond during protein synthesis (Tsui et al., 2004), leading to cell death (Leclercq & Courvalin, 1991 & Yao et al., 2019).

Many genes have been identified that encode enzymes that either act upon this group of antibiotics or change the target site, making the antibiotic molecules unable to bind. A common class of genes is the erm (erythromycin resistance methylase) group, which add a methyl group to the side-chain of the antibiotic binding site, which in turn prevents the binding of the antibiotic to the binding site in the 50S ribosome subunit (Svetlov et al. 2021).

1.7.4 Sulfonamide

Sulfonamides have a long history of antibiotic use, being the first drugs to act on bacteria while being exclusive of mammalian cells. The target of sulfonamides is the enzyme dihydropteroate

synthase, which most mammalian cells lack. Inhibition of this enzyme interferes with the folic acid metabolism pathway, leading to the inability to synthesise nucleic acid (Sköld, 2000).

Sulfonamide resistance is widespread due to its long history of use and its being a broad-spectrum antibiotic (Ovung & Bhattacharyya, 2021). Because of this, many genes from different species of bacteria conferred resistance to sulfonamides. One class of resistant genes is the sul genes. These genes encode dihydropteroate synthase and are resistant to sulphonamides. Dihydropteroate synthase lowers the affinity for sulfonamides through modifications to the antibiotic (Phuong Hoa et al., 2008 & Adekanmbi et al., 2020).

1.7.5 Tetracycline

Tetracyclines are broad-spectrum antibiotics that have been in use since the 1940s. They function by inhibiting protein synthesis in both gram-positive and gram-negative bacteria. Tetracyclines prevent the attachment of tRNA to the ribosomal A site, rendering the ribosome non-functional (Chopra & Roberts, 2001).

Resistance to tetracycline antibiotics can be characterised into three different mechanisms. (1) tet genes that code for efflux proteins that specifically export tetacyclines from the cell. This reduces the concentration of tetracycline within the cell, protecting the ribosome (Levy et al., 1999). (2) Specific ribosomal protection proteins that compete to bind to the active A site of the ribosome. Once these proteins are bound, tetracycline antibiotics cannot act (Chopra & Roberts, 2001). (3) Enzymatic inactivation of tetracycline that modifies tetracyclines' structure, rendering it unable to act on the ribosome (Speer et al., 1991).

1.7.6 Trimethoprim

Trimethoprim is in the diaminopyrimidine class of organic antibiotics. It functions by inhibiting the ability of dihydrofolate reductase (DHFR) to convert dihydrofolate (DHF) to tetrahydrofolate (THF) (Fierke et al., 1987). In bacteria, THF is needed to synthesise DNA (Liu et al., 2013) and for the metabolism and regulation of gene expression (Gleckman et al., 1981).

Bacteria have gained resistance to this antibiotic through five primary mechanisms: (1) modifications to the target enzyme DHFR (Brolund et al., 2010), (2) amino acid mutations to the target enzyme DHFR, (3) changes in the permeability of the cell wall or protein efflux pumps on the cell wall, (4) naturally insensitive target enzymes, (5) acquired resistance through random mutations (Eliopoulos & Huovinen, 2001)

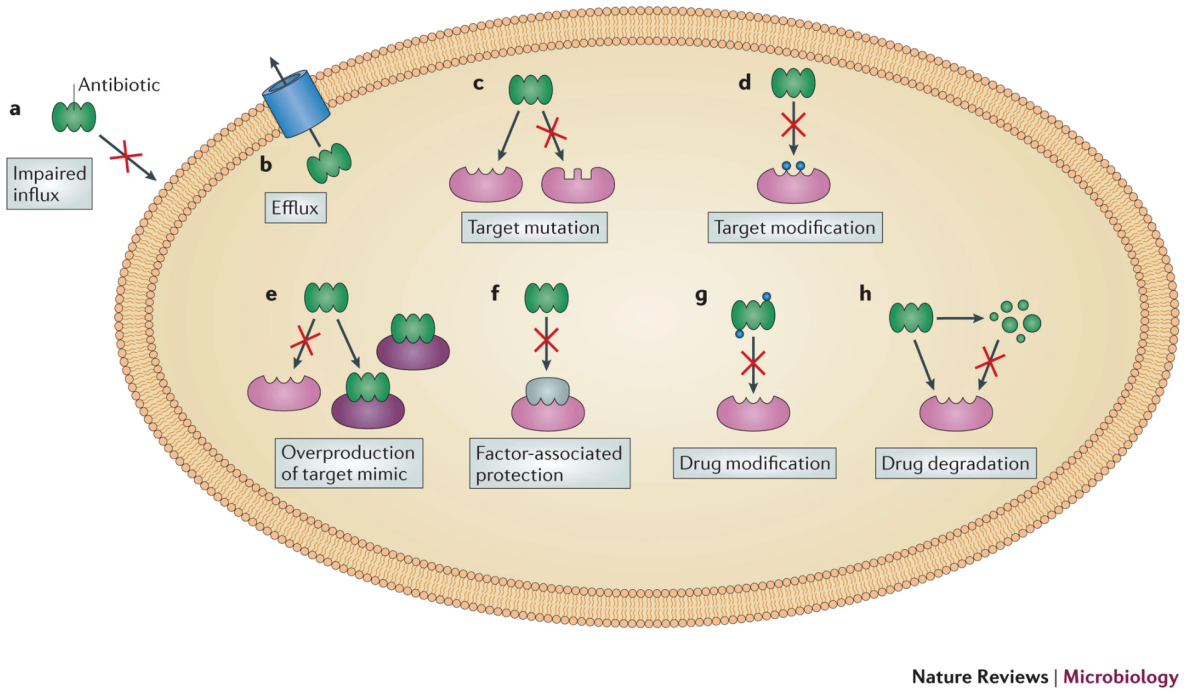

Figure 1.2. Resistance mechanisms of common antibiotics. Alterations to the porin in the cell membrane impair its influx, resulting in low membrane permeability (a). A direct efflux of the antibiotic from the cell (b). Mutation (c) or modification (d) of the antibiotics target, interrupting the antibiotics binding site or lowering the drug's affinity for the target. Overproduction of a molecular that mimics the antibiotics target (e), diluting the drug concentration so that the target remains unbound. Actively removing the drug from its target via protein factor protection (f). Modification (g) or degradation (h) of the active antibiotic. Image from Wilson (2014).

1.3 The burden of antibiotic resistance

Microbes' utilisation of these defence mechanisms has significantly strained numerous industries, burdening humans with associated challenges. As mentioned, antimicrobial resistance (AMR) and the use and misuse of antimicrobial drugs through antibiotic discharge (improper disposal of antibiotics), wastewater treatment, agricultural practices, and ineffectiveness of treatment have become global health concerns. This has had unintended, but not unexpected, consequences on the public health sector, agriculture, the food processing industry and the environment (WHO, 2021; Dadgostar, 2019; Cheng et al., 2013; Dhingra et al., 2020 & Majumder et al., 2020). Due to antibiotic resistance, there is a burden imposed on society in terms of increased morbidity and mortality (Centers for Disease Control and Prevention, 2019 & Agyeman et al., 2022), reduced treatment options (Roca et al., 2015 & Review on Antimicrobial Resistance, 2014), increased healthcare cost and economic losses

(Hofer, 2019; Morel et al., 2020 & Ahmad & Khan, 2019), and its threat to global health security (Ayukekbong et al., 2017).

As of 2019, the burden of AMR directly attributed, cause and effect, to human life is estimated at around 1.27 million deaths and 4.95 million associated deaths annually, showing a relationship between antibiotic resistance and infection deaths but not a direct cause and effect (Antimicrobial Resistance Collaborators, 2022). The evidence is unequivocal; antibiotic resistance is a global concern that is worsening due to the misuse of antibiotics. Six species of bacteria are the prominent cause, accounting for 73% of those 1.27 million deaths. Species are listed by order of number of deaths. *Escherichia coli*, *Staphylococcus aureus, Klebsiella pneumonia, Streptococcus pneumonia, Acinetobacter baumannii*, and *Pseudomonas aeruginosa* (Antimicrobial Resistance Collaborators, 2022).

1.3.1 Antibiotic resistance in healthcare

As mentioned in section 1.3, only a small number of antibiotic-resistant species cause the vast majority of infections. In addition, many of these species are multidrug-resistant (MDR) (Abbo et al., 2007; Cao et al., 2004; Wang et al., 2020 & Medugu et al., 2022). A recent meta-analysis found that such MDR infections significantly increase hospitalisation time, associated costs, and mortality (Serra-Burriel et al., 2020). The consequences of resistance also lead to delays in the prescription of effective therapy – the most significant factor in delaying effective therapy is the mismatch between the antibiotic susceptibility test results and empirical therapy (Kollef et al., 2021; Eliopoulos et al., 2003 & Schwaber & Carmeli, 2007). This highlights a critical need for effective methods to detect and profile antibiotic resistance in MDR bacteria.

1.3.2 Antibiotic Resistance in Agriculture and the Food Processing Industry

Antibiotics are widely used in agricultural settings and the food processing industry to prevent and cure crop diseases as well as for livestock growth promotion. Since the 1940s, streptomycin and other aminoglycosides have been used in agriculture; in the 1950s, tetracycline was introduced, and since the introduction of these antibiotics, there have been increases in resistant strains such as *E. coli*, *Staphylococcus* and *Streptococcus* (Roberts, 1996; Cadena et al., 2018 & Magnet & Blanchard, 2005). A primary concern in using antibiotics in livestock is that a fraction of the excreted metabolites convert back into the active antibiotic and are returned to the environment (Sarmah et al., 2006). This leads to the selection of microbes to develop resistance to those excreted antibiotics (Mokni-Tlili et al., 2022, & Guo et al., 2018).

This has led to a growing concern that the increasing presence of ARGs and antibiotic resistance in soils may lead to even further increases in resistant bacteria in humans and livestock food chains (Hu et al., 2016 & Marti et al., 2013). When antibiotics are returned to the environment (for example, after use in agriculture), this creates selection for the evolution and maintenance of resistant bacteria. From these bacteria, transfer of antibiotic-resistant genetic elements can occur (from innocuous soil bacteria or more harmful strains present in the environment) into plasmids or chromosomes of pathogenic bacteria through HGT and MGE (Berendonk et al., 2015; Dancer, 2014 & Larsson & Flach, 2022). This leads to a situation in which low-level use of antibiotics in agricultural settings creates a vast reservoir of MGEs containing resistance elements. Numerous reports have highlighted the consequences associated with antibiotic resistance (O'Neill, 2016, O'Neill, 2014; WHO, 2021; CDC prevention, 2013 & Prestinaci et al., 2015). If the spread and development of antibiotic resistance continue unchecked, there could be much more severe repercussions to face in the future.

1.4 What are we doing about resistance? How can we slow the spread?

Over the past decade, additional regulations have been placed on antibiotics in healthcare and agriculture, thereby minimising their use. However, this is not a simple issue, as different countries have and will regulate antibiotic use to different standards (Årdal et al., 2016). What other strategies could be used instead of simply placing more regulations on antibiotic use? We are entering an age of gene editing technology. Through the application of various editing technologies or surveying techniques, resistant pathogenic bacteria can be inhibited before they lead to widespread infections. One technique being developed is the use of CRISPR-based systems that can efficiently target resistant microbes (Aslam et al., 2021).

Having efficient tools to uncover novel ARGs, rapidly decreasing the time to profile ARGs, and detecting ARGs before they become widespread are also ways that can contribute to reducing the burden of antibiotic resistance while gene editing technology is still being developed.

1.5 Culture-based methods for antibiotic resistance gene detection

The current gold standard to profile and detect ARGs in bacteria is culture-based methods in which bacteria are grown on permissive or selective media in the presence of the tested antibiotic. Culture-based methods include antimicrobial gradient methods, disc diffusion and commercially available automated systems (Sheka et al., 2021). These methods are relatively low-cost, easy to implement, and require minimal training (Zhang et al., 2021). However, culture-based methods have limitations such as variable growth times among bacterial strains, low sensitivity regarding false positives/negatives, the lack of differentiation between target and other non-target bacteria if the sample is not pure culture, and the inability to detect non-culturable or culture-resistant microorganisms (De, 2019 & Sohier et al., 2014).

Because culture time can vary between 24 and 72+ hours and, in some cases, weeks (e.g. eight weeks for *Mycobacterium tuberculosis*) (Pulido et al., 2013 & Koch et al., 2018), a broad-spectrum therapy is prescribed to manage an infection (Cassini et al., 2018 & Maugeri et al., 2019). However, this may be ineffective at treating the causative pathogen as it may be resistant, and every hour there is a delay in targeted infection treatment, there is a significant increase in infection length (Kumar et al., 2006). Therefore, molecular methods that can rapidly detect antibiotic resistance could decrease the time to initiate specific antibiotic treatment that can actively target the corresponding causative bacteria.

1.6 Molecular methods

Currently, a range of molecular and spectroscopic techniques for profiling AMR is already in use, such as metagenomics and functional metagenomics (Forbes et al., 2017 & Moragues-Solanas et al., 2021), whole-genome sequencing (WGS) (Shelburne et al., 2017), polymerase chain reaction (PCR) combined with nanopore sequencing (Sheka et al., 2021), mass spectrometry (Yoon & Jeong, 2021 & Florio et al., 2021), and CRISPR (Sajuthi et al., 2020).

1.6.1 Metagenomics versus targeted approaches

Both metagenomic sequencing and qPCR are two widely used strategies to detect and profile ARGs in both environmental and clinical settings (Lu et al., 2022; Diao et al., 2022; Xiao et al., 2016; Waseem et al., 2019; Burcham et al., 2019). In recent years, CRISPR has also been developed to target and amplify ARGs (Sajuthi et al., 2020). What are the benefits of targeted vs. non-targeted (metagenomics)? Metagenomics is a nontargeted method that can detect all ARGs within a particular sample (Munk et al., 2017 & Lanza et al., 2018). In contrast, as qPCR and CRISPR are targeted methods, they are capable of finding only specific ARGs. Ferreira et al. (2023) performed a comparative study between metagenomics and qPCR and found that metagenomic sequencing detects more ARGs overall. In contrast, qPCR was more sensitive but detected significantly lower numbers of ARGs. The authors suggest that qPCR can be advantageous for ARG monitoring purposes and is easily customised to monitor ARG profiles in different environments. At the same time, CRISPR-based methods can be rapid and sensitive. However, CRISPR-based methods have limitations when the sample is complex, i.e. from soil or faeces, as this can interfere with the CRISPR-Cas system (Rasheed et al., 2021). While this is also a possibility for qPCR, such assays are often more robust.

1.6.1 Oxford nanopore sequencing as a platform to profile antibiotic resistance genes

Oxford Nanopore Technologies (ONT) is a DNA sequencing platform that offers long-reads, usually from thousands to hundreds of thousands of base pairs long. However, the number of base pairs in a single read can be as low as 50 base pairs (bp) and can reach as high as 2.3

megabase pairs (Mb) (Amarasinghe et al., 2020 & Payne et al., 2018). ONT sequencing offers real-time data that can be analysed while sequencing (Jain et al., 2016), which is beneficial for rapid analytics. The standard sequencing platform, the ONT MinION device, is smaller than a mobile phone. This opens another aspect of this platform regarding accessibility and usability.

Due to the real-time nature and portability, it has been used in disease outbreaks such as the 2014 Ebola outbreak in Africa (Hoenen et al., 2016) and more recently during the SARS-CoV-2 pandemic in 2019 (Bull et al., 2020 & Freed et al., 2020). Rapid sequence data is crucial in disease outbreaks to monitor evolutionary patterns and investigate transmission chains (Mate et al., 2015). ONT sequencing has also been found to be sufficient to resolve the structures of an antibiotic-resistant island despite having a high error rate compared to other sequencing platforms. ONT sequencing has also been used to track antibiotic resistance and plasmid evolution in a clinical setting (Zhao et al., 2023). Peter et al. (2020) found it to be an efficient platform for sequencing an MDR Gram-negative bacteria collection.

In 2022, ONT released new reagents (10.4.1 flowcells and V14 chemistry) and a basecalling method (dorado) that decreased error rates such that they are now comparable to other sequencing platforms (with the majority of reads having 99% accuracy and above) (Linde et al., 2023).

Two studies to date have researched the capabilities of multiplex PCR paired with ONT to profile and detect ARGs in bacteria from clinical samples. Firstly, Zhang et al. (2020) designed a protocol to target 13 ARGs in *Neisseria gonorrhoeae* with high sensitivity and accuracy. The authors could detect the target ARGs within 7 hours 40 minutes to 10 hours 40 minutes and in isolates between 5 hours 20 minutes to 8 hours 20 minutes. Zhao et al. (2022) reported that they could profile seven ARGs in *Mycobacterium tuberculosis* within 12 hours using multiplex PCR and ONT as a sequencing platform. These two methods highlight the efficiency of ONT as a sequencing platform to decrease the time to analyse ARG data.

1.8 Research hypothesis and objectives

In this study, we aimed to develop a proof-of-principle method to demonstrate that through molecular techniques, ARGs could be profiled in a rapid and sensitive manner in both single colonies and metagenomic samples. We compared its performance with metagenomic sequencing in terms of time and ease of use. Furthermore, we developed this method to allow profiling both the ARGs of interest and the genomic or genetic context in which those ARGs were contained.

To test our hypothesis, we addressed these objectives:

1. Developed and optimised a PCR protocol that allowed amplification of targeted ARGs and surrounding genomic regions.
    a. We designed primers that amplified specific ARGs and designed and tested degenerate primers that amplified random regions close to the target ARG.

2. Test degenerate primers' capabilities to determine the target ARGs' genome context.
    a. We tested the effectiveness of a pooled primer set that allowed us to provide genomic context to each target ARG.

3. Test the protocol on single bacterial isolates.
    a. We tested how our protocol worked on a single colony and adjusted to optimise the protocol by changing the primer pools or PCR temperatures and cycle times.

4. Compare the performance of the PCR-based protocol to standard metagenomic approaches using complex faecal samples.
    a. We tested how the developed protocol worked on metagenomic fecal samples and compared the results to metagenomic sequencing.

Chapter 2: Materials and Methods

2.1 E. coli L3Cip3

E. coli L3Cip3 is a strain of *E. coli* with nine ARGs that are either chromosomal or plasmid-borne. Due to its extensive complement of ARGs, we used it to determine the efficiency of our ARG primers or primer pools (**Table 2.3**). Only ARGs identified in a previous study using *E. coli* L3Cip3 (Sajuthi et al., 2020) were used to develop primers.

2.1.1 DNA extraction

E. coli L3Cip3 was streaked onto Lysogeny broth (LB) agar and grown for at least 12 hours at 37°C. We confirmed single colonies and grew one in 1mL of LB for 12 hours at 37°C. Genomic DNA (gDNA) was extracted from this culture using the Promega Wizard® genomic DNA purification kit. DNA was eluted using DNAase-free H_2O. DNA quantification was performed using the broad-range double-stranded DNA (dsDNA) assay kit on a Qubit 4.0 fluorometer (Thermo Fisher Scientific, US). gDNA samples were diluted into 1:10, 1:100 and 1:1000 (DNA: H_2O) batches for use as PCR templates.

2.1.2 Selecting Target ARGs

We selected nine ARGs (**Table 2.1**) to target within *E. coli* L3Cip3. The L3Cip3 chromosome is 4,932,700 bp, the largest plasmid is 177,032 bp (referred to as plasmid 1 below) and contains most of the target ARGs. The three following largest plasmids are 87,471 bp, 83,916 bp, and 44,671 bp in size and below are referred to as plasmids 2, 3, and 4, respectively; L3Cip3 has a total of seven plasmids.

Table 2.1. Target ARGs for *E. coli* L3Cip3. Position, location, size, resistance mechanism and drug class were all found using Proksee (Grant et al., 2023), which uses the Comprehensive Antibiotic Resistance Database (CARD) to annotate ARGs.

ARG	Location	Position	Size (bp)	Resistance Mechanism	Drug class
rmtB	Chromosome	3,602,713bp - 3,604,251bp	1539	Target alteration	Aminoglycosides
aph(6)-Id	Plasmid 1	79,639bp - 80,475bp	837	Inactivation	Aminoglycosides
aph(3)-Ib	Plasmid 1	78,836bp - 79,639bp	804	Inactivation	Aminoglycosides
bla-$_{TEM-1}$	Plasmid 1	80,706bp - 81,566bp	861	Inactivation	Monobactam, cephalosporin
dfrA14	Plasmid 1	71,605bp - 72, 078bp	474	Target replacement	Diaminopyrimidine
sul2	Plasmid 1	77,960bp - 78,775bp	816	Target replacement	Sulfonamide
tet(A)	Plasmid 1	63,906bp - 65,105bp	1200	Efflux	Tetracycline
bla-$_{CTX-M-55}$	Plasmid 2	73,117bp - 73,992bp	876	Inactivation	Cephalosporin, Penicillin
aph(4)-Ia	Plasmid 3	6268bp - 7293bp	1026	Inactivation	Aminoglycoside
ermB	Plasmid 4	39,704bp - 40,441bp	738	Target alteration	macrolide, lincosamide, streptogramin

2.2 Metagenomic samples.

All metagenomic samples were collected from five different New Zealand farms. All samples were from dairy calf faeces. Each sample is a collection of 25 different collection points on each farm, and each collection point are individual faeces. The location and dates collected are outlined in **Table 2.2**.

Table 2.2. Metagenomic faecal samples.

Sample ID	Region	Collection date
04	Waikato	9-Aug-2021
10	Waikato	10-Aug-2021
13	Waikato	13-Sept-2021
69	Waikato	24-Sept-2021
77	Canterbury	28-Sept-2021

2.2.1 Metagenomic DNA extraction

DNA was extracted using two methods: the Zymobiomics (Zymo Research) miniprep kit was used to extract DNA from 100-150mg of faecal sample following the manufacturer's instructions. The Qiagen DNeasy Powersoil kit was used to extract DNA from 150-200mg of faecal sample following the manufacturer's instructions. DNA quantification was performed using the broad-range double-stranded DNA (dsDNA) assay kit on the Qubit 4.0 fluorometer (Thermo Fisher Scientific, US).

2.3 Nested PCR

A nested PCR (N-PCR) method was used to amplify target ARGs to increase detection sensitivity and provide genomic context for the target ARG. N-PCR functions by implementing two rounds of PCR. In the first, amplification occurs via a primer binding to the ARG(s) of interest and non-specifically to the genomic region downstream. This downstream primer contains a tail at the 3' of the known sequence. In a second round of PCR, to increase specificity, a second primer targeting the ARG that is downstream of the first ARG primer is used. In addition, a primer complementary to the tail on the degenerate primer is used. To identify the genomic context, we stipulated a minimum requirement of over 25 base pairs downstream of the ARG was present. This should allow unique determination of the region to at least a genus level; however, more repetitive regions such as transposons, IS elements, or others would require substantially longer sequence context outside of the ARG. **Figure 2.1**

outlines the basis of using degenerate primers in conjunction with ARG primers to amplify ARGs.

Table 2.3. ARG primer pool containing all target ARGs. The primers listed here were multiplexed into two pools. One for the first round of N-PCR and one for the second round of N-PCR. Primers designed using Primalscheme v1.4.1 (Quick et al., 2017).

First-round primer pool	Primer sequence (5'-3')	Position of primer in ORF	Second-round primer pool	Primer sequence (5'-3')	Position of primer in ORF
aph(3'')-Ib_5_AF321551:+24	TGGTGAATCGCATTCTGACTGG	377	aph(3'')-Ib_5_AF321551:+332	CTGTTCACAGCCTATCGGTTGA	376
aph(4)-Ia_1_V01499:+25	ACGTCTGTCGAGAAGTTTCTGA	380	aph(4)-Ia_1_V01499:+617	CGGACAATGGCCGCATAACA	388
aph(6)-Id_4_CP000971:+5	CGCCTGTTTTTCCTGCTCATTG	377	aph(6)-Id_4_CP000971:+283	GACTACCAGGCGACCGAAATTG	379
blaCTX-M-55_1_DQ810789:+8	AAAAATCACTGCGCCAGTTCAC	381	blaCTX-M-55_1_DQ810789:+331	ATTGCGGAAAAGCACGTCAATG	367
blaTEM-1B_1_AY458016:+15	TTTTCGTGTCGCCCTTATTCCC	374	blaTEM-1B_1_AY458016:+326	AGCATCTTACGGATGGCATGAC	388
dfrA14_1_KF921535:+6	AGTATCATTGATGGCTGCGAAAG	378	dfrA14_1_KF921535:+59	ACATACCCTGGTCCGCGAAA	384
erm(B)_1_JN899585:+37	ACGAGTGAAAAAGTACTCAACCAAA	372	erm(B)_1_JN899585:+295	GGGAATATTCCTTACCATTTAAGCACA	379
rmtB_1_AB103506:+22	ACCTCCATCCTGGCCTCAAAAA	378	rmtB_1_AB103506:+340	CTTAACCCCTTGGCGCTATACG	366
sul2_2_AY034138:+35	ACATAACCTCGGACAGTTTCTCC	393	sul2_2_AY034138:+355	GCGAAATCATCTGCCAAACTCG	372
tet(A)_4_AJ517790:+3	GAAACCCAACAGACCCCTGATC	398	tet(A)_4_AJ517790:+531	CTGTTTCCTTTTGCCGGAGTCG	384

Table 2.4. Description of degenerate primers and constant primers. Freed (F) primers were designed by Freed et al. (2016). Manoil (M) primers were designed by Manoil (1999). N denotes any possible base (A, T, C or G)

Degenerate primers	Primer sequence (5'-3')
F-NNN	GTG ACT GGA GTT CAG ACG TGA NNN NNN NNN NNN NNN
F-ATG	GTG ACT GGA GTT CAG ACG TGA NNN NNN NNN NNA TGN
F-TAA	GTG ACT GGA GTT CAG ACG TGA NNN NNN NNN NNT AAN
F-TGA	GTG ACT GGA GTT CAG ACG TGA NNN NNN NNN NNT GAN
M-NNN	GGC CAC GCG TCG ACT AGT ACN NNN NNN NNN NNN NN
M-ATG	GGC CAC GCG TCG ACT AGT ACN NNN NNN NNN NAT GN
M-TAA	GGC CAC GCG TCG ACT AGT ACN NNN NNN NNN NTA AN
M-TGA	GGC CAC GCG TCG ACT AGT ACN NNN NNN NNN NTG AN
Constant primers	**Primer sequence (5'-3')**
nested-freed-AMR-constant	GTG ACT GGA GTT CAG ACG TGT
nested-manoil-AMR-constant	GGC CAC GCG TCG ACT AGT AC

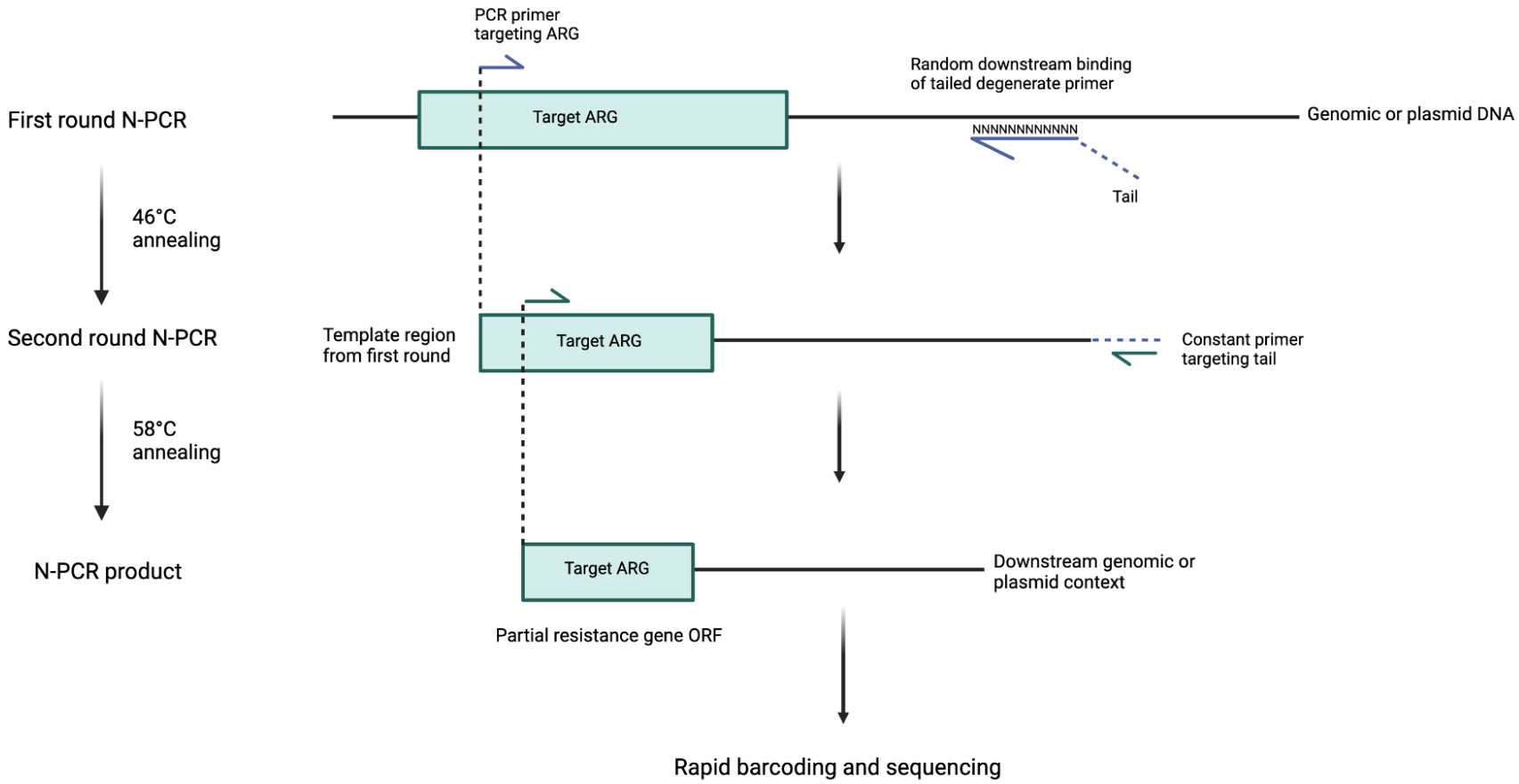

Figure 2.1. Degenerate primers paired with ARG primers produce sequences that can provide a genomic context to an ARG. This nested PCR protocol included two rounds of PCR. The first round aims to amplify a target ARG and include an unknown number of base pairs up or downstream of that ARG. To achieve this, a forward primer for a target ARG and a degenerate primer with a random degenerate sequence are used during the first round. This produces an amplicon with part of the target ARG and a fragment of unknown length with an introduced constant region within it. The second round of PCR will further amplify this amplicon using a constant primer, another forward ARG primer targeting inside the same ARG. The constant primer will anneal to the introduced constant region (tail) from the first-round PCR. For simplicity, this illustration only shows a downstream unknown region attached to the target ARG. However, the unknown region can be either upstream or downstream.

2.3.1 First round PCR

The reaction mix included 10µL Q5® High-Fidelity 2X Master Mix (Master mix includes Q5 High-Fidelity DNA Polymerase, deoxynucleotide triphosphates (dNTPs), and Mg^{++} in a broad-use buffer), 4µL ddH2O, 2µL first-round ARG primer pool (10µM), 2µL degenerate primer (10µM) (**Table 2.3**), or a degenerate primer pool (10µM) (**Table 2.4**), depending on the experiment, and 2µL gDNA. The PCR cycling profile consisted of initial denaturation at 95ºC for 3 minutes, followed by eight cycles of denaturation at 95ºC for 30 seconds, annealing at 46ºC (varying temperatures during primer optimisation, section **3.1**) for 30 seconds, and extension at 72ºC for 1 minute. The final extension temperature was 72ºC for 3 minutes, followed by a hold at 4ºC to complete the run. The products were electrophoresed on a 1% agarose gel at 100 volts for one hour to check whether the N-PCR was successful. No specific size fragments were seen due to the degenerate primers producing amplicons of an unknown size.

2.3.2 PCR Cleanup

10µL PCR product from first-round nested PCR and 7ul of AMPure XP beads (Beckman Coulter, Life Sciences) was added to a new 1.5mL Lobind tube to obtain a 0.7:1 ratio of sample to beads (0.7x beads (sample volume)). Samples were incubated on HulaMixer (Thermo Fisher Scientific, US) for five minutes at room temperature. Samples were placed in a magnetic rack for three minutes until the supernatant was clear. The supernatant was removed without disturbing the pellet. The pellet was washed with 500µL of freshly prepared 70% ethanol. Ethanol was removed, and this step was repeated. Samples were spun down briefly and placed back on a magnetic rack. Any excess ethanol was removed, and the tube air dried for 30 seconds without cracking the pellet. 10µL nuclease-free H_20 was added to samples, and the pellet was resuspended to elute the DNA from the AMPure beads. The sample was left to sit at room temperature for two minutes. Samples were placed back on a magnetic rack for at least one minute, and 10µL supernatant containing the second round PCR template was removed and placed into a new 1.5mL Lobind tube

2.3.3 Second-round nested PCR

The bead-cleaned N-PCR product from the first round of PCR was used as the template for the second round of N-PCR. The reaction mix included 10µL Q5® High-Fidelity 2X Master Mix (Master mix includes Q5 High-Fidelity DNA Polymerase, dNTPs, and Mg^{++} in a broad-use buffer), 4µL ddH2O, 2µL second-round ARG primer pool (10µM) (**Table 2.3)**, 2µL degenerate primer pool (10µM) (**Table 2.4)**, and 2µL bead-cleaned first round PCR product. The PCR cycling profile consisted of initial denaturation at 95°C for 3 minutes, followed by 35 cycles of denaturation at 95ºC for 30 seconds, annealing at 58ºC (varying temperatures during primer optimisation, section **3.1**) for 30 seconds, and extension at 72ºC for 1 minute. Final extension at 72ºC for 3 minutes, followed by 4ºC hold to complete the run. The products were

electrophoresed on a 1% agarose gel at 100 volts for one hour to check whether the N-PCR was successful. No specific size fragments were seen due to the degenerate primers producing amplicons of an unknown size.

2.4 Oxford Nanopore Sequencing

2.4.1 Rapid barcoding - R9.4.1

The rapid barcoding kit (SQK-RBK004) from ONT offers a relatively quick and cheap method to sequence genomes, plasmids or amplicons. Rapid barcoding functions by attaching barcodes to each sample at non-specific regions within the DNA fragment. This is accomplished with a barcoded transposome complex, which cleaves and adds barcodes within a DNA fragment. For each library preparation, we had different numbers of samples from each N-PCR run, ranging from two up to 26 samples, depending on what was being tested. The ONT rapid barcoding is offered in 12 sample kits (SQK-RBK004) and 96 sample kits (SQK-RBK110.96), providing the ability to sequence one to 96 samples on a single MinION R9.4.1 flowcell. The library was prepared following the manufacturer's instructions. One modification was made to the RBK004 and RBK110.96 protocol during library preparation. A 0.7x AMPure XP beads of sample volume was implemented to remove DNA fragments under 200 bp. DNA fragments of 200 bp or less are less likely to provide information on genomic context. Once library preparation was completed, the library was loaded onto an R9.4.1 flowcell and run for an average of 1.5 hours. The time needed for the collection of sufficient sequence data depended on the health (pore availability) of the flowcell being used (the majority of experiments were performed on used flowcells).

2.4.2 Rapid barcoding - R10.4.1

During our experiments, access to ONT's new chemistry opened up. This included the new rapid barcoding kit RBK114 and R10.4.1 flowcells. We thus also sequenced the PCR product using the RBK114 kit, which provides similar barcodes to the old chemistry but produces 1-2% higher accuracy reads (Sereika et al., 2022). The library was then prepared following the manufacturer's instructions. One modification was made to the RBK114 protocol: a 0.7x AMPure XP beads to sample volume was implemented to remove DNA fragments under 200 bp. The library was loaded onto a P2 PromethION R10.4.1 flowcell and run for 30 minutes. The time needed to sequence will depend on the health (pore availability) of the flowcell being used.

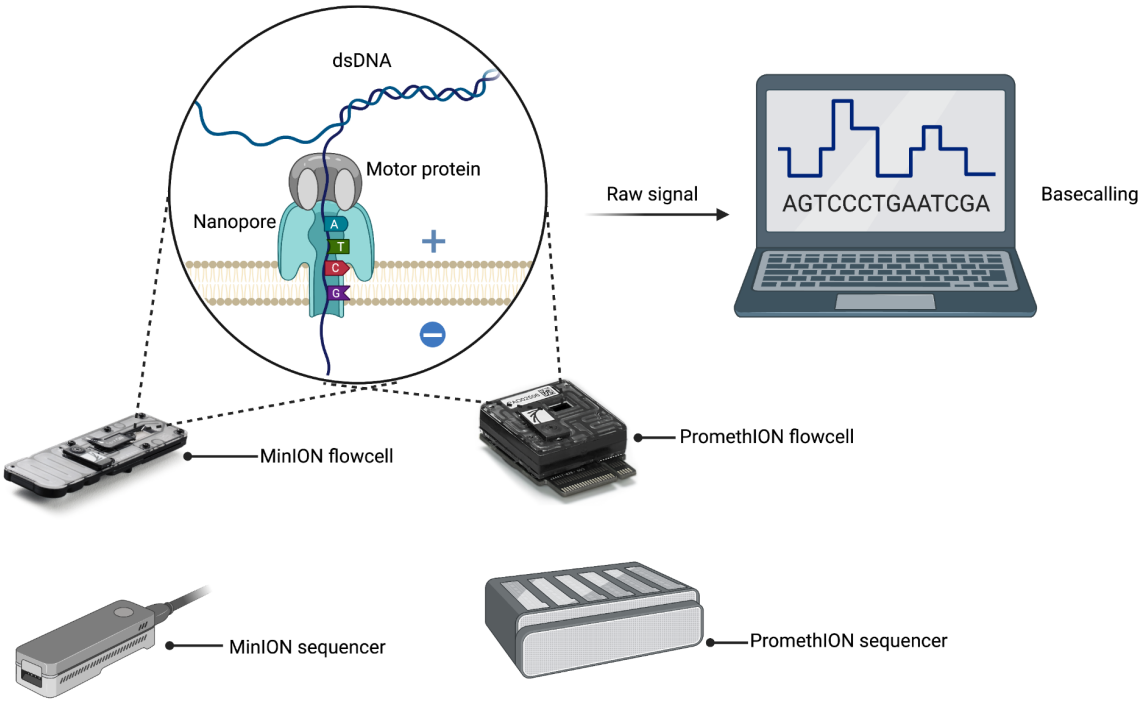

Figure 2.2. Principle of Oxford Nanopore sequencing. The MinION and PromethION sequencers are two devices offered by ONT and have different flowcells that produce differing amounts of data. However, the method of sequencing remains the same. The MinION flowcell contains 2048 nanopores and can produce 50Gb of data, while the PromethION flowcell contains 10,700 nanopores and can produce up to 290Gb of data. When a single DNA strand passes through a nanopore, there is a disturbance of the ionic current that is constantly flowing through the membrane. This produces a raw signal that a basecaller can decode to uncover the DNA bases. Image created using BioRender.com. Flowcell images from https://nanoporetech.com/how-it-works/flow-cells-and-nanopores.

2.5 Bioinformatic Workflow

2.5.1 Basecalling and quality control

As illustrated in **Figure 2.2**, Nanopore sequencing functions by a single strand of DNA passing through nanopores embedded within a sensor assay of a flowcell. The constant ionic current is disrupted as the strands pass through the nanopore, producing varying signals. Basecalling is a method to decode that signal to uncover the single bases within that strand. A wide variety of basecallers are offered by third parties (Pagès-Gallego & Ridder, 2023 & Wick et al., 2019). However, during this research, we exclusively used the basecaller Guppy v6.3.4 high accuracy (hac), ONT's basecaller. Three different accuracy modes can be implemented while using Guppy (fast, hac, and sup). Guppy basecaller_fast is significantly faster than the other two. However, accuracy is sacrificed for speed. Guppy basecaller hac is the middle ground of the three modes and significantly increases accuracy compared to the fast mode. Super accuracy (sup) produces the most accurate reads, but speed is sacrificed. We chose Guppy_hac as this

took, on average, less than 10 minutes to basecall 100k reads per run. Guppy_basecaller was used to demultiplex the barcodes from the rapid barcoding kits and sort them into individual files. We filtered our reads using FIltlong v0.2.1 (https://github.com/rrwick/Filtlong) to remove any reads under 100 bp.

2.5.2 Mapping

Reads from each sample were mapped against ResFinder (Florensa et al., 2022) (https://bitbucket.org/genomicepidemiology/resfinder_db/src/master/), an open-source database to identify ARGs using next-generation sequencing (NGS). Using cd-HIT, this database was reduced to only contain ARGs that are 90% similar, as a very large number of ARGs are highly similar, differing only by a few bp. However, for the most part, they provide similar, if not identical, functionality. In order to simplify the analysis pipeline, we aimed to determine only whether a sample contained a specific type of ARG rather than a specific allele of a specific type. For this reason, we collapsed the database.

Reads from each sample were also mapped against the L3Cip3 reference FASTA file previously sequenced. Mapping was completed using minimap2 v2.26 (https://github.com/lh3/minimap2). After all mapping steps, we removed all reads with mapping quality below 20.

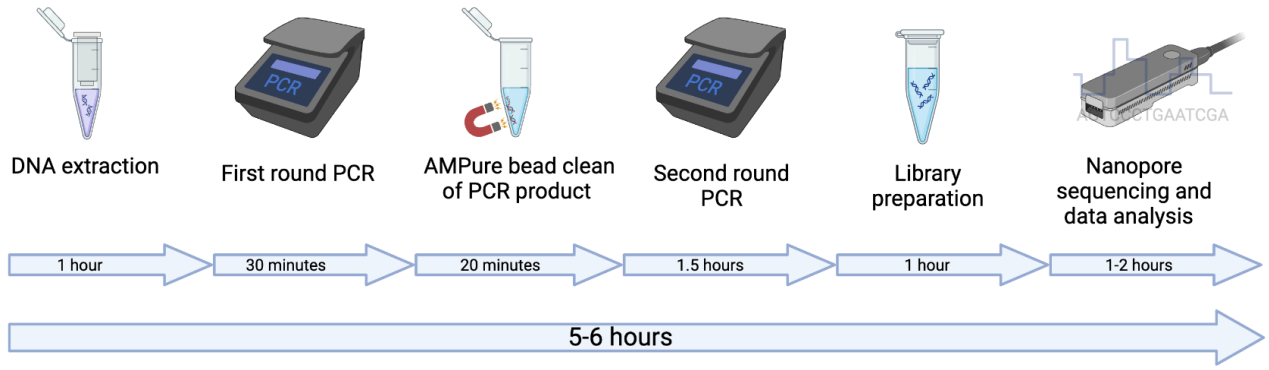

Figure 2.3. Nested PCR with ONT sequencing can be completed within 5-6 hours. Average time of each component of N-PCR protocol. DNA extraction is completed using the Promega Wizard® genomic DNA purification kit for single strains and the Zymobiomics miniprep kit or Qiagen DNeasy Powersoil kit for metagenomic samples. PCR is completed using a nested PCR protocol with two rounds of PCR; between the first and second rounds of PCR, the product is purified using AMPure beads at a 0.7x beads-to-sample. Library preparation is completed using ONT's rapid barcoding kits (RBK004, RBK110.06 or RBK114). DNA sequencing was completed on ONTs R9.4.1 MinION flowcells' or R10.4.1 PromethION P2 solo flowcells'. Reads basecalled and demultiplexed using Guppy, and reads mapped using minimap2. Sequencing time will depend on flowcell health, pore availability and quality of library preparation.

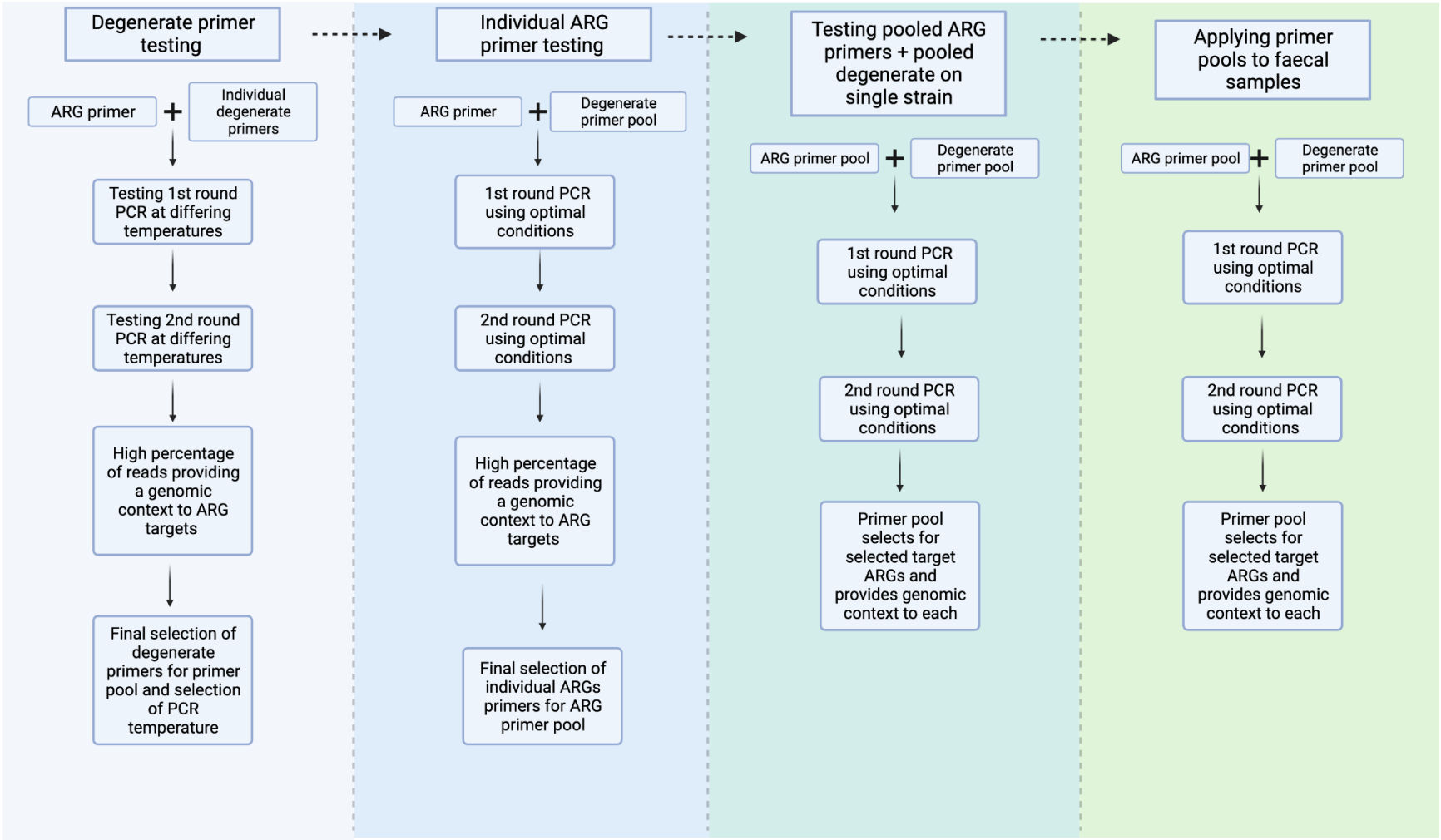

Figure 3.1. Strategy to develop functional primer pools with degenerate primers and ARG primers. First panel: Starting with initial testing of degenerate primers to find the optimal conditions needed for these to anneal at high rates while also finding which primers provide a genomic context to target ARG and which might work well together in a multiplex pool. Second panel: Testing individual ARG primers with a degenerate primer pool to determine if pooling degenerate primers is necessary and finding ARG primers that work in these optimised conditions. Third panel: Testing how the developed degenerate and ARG primer pools work together on a single strain. Fourth panel: Testing how the developed primer pools work with metagenomic samples.

Chapter 3: Single Strain Results

3.1 Primer Optimisation

To efficiently amplify target ARGs while providing genomic context, we needed a strategy to amplify target ARGs and know if they reside on the chromosome or are plasmid-borne. We used a nested degenerate-primer strategy to pursue this goal (**Fig. 3.1**). We designed eight different degenerate primers containing a 3' region that could anneal non-specifically. These primers had three base pairs binding to a sequence complementary to a start or stop codon, with the exception of the primers we refer to as F-NNN and M-NNN, which are fully degenerate (**Table 2.4**). This three-base pair sequence is followed by ten base pairs of entirely random sequences (N_{10}) and a 5' leader having a known (constant) sequence. We designed two constant primers to anneal to this introduced constant region from the first round PCR primers (**Table 2.4**). We also designed a panel of ARG primers to anneal to target ARGs (**Supp. Table 6.1**) with the purpose of multiplexing all of the primers into two pools, one for round-one N-PCR and one for round-two N-PCR (principle outlined in **Fig. 2.1**).

3.1.1 Testing Degenerate Primers

We first tested the eight degenerate primers (described above and in **Table 2.4**) with a single forward ARG primer complementary to the dihydrofolate reductase gene (*dfrA14*), positions 71,605bp to 71,628bp on plasmid 1 of L3Cip3. We tested the efficiency of these eight degenerate primers at different annealing temperatures (42ºC, 44ºC, and 46ºC) during the first round of N-PCR. In the second round of N-PCR, we tested different annealing temperatures (58ºC, 60ºC, and 62ºC). During this round, we used constant primers (**Table 2.4**) and a second forward *dfrA14* primer complementary to positions 71,664 to 71,684 on plasmid 1 of L3Cip3, again at differing annealing temperatures. This combinatorial design resulted in seven different combinations of annealing temperatures across all eight degenerate primers, a total of 56 different PCR reactions. We sequenced each PCR product using the ONT rapid barcoding kit (RBK004) on MinION R9.4.1 flowcells, allowing us to sequence up to 12 samples in a single sequencing run. We completed six different sequencing runs (**Table 3.1**), running each for an average of one hour.

We selected the optimal PCR conditions based on the highest average frequency of reads that provided a genomic context for the *dfrA14* gene. We found that the degenerate primers functioned the best at 46ºC during annealing for the first round of N-PCR (providing a low enough temperature for degenerate priming) and 62ºC annealing during the second round (providing a high enough temperature to ensure specificity of amplification) (**Fig. 3.1)**. However, Optimal behaviour for this single gene at a single temperature was not our only consideration.

As is apparent from **Figure 3.1**, when using an initial temperature of 44ºC, the best temperature in the second round (across all primers) is 58ºC. At 46ºC (first round), 60ºC performs poorly in the second round. Thus, there appears to be a non-trivial relationship between temperature, primer, and performance. Nevertheless, we selected a pair of temperatures that appeared to balance robustness and repeatability, settling on 46ºC+58ºC annealing as our N-PCR temperatures for all remaining experiments. In addition, we found that the degenerate primers F-NNN and M-NNN seemed to function robustly across all annealing temperatures, except 44ºC+62ºC for F-NNN and 42ºC+58ºC for M-NNN. This suggested that these two primers may be the most robust when used singly. The highest percentages of reads that provided a genomic context to *dfrA14* were noted at our selected temperature combination (46ºC + 58ºC): M-TAA (35%), M-TGA (28%) and F-TGA (38%). We pooled the primers M-TAA, M-TGA and F-TGA for future tests.

Table 3.1. ONT sequencing reports for each run. Reads generated are in the thousands (k), data produced in gigabytes (GB), and estimated bases in mega base pairs (Mb). N50 is the sequence length of the shortest read at 50% of the total assembly length (Thrash et al., 2020).

Sequencing run	Reads generated (k)	Data produced (GB)	Estimated bases (Mb)	Estimated N50	Run time (hours)
1	246	1.32	79	347	1.19
2	433	2.94	154	419	1.13
3	366	2.13	114	322	1
4	265	1.53	88	348	1.65
5	476	2.75	151	330	1
6	177	1.09	54	305	1.84
Average	327	2	107	345	1

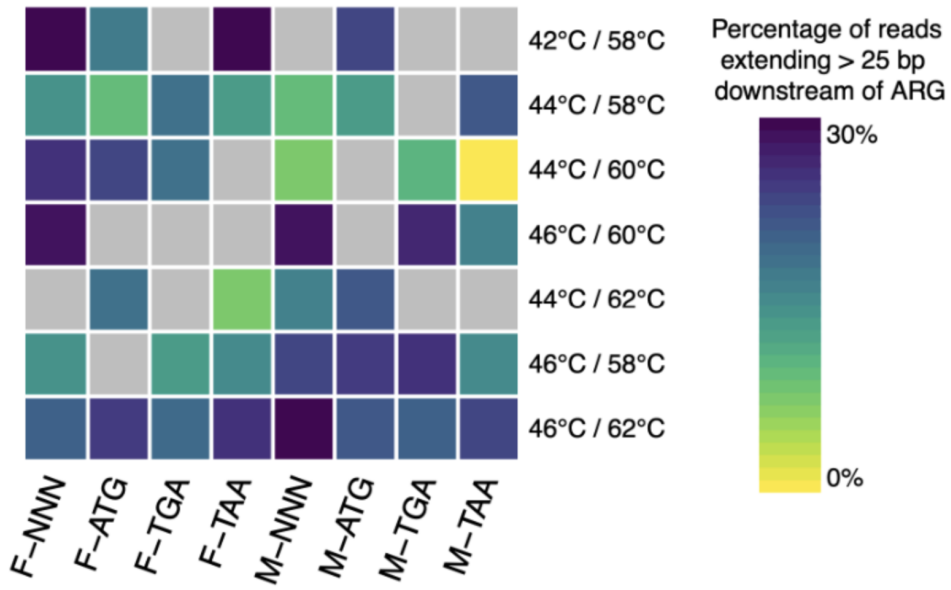

Figure 3.1. 46℃+62℃ is the best annealing temperature condition for all degenerate primers during N-PCR. The y-axis is the annealing temperatures for both rounds of N-PCR (1st round annealing + 2nd round annealing). The x-axis indicates the degenerate primers tested at these temperatures. Grey boxes show that primers did not work at these temperatures. Products were produced using a nested PCR protocol with individual degenerate primers and the primer annealing to the dfrA14 gene of *E. coli* L3Cip3, each degenerate primer corresponding to an individual reaction. We sequenced the products using the RBK004 rapid barcoding kit on a MinION R9.4.1 flowcell over six sequencing runs. We mapped these reads to the *E. coli* L3Cip3 reference genome and the ResFinder AMR database using minimap2. We cross-referenced the reads mapping to the L3Cip3 reference genome and the ResFinder AMR database to find reads with nucleotides extended 25bps or more up or downstream of dfrA14. The percentage was calculated by dividing the number of reads proving a genomic context by the number of reads mapping to the target ARG.

3.2 Testing individual ARG primers with pooled degenerate primers

We next wanted to test how individual ARG primers functioned with the degenerate primer pool containing M-TAA, M-TGA and F-TGA. We completed our N-PCR protocol (**Methods section 2.3**) using individual ARG primers targeting ARGs *aph(3), aph(6), bla-$_{CTX}$, bla-$_{TEM}$, dfrA14, sul2* and *tet(A)* (resistance and locations outlined in **Table 2.1**), and the degenerate primer pool in single reactions. We sequenced the N-PCR products using the RBK004 rapid barcoding kit on an R9.4.1 flowcell. In 1.5 hours, we produced 143k reads and 1.46 Gbp from a used flowcell containing approximately 600 active pores. We mapped the reads against the *E.coli* L3Cip3 reference genome and the Resfinder AMR database to find reads that map to all target ARG and provide genomic context to each target. We found significant enrichment of *aph(6)* (encoding resistance to aminoglycoside antibiotics) and *sul2* (encoding sulfonamide-resistant dihydropteroate). In addition, we found that the degeneracy of the N-PCR and the length of the reads provided genomic context (i.e. 25 bp or more of adjacent nucleotide sequence from the ARG) with the exception of tet(A).

We found over 223 reads mapping to the *tet(A)* gene, showing we can enrich this target to a significant level. However, few extended 25 bp upstream or downstream of t*et(A)*. This failure, in conjunction with the fact that the *tet(A)* gene encodes resistance to tetracycline, a highly prevalent antibiotic used in New Zealand agriculture (Jahantigh et al., 2020), motivated us to attempt this experiment a second time to determine the genomic context adjacent to *tet(A)* at a higher rate. In addition, these additional experiments allowed to test the repeatability of the assay.

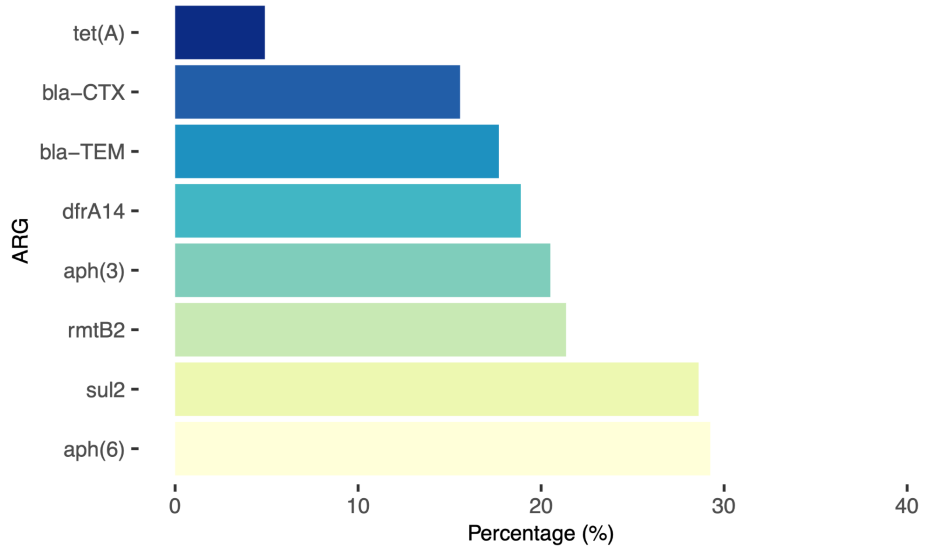

Figure 3.2. The *aph(6)* and *sul2* primers working with the degenerate primer pool produced the highest percentage of reads providing a genomic context. We produced reads by sequencing on ONT's MinION device using a MinION 9.4.1 flowcell after completing a nested PCR protocol. Using minimap2, we mapped these reads to the *E. coli* L3Cip3 reference genome and the Resfinder ARM database. To find reads with nucleotides extended up or downstream of the target gene, we cross-referenced the reads mapping to the L3Cip3 reference genome and the Resfinder AMR database. We found reads extending up or down from the target ARG above 25bps. The percentage was calculated by dividing the number of reads proving a genomic context by the number of reads mapping to the target ARG.

We thus performed two additional experiments to determine if the amplification of the region surrounding tet(A) was consistently low. We completed both experiments with the same conditions as the first. In the first sequencing run, we produced 68k reads and 27.77 megabase pairs (Mbp), with an N50 of 413 bp over 1.5 hours on a used flowcell containing approximately 500 active pores. In the second run, we produced 66k reads and 28.4 Mbp, with an N50 of 448 bp over 1.5 hours on a used flowcell containing approximately 400 pores.

The two genes that encode resistance to beta-lactam antibiotics, *bla-$_{CTX}$* and *bla-$_{TEM,}$* were the most consistently amplified together with the surrounding genomic region, with the percentage of reads that provide a genomic context averaging 15% ± 0.8% and 19% ± 3%, respectively. Interestingly, the ARGs *sul2, dfrA14* and *rmtB2* were less consistent over the three experiments, demonstrating that assay robustness is not fully optimised. Finally, we found that the percentage of reads providing *tet(A)* genomic context was consistently below 5% in all three experiments (**Figs. 3.2 & 3.3).** However, over all three sequencing runs, we produced, on average, 284 reads mapping to *tet(A)*. Showing we can enrich this target – and that the lack of reads providing genomic context is not due to poor amplification in general, but rather the degenerate primer pool annealing infrequently to regions outside the *tet(A)* gene.

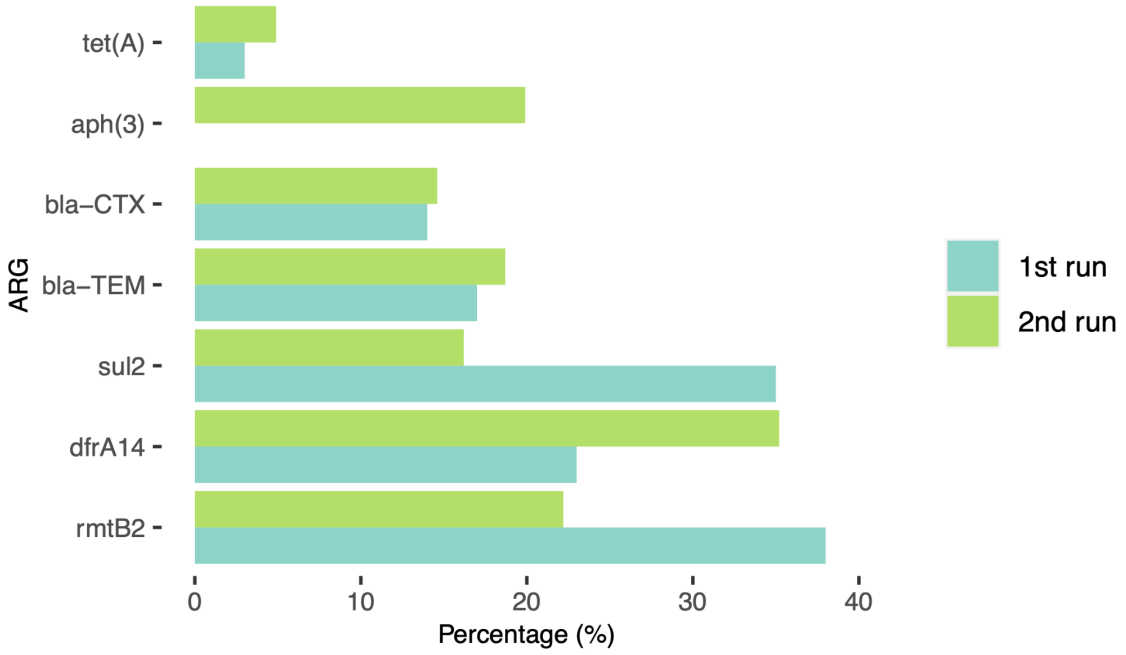

Figure 3.3. The primer for *tet(A)* working with the degenerate primer pool does not produce reads that provide a genomic context at high percentages. We produced reads by sequencing on ONT's MinION device using a MinION 9.4.1 flowcell after completing a nested PCR protocol. Using minimap2, we mapped these reads to the *E. coli* L3Cip3 reference genome and the Resfinder ARM database. To find reads with nucleotides extended up or downstream the target gene, we cross-referenced the reads mapping to the L3Cip3 reference genome and the Resfinder AMR database and found reads that would extend up or down from the target ARG above 25bps. The percentage was calculated by dividing the number of reads proving a genomic context by the number of reads mapping to the target ARG.

3.3 Improving tetracycline genomic context frequency

The degenerate primer pool containing M-TAA, F-TGA and M-TGA produced high-frequency mapping to the target ARGs outlined in section **3.2**. It also provided genetic context to all targets except *tet(A)*. To test whether we could increase the percentage of reads providing a genomic context for *tet(A)*, we tested all eight individual degenerate primers with the *tet(A)*-specific ARG primer complementary to positions 63,909bp - 63,929bp for the first round of N-PCR. During the second round of N-PCR, we used the pooled constant primers with the nested *tet(A)* primer complementary 64,437bp - 64,459bp (**Methods section 2.8**). We sequenced products using the RBK004 rapid barcoding kit on an R9.4.1 flowcell with an initial 200 active pores. This produced 122.83k reads and 1.23 Gbp in four hours. We mapped all reads against the *E .coli* L3Cip3 reference genome and the Resfinder AMR database to find reads mapping to *tet(A)* and providing a genomic context.

We found that the primer combination of F-TGA with the forward primer for *tet(A)* enriched the *tet(A)* locus the most. However, this primer combination did not yield a high percentage of reads that also provided a genomic context. Of note, the top three primer combinations that produced the highest number of reads mapping to *tet(A)*, (F-NNN, F-TGA and M-ATG), all produced relatively low percentages of reads providing a genomic context (**Table 3.2**). F-TAA produced the highest percentage of reads, giving a genomic context to tet(A) at a percentage comparable to other target ARGs in previous experiments. Due to this, we added the degenerate primer F-TAA to the degenerate primer pool. Our degenerate primer pool now contained M-TAA, M-TGA, F-TGA, and F-TAA.

Table 3.2. The degenerate primer F-TAA produced reads that provide a genomic context for *tet(A)* at high frequencies.

Degenerate primer	Reads mapping to ARG	Reads mapping to ARG + providing a genomic context
F-NNN	100	7 (7%)
F-ATG	38	2 (5%)
F-TAA	98	19 (20%)
F-TGA	143	5 (3%)
M-NNN	80	10 (13%)
M-ATG	110	8 (7%)
M-TAA	0	0 (0%)
M-TGA	57	3 (5%)

3.4 Developing an ARG primer pool

3.4.1 Testing individual degenerate primers with pooled ARG primers

In testing our degenerate primers, we developed a functional pool that works with individual ARG primers. These allowed successful amplification of genomic regions outside of the ARG and determination of genomic context (or, in our case, plasmid context). However, our goal is to develop a simple assay that allows rapid detection of multiple ARGs. The simplest assay should perform robustly in a single reaction. We first wanted to test how pooling ARG primers would work with individual degenerate primers to decide if pooling the degenerate primers was necessary in the first place.

We developed an ARG primer pool to target specific ARGs within the *E. coli* L3Cip3 genome. The target ARGs within this pool are *aph(3), aph(4), aph(6), bla-*$_{CTX}$*, bla-*$_{TEM}$*, dfrA14, erm(B), rmtB, sul2* and *tet(A)* (**Table 1.1**). Using the ONT rapid barcoding kit, we produced 294k reads and 3.02 Gbp, after sequencing for 3 hours and 10 minutes on a fresh flowcell. On average, 19,179 ± 6,025 reads mapping to all target ARGs, with 321 ± 122 reads, providing a genomic context. The degenerate primer M-ATG produced the most reads mapping to target ARGs and reads that provide a genomic context. Surprisingly, and in contrast to our previous results, this was only 2% and even lower for other target ARGs (**Table 3.3**).

Interestingly, from this experiment (**Supp. Table 6.11**), we sequenced significantly more reads than any previous runs, and the percentage of reads mapping to ARGs (i.e. the relative enrichment over non-specific binding and amplification of chromosomal regions) was also significantly higher (52%). This can be contrasted with the results above (section **3.1**), in which we found only 2.5% of reads mapped to target ARGs. We are uncertain why the relative enrichment levels varied so drastically, nor why this was inversely correlated with the fraction of reads providing genomic context.

Table 3.3. Testing individual degenerate primers with an ARG primer pool.

Degenerate primer	Reads mapping to target ARGs	Reads mapping to ARG + provides genomic context
F-NNN	22605	367 (1.7%)
F-TAA	21432	372 (1.7%)
F-ATG	9722	165 (1.7%)
F-TGA	20131	291 (1.4%)
M-NNN	18430	285 (1.6%)
M-TAA	21270	380 (1.8%)
M-ATG	28317	540 (2%)
M-TGA	11525	175 (1.5%)

3.4.2 Pooling of ARG primers results in amplification bias toward specific ARGs

There was successful amplification of each target ARG when the pooled ARG primers are paired with each degenerate primer singly (**Fig. 3.4**). However, we amplified several genes significantly more than others. Genes encoding resistance to beta-lactam antibiotics, *bla-$_{CTX}$* and *bla-$_{TEM}$*, were consistently enriched the most, except in tests with F-TAA or M-TAA as the degenerate primer. In these two cases, tet(A) and aph(6) had slightly more enrichment than *bla-$_{TEM}$*. However, across all tests, there was a clear pattern. We enriched bla-$_{CTX}$ to the highest extent, followed by *bla-$_{TEM}$, tet(A) or aph(6); then sul2, aph(3)* or *dfrA14*. The genes with the lowest enrichment were consistently *rmtB, erm(B)* and *aph(4)*. As each degenerate primer is binding to random regions within the genome, we would expect to see less of a trend between samples. We propose that this repeatable pattern of high or low ARG enrichment, independent of the degenerate primer, is due to a combination of (1) ARG copy number and accessibility (a function of both plasmid copy number and location on the plasmid); (2) the efficiency of binding of the primers within the ARG (at the first or second round of PCR, or both); (3) the specific context of the ARG (e.g. whether it is adjacent to an element that is highly repetitive within the genome, possibly causing secondary binding of the amplified products).

3.4.3 Amplification of specific ARGs is more likely to yield genomic context

There was also a trend when examining the individual ARGs and the fraction of reads providing a genomic context (i.e. extending more than 25 bp into the region adjacent to the ARG) (**Fig. 3.5**). We consistently produced reads that provided genomic context adjacent to the gene rmtB gene at high percentages, ranging from 11%-14%. This gene encodes 16S rRNA methyltransferase, which can alter the binding of aminoglycoside antibiotics, rendering them inactive. *rmtB* was the only targeted ARG present on the chromosome. For all other genes, the percentage of reads providing genomic (plasmid) context ranged from 0%-2.8%. This suggests that any combination of degenerate primers with the primers targeting rmtB can successfully amplify the region surrounding the *rmtB* gene. Again, we note that *rmtB* is the only chromosomal ARG that we targeted, which may provide some insight into why this ARG contrasted with others.

While the target ARGs *bla-$_{CTX}$, bla-$_{TEM}$* and *dfrA14* were amplified with the contextual adjacent regions relatively consistently across all degenerate and ARG primer combinations, this was not true for *aph(3), aph(4), tet(A)* and *sul2*. Only rarely did the amplification products for these ARGs provide a genomic context. Overall, these results suggest that there is a consistent bias in the likelihood of amplifying and sequencing adjacent genomic context. However, these results were obtained when relying on only a single degenerate primer. We thus next tested whether a dual-pool system would improve the situation: pooled degenerate primers and pooled ARG-targeting primers.

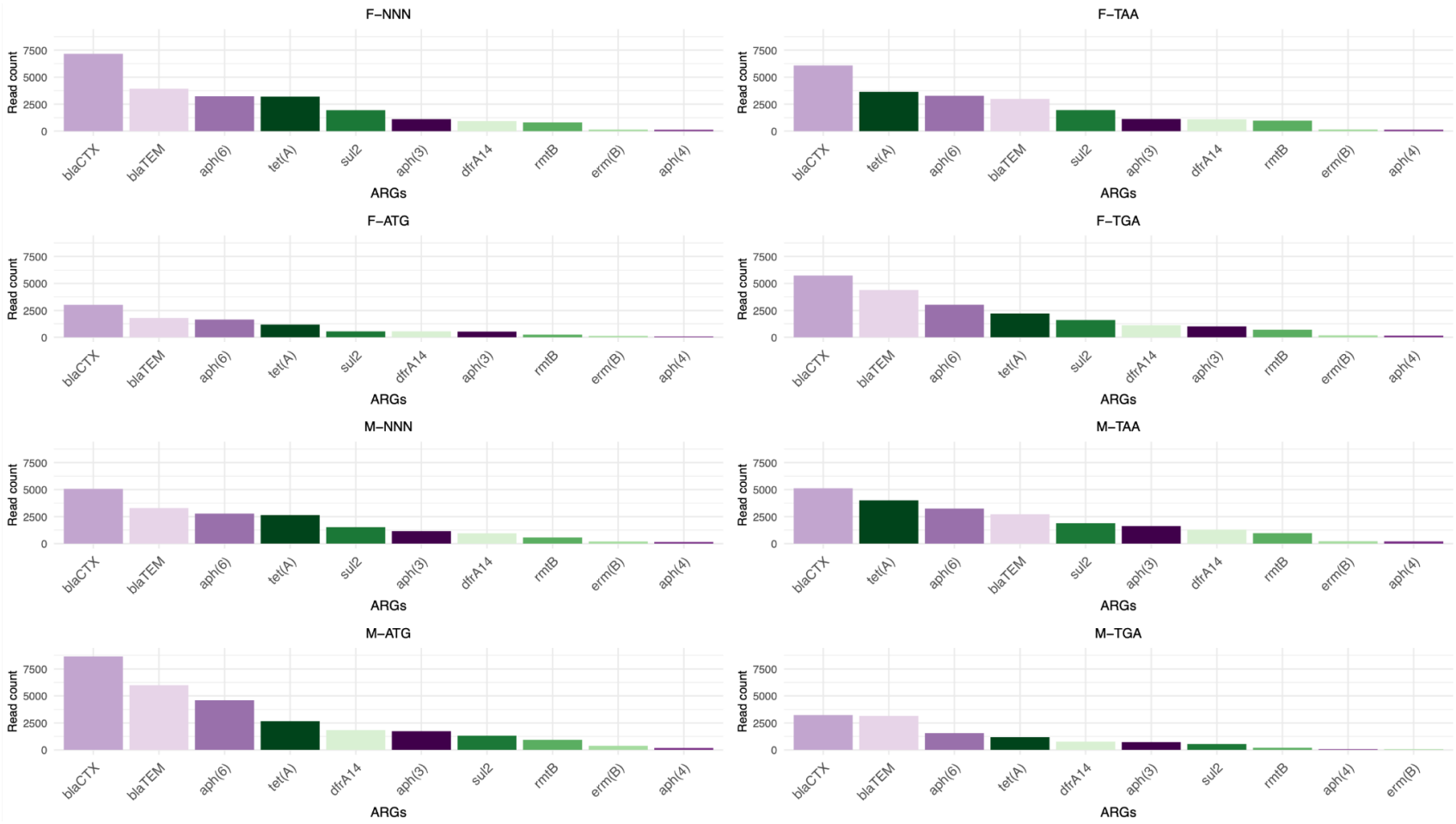

Figure 3.4. bla-$_{CTX}$ is consistently enriched the most regardless of the degenerate primer set. The nested PCR protocol was completed with each of eight different degenerate primers and the pooled ARG-specific primers. (*aph(3), aph(4), aph(6), bla-$_{CTX}$, bla-$_{TEM}$, dfrA14, erm(B), rmtB, sul2* and *tet(A)*). The reads were mapped to the *E. coli* L3Cip3 reference genome to find reads mapping to target ARGs. The total number of reads mapping to each ARG is indicated on the y-axis.

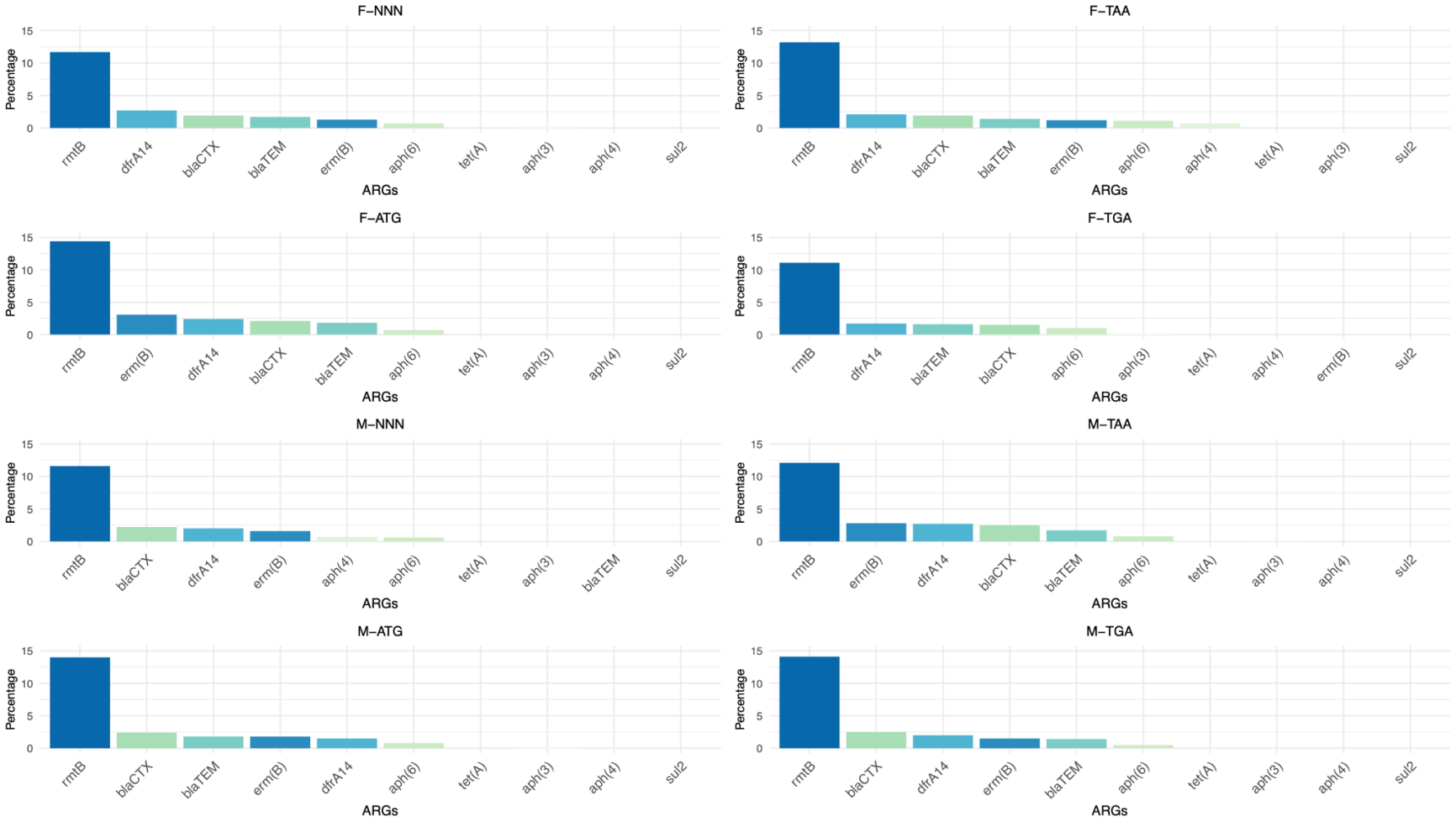

Figure 3.5. Reads mapping to rmtB consistently provide genomic context at higher percentages than other ARGs. The nested PCR protocol was completed with each of eight different degenerate primers and the pooled ARG-specific primers. (*aph(3), aph(4), aph(6), bla-$_{CTX}$, bla-$_{TEM}$, dfrA14, erm(B), rmtB, sul2* and *tet(A)*). The reads were mapped to the *E. coli* L3Cip3 reference genome and the Resfinder AMR database to find reads mapping to target ARGs and had more than 25 base pairs extending up or downstream from that gene to determine the genomic context. The percentage of reads providing such context is indicated on the y-axis. Each plot shows the result of one of the eight degenerate primers.

3.4.2 Combining the ARG primer pool with the degenerate primer pool

Testing individual degenerate primers with pooled ARG primers did not yield significant results in providing a genomic context for each targeted ARG, except in the case of rmtB. Therefore, we tested whether using a dual pooling strategy could improve the efficiency and robustness. We used the pooled ARG primers together with a pooled degenerate primer set containing M-TAA, M-TGA, F-TGA, and F-TAA. In the second round of N-PCR, we used the pooled interior ARG primers and the two constant primers that bound to the tails of the M (Manoil) and F (Freed) primers (**Table 2.3 & 2.4**). After PCR and library preparation, we sequenced the library on a single new MinION 9.4.1 flowcell with approximately 800 active pores for 1 hour (this number of pores is uncommonly low for a new flowcell). We generated 45k reads, totalling 19.4Mbp with an average length of 247 bp. However, in this experiment, we ran multiple samples from unrelated experiments using the rapid barcoding kit. For the barcode relevant to our experiment, we generated 4085 reads. 2081 of those reads mapped to the L3Cip3 genome, and 1092 reads (52%) mapped to ARGs within the L3Cip3 genome.

Using a dual-pool strategy (ARG primer pool and degenerate primer pool), we enriched all target ARGs and provided a genomic context for all at 10% or more, with an average of 38% across all ARGs (**Table 3.4**).

However, we again found that the total number of reads mapping to each target ARG differed substantially. More than 300 reads mapped to both *bla-*$_{CTX}$ and *bla-*$_{TEM}$, while far fewer mapped to *aph(6)* (36 reads), *dfrA14* (30 reads), *rmtB* (12 reads), and *tet(A)* (33 reads). This echoed previous results with the individual primers, in which *bla-*$_{TEM}$ and *bla-*$_{CTX}$ were consistently the most efficiently amplified. Surprisingly, this contrasted strongly with the results for the unpooled degenerate primers (above): In that case, only a small fraction of reads mapping to *bla-*$_{CTX}$ and *bla-*$_{TEM}$ also provided genomic context.

Table 3.4. Percentage of reads mapping to target ARGs while providing a genomic context.

ARG	Total reads mapping to ARG	Reads mapping to target ARG and provide genomic context
aph(3)	81 (7.42%)	39 (48%)
aph(4)	140 (12.83%)	40 (28.5%)
aph(6)	36 (3.30%)	14 (38%)
bla-$_{CTX}$	320 (29.33%)	139 (43%)
bla-$_{TEM}$	311 (28.51%)	125 (40%)
dfrA14	30 (2.75%)	7 (23%)
rmtB	12 (1.10%)	5 (41%)
sul2	94 (8.62%)	41 (43.6%)
tet(A)	33 (3.02%)	4 (12%)
Total	1092	414 (38%)

Chapter 4: Metagenomic Results

4.1 Metagenomic sequencing

Until this point, we had focussed on testing the pooled primer strategy on relatively pure DNA from a single isolate. We wanted to test how our N-PCR method would fare on a more complex and recalcitrant sample and, furthermore, compare its performance to standard metagenomic sequencing. To this end, we first obtained a set of faecal samples likely to contain a wide range of ARGs. These samples were collected on a number of farms across New Zealand (**Table 2.2**). We extracted DNA from these samples using two different protocols (**Methods section 2.2.1**) and sequenced all ten samples on a single PromethION P2 R10.4.1 flowcell (**Methods section 2.4.2**). This generated 3.95 million reads and 14.86 Gbp over 48 hours (**Table 4.1**). To identify the different classes of ARGs in each faecal sample, we mapped the reads from each barcoded sample against the Resfinder ARG database. 2517 reads mapped to at least one ARG, with 55 different ARGs across all 10 samples. While the fraction of reads mapping to each ARG differed between faecal samples, both methods of DNA isolation (Zymobiomics and Qiagen) exhibited somewhat concordant fractions (**Fig. 4.1).**

Of the ARGs found in the faecal samples, six were also contained within the ARG primer pools we had designed., Several were present at relatively high abundances in the metagenomic samples (**Fig. 4.1**). We found that sul2, a sulfonamide-resistant gene, was present in all samples except for 13 and 77 (for both the Zymo and Qiagen preps). Both *aph(3)* and *aph(6)*, aminoglycoside-resistance genes, were present in all samples except 13 (again, for both Zymo and Qiagen preps). *tet(A)*, a gene that encodes tetracycline resistance, was present in samples 10 and 4 (but only in the Qiagen prep for the latter case). *erm(B)* (MLS resistance) was detected in samples 13, 69, and 04 (but again, only for the sample 04 Qiagen prep). Finally, *bla-$_{TEM}$* (beta-lactam resistance), was detected in samples 04 and 10 (but only for the Zymo prep in the latter case). The presence of these ARGs across samples suggested that if our N-PCR was sufficiently robust, we should be able to enrich for *sul2, aph(3), aph(6), tetA(P), erm(B)* and *bla-$_{TEM}$*, while also providing a genomic (plasmid) context for each ARG.

Table 4.1. Sequence statistics for unfiltered reads from each faecal sample and prep method. Two extraction methods were used: Zymobiomics mini prep (zymo) or Qiagen Power soil (qiagen). N50: The sequence length of the shortest contig at 50% of the total assembly length (Thrash et al., 2020). Q1, Q2, and Q3 indicate the length of sequences (in bp) at the 25th, 50th, and 75th quartile Q20(%) is the percentage of bases with a quality score (phred score) greater than 20. Q30 is the(percentage of bases with a quality score greater than 30. Sequencing statistics were produced using seqkit stats (Shen et al., 2016).

Sample	N50	Total number	Max length (bp)	Q1	Q2	Q3	Q20(%)	Q30(%)
04-zymo	3,954	32,895	337,367	175	314	1,017	64.91	41.46
04-qiagen	2,823	262,612	218,631	166	265	696	63.35	39.86
10-zymo	4,645	110,446	627,640	208	415	1,386	63.6	40.36
10-qiagen	2,115	259,680	336,195	190	323	814	62.48	38.26
77-zymo	3,711	768,078	361,368	186	368	1,326	63.79	40.12
77-qiagen	2,124	332,202	155,194	182	277	606	62.74	39.1
13-zymo	3,452	82,823	75,816	217	393	1,029	63.68	40.26
13-qiagen	2,199	162,165	705,801	177	366	945	63.41	40.02
69-zymo	4,568	301,582	151,726	236	482	1,663	65.07	41.6
69-qiagen	3,458	169,546	436,593	190	337	1,005	62.76	39.38

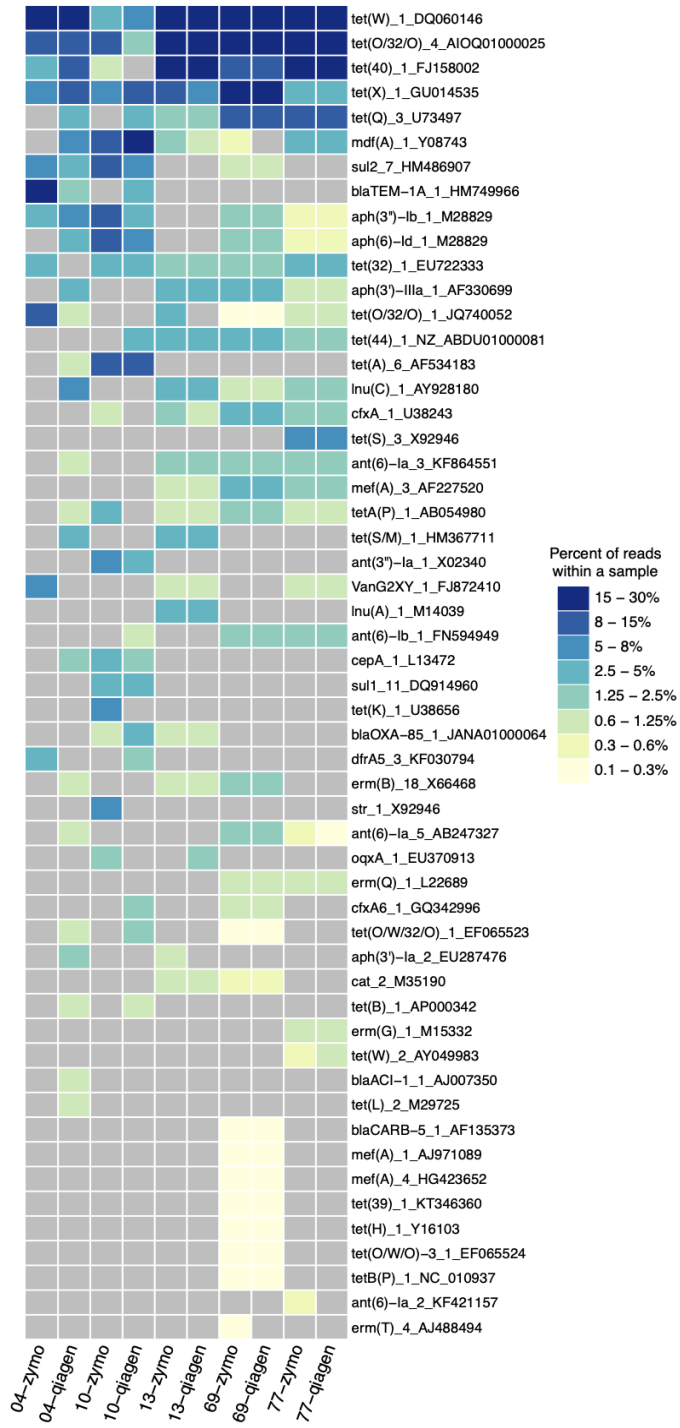

Figure 4.1. ARGs encoding resistance to tetracycline are the most abundant across all metagenomic samples. DNA was extracted using Zymobiomics miniprep kit (zymo) or Qiagen DNeasy Powersoil kit (qiagen). Grey is showing that no ARGs were deterred in that sample. Samples were sequenced using the RBK114.96 rapid barcoding kit on an R10.4.1 P2 flowcell. Samples were basecalled and demultiplexed using Guppy, and reads were mapped to the Resfinder AMR database with minimap2.

We found a high abundance of tetracycline resistance genes within each sample, with all five of the most abundant ARGs (averaged across samples) involved in tetracycline resistance (**Figure 4.1**): *tet(W)DQ060146, tet(O/32/O)AIOQ01000025, tet(40)FJ158002 and tet(X)GU014535, tet(Q)U73497* were consistently high abundance across all samples. Of the 55 ARGs that we detected, a total of 18 (32%) provided resistance to tetracycline; the next most common ARG category was aminoglycoside resistance, with 9 (16%) ARGs providing resistance, followed by macrolide resistance (**Figure 4.2**).

4.2 Difference between extraction methods

We extracted DNA using two different methods, Zymobiomics DNA miniprep and Qiagen DNeasy Powersoil kit (**Methods section 2.2.1**) to determine if there was a difference in the profile and diversity of resistance genes discovered with each method. **Table 4.1** shows the difference in sequence data produced from each sample. The average number of sequences from the Zymobiomics was 259,165, and the average from the Qiagen samples was 237,241. The data produced from the Qiagen samples was more consistent regarding the number of sequences, although there was no strong pattern. However, the sequence lengths produced by the Zymobiomics preps were, on average, considerably longer, with Zymobiomics N50 and Q3 lengths being, on average, 65% and 62% longer, respectively, than the paired Qiagen samples. In addition, the Zymobiomics samples resulted in slightly higher quality reads, an average of 3.7% more Q30 bases compared to Qiagen.

A total of 1,147 reads from the Zymobiomics preps mapped to an ARG, and Qiagen samples produced 1,196 total reads mapped to an ARG. At first glance, sample 04 exhibited very different resistance profiles between the two extraction types: the Zymo prep had reads mapping to 11 different ARGs, whereas the Qiagen prep had reads mapping to 25 different ARGs. However, this is at least partly explained by the differences in read numbers: the Zymo prep produced a total of 32,895 reads, whereas the Qiagen prep produced 262,612 reads, a difference of almost eight-fold. The other samples exhibited similar fractions of reads mapping to each ARG, with the exception of one or two genes.

Interestingly, the number of reads mapping to tetracycline-resistance genes from Zymobiomics samples was significantly higher compared to Qiagen samples: 1,203 compared to 596, respectively, despite very similar overall read numbers (1.3 million versus 1.19 million, respectively). This suggests a possible bias toward specific ARG types between these two extraction methods. This could occur, for example, if tetracycline genes are more common on large plasmids, and the Zymobiomics kit enriches to a greater extent for large plasmids.

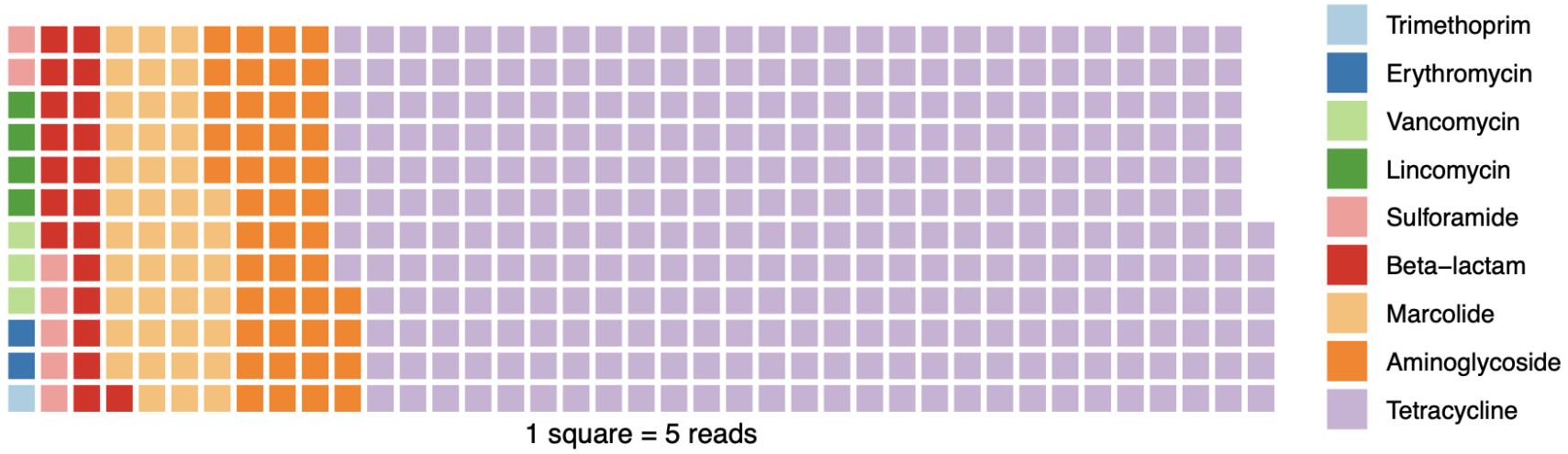

Figure 4.2. Tetracycline resistance is the most abundant within metagenomic samples. All reads from each sample 04-zymo, 10-zymo, 13-zymo, 69-zymo, 77-zymo, 04-qiagen, 10-qiagen, 13-qiagen, 69-qiagen and 77-qiagen) were grouped to find which group of antibiotics was most abundant. DNA was extracted using two methods: Zymobiomics miniprep kit (zymo) or Qiagen DNeasy Powersoil kit (qiagen). Samples were sequenced using the RBK114.96 rapid barcoding kit on an R10.4.1 P2 flowcell. Samples were basecalled and demultiplexed using Guppy, and reads were mapped to the Resfinder AMR database with minimap2.

4.3 Application of the N-PCR protocol on faecal samples (L3Cip3 enriched)

During metagenomic sequencing, we detected six genes that could be enriched, described in section **4.1**. We applied our N-PCR protocol to the faecal samples to compare to the metagenomic sequence data. We first tested whether the N-PCR method could enrich for ARGs (and adjacent genomic context) in a more complex, recalcitrant faecal sample compared to pure gDNA from a cultured isolate. To this end, we spiked 1µL of *E. coli* L3Cip3 DNA to 9µL of 04-zymo DNA and completed our N-PCR protocol. We sequenced the PCR products on a used R9.4.1 flowcell with 500 active pores using the RBK004 rapid barcoding kit, producing 28.29 K reads, 353 Mbp, and an N50 of 564 in 1.5 hours. We mapped the reads to the Resfinder AMR database and filtered the reads only to include reads with a mapping quality above 20. We found that 5% (1488) of reads mapped to our target ARGs and 50% (750) of those reads provided a genomic context.

These results showed we can successfully enrich ARGs from a complex faecal sample (**Table 4.2**). We produced numerous reads that provide a genomic context for *aph(3), aph(6), bla-$_{CTX}$, bla-$_{TEM}$*, and *sul2*. We amplified *bla-$_{TEM}$* at a high level, consistent with our single isolate L3Cip3 experiments.

Table 4.2. Percentage of reads mapping to target ARGs that provide a genomic context in a metagenomic sample spiked with E. coli L3Cip3.

ARG	Total reads mapping to ARGs	Reads mapping to ARG + Providing genomic context
aph(3)	312 (20%)	161 (53%)
aph(4)	6 (0.4%)	1 (17%)
aph(6)	292 (18%)	161 (55%)
bla-$_{CTX}$	107 (7%)	40 (37%)
bla-$_{TEM}$	421 (28%)	205 (48%)
dfrA14	11 (0.7%)	3 (27%)
sul2	316 (21%)	167 (53%)
tet(A)	15 (1%)	4 (27%)
Total	1488	750 (50%)

4.4 Application of N-PCR protocol on pure faecal samples

Having tested the performance of the N-PCR protocol on complex samples spiked with known DNA, we next tested the performance on the DNA from the faecal samples. We used the RBK114 rapid sequencing kit on a used R10.4.1 flowcell with approximately 2000 active pores using the P2 solo device. We produced 67.15k reads and 110.67 Mbp, with an N50 of 336 bp in 30 minutes of sequencing. Across all samples, an average of 2,848 reads mapped to ARGs, we compared these results to the results from metagenomic sequencing. We found that N-PCR enrichment increased target frequency by 15 to 1000-fold compared to metagenomic sequencing (**Table 4.3**). PCR-enriched samples had an average of 1% reads mapping to target ARGs, whereas all metagenomic samples had an average of only 0.0086% reads mapping to target ARGs. These findings suggest that PCR enrichment could be a more effective method for detecting target ARGs, even in complex samples. Furthermore, the N-PCR method provides a way of establishing the genomic (or plasmid) context of ARGs without the effort required (both in terms of reagent cost and compute cost) required by metagenomic sequencing.

Comparing the DNA extraction methods regarding fold-increase, no method outperformed the other across all samples, and the difference between all samples is likely to be the nature of the samples themselves. For samples 04-zymo, 77-zymo, 04-qiagen, 10-qiagen, 77-qiagen and 69-qiagen, we enriched aph(6) more compared to all other ARGs Interestingly, we did not observe more significant enrichment of *bla-*$_{TEM}$, present in samples 04-zymo, 04-qiagen and 10-zymo. This is most likely due to this ARG not being present at high levels in the metagenomic samples (further evidenced by the metagenomic sequencing (**Figure 4.1**). The most significant enrichment we found was for *sul2*, a gene that encodes sulfonamide resistance, in sample 04-zymo. Interestingly, *sul2* was not enriched to this extent in other faecal samples for which metagenomic sequencing indicated its presence. It is unclear as to why, although there are a wide range of possible explanations. Critically, our N-PCR method enriches ARGs not within the pure metagenomic sequence results, notably *sul2* in sample 77-qiagen and *dfrA14* in sample 04-qiagen (**Figure 4.3**), although both to a minimal extent. This indicates that the metagenomic sequencing did not detect several ARGs within the sample.

Table 4.3.Comparison of metagenomic sequencing and PCR-targeted sequencing.

Sample	Number of metagenomic reads mapping to target ARGs (%)	Number of reads mapping to target ARG loci (PCR enriched)	Fold-increase
04-zymo	10 (0.024%)	81 (3%)	124
04-qiagen	21 (0.0082%)	35 (1.7%)	206
10-zymo	42 (0.025%)	21 (0.4%)	15
10-qiagen	6 (0.0025%)	30 (0.4%)	159
77-zymo	12 (0.0008%)	24 (0.8%)	1000
77-qiagen	6 (0.0021%)	25 (1.5%)	713
13-zymo	0(0%)	0 (0%)	NA
13-qiagen	0 (0%)	0 (0%)	NA
69-zymo	16 (0.0032%)	12 (0.5%)	155
69-qiagen	16 (0.0078%)	26 (2.4%)	306

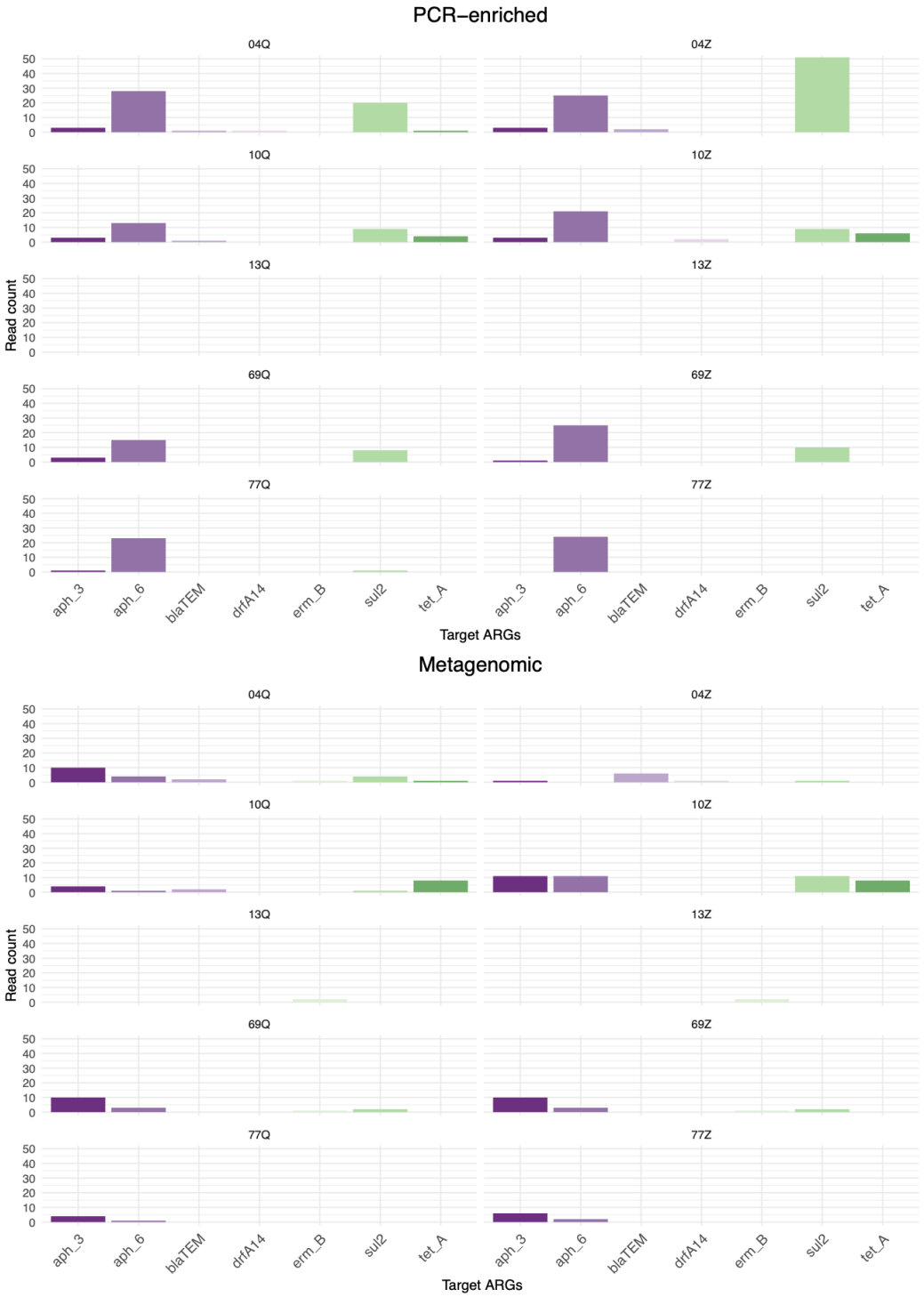

Figure 4.3. Comparison of PCR-enriched samples to metagenomic sequencing. PCR-enriched samples were amplified using an N-PCR protocol with degenerate and ARG primer pool, targeting the ARGs *aph(3), aph(4), aph(6), bla-$_{CTX}$, bla-$_{TEM}$, dfrA14, erm(B), rmtB, sul2* and *tet(A)*. Metagenomic DNA was extracted using two methods, Zymobiomics miniprep kit (Z) or Qiagen DNeasy Powersoil kit (Q). Samples, PCR-enriched and metagenomic, were sequenced using the RBK114.96 rapid barcoding kit on an R10.4.1 P2 flowcell. Samples were basecalled and demultiplexed using Guppy, and reads were mapped to the Resfinder AMR database with minimap2.

4.5 Genomic context in metagenomic samples

To differentiate our method from other molecular methods that use ONT as a sequencing platform, including qPCR and CRISPR, we aimed to provide a genomic context to each of our target ARGs using degenerate primers. Degenerate primers can anneal to random regions within the genome and extend those regions, producing a template to have both part of the target ARG and downstream region of either the chromosome or plasmid, allowing us to determine where in the genome it resides (Principle outlined in **Fig. 2.1**). We have shown that we can enrich target ARGs with our ARG primer pool and provide a genomic context for each in a single strain sample (**Table 3.4 & Fig. 3.4**) and a metagenomic sample enriched with *E. coli* (**Table 4.3**). Our sequencing run outlined in section **4.4** provided a genomic context for some of the target ARGs in the pure metagenomic samples (**Table 4.4**) at comparable percentages to our single-strain tests (**Table 3.4**). Although the number of reads is substantially lower compared to our single strain test, we note that for this experiment, sequencing occurred for only 30 minutes on a used flowcell (67 thousand reads total). The additional depth created by additional sequencing effort – easily ten- or even 100-fold more reads) should easily make up for this decreased read number. However, when analysing the individual genes (**Fig 4.4**) we are consistently amplifying *aph(6)* significantly more than all other target ARGs, suggesting that our primer pool day have a bias towards *aph(6)* and may need to trial a lower concentration of the *aph(6)* primer.

Table 4.4. Genomic context of PCR-enriched metagenomic samples.

Sample	Reads mapping to target ARG	Reads providing genomic context
04-zymo	81 (26%)	26 (32%)
10-zymo	41 (13%)	8 (19%)
77-zymo	24 (8%)	4 (16%)
13-zymo	0 (NA)	0 (NA)
69-zymo	36 (11%)	7 (19%)
04-qiagen	54 (17%)	10 (18%)
10-qiagen	30 (9%)	6 (20%)
77-qiagen	25 (8%)	12 (48%)
13-qiagen	0 (NA)	0 (NA)
69-qiagen	26 (8%)	11 (42%)
total	317	84 (26%)

Figure 4.4. Genomic context for aph(6) is consistently high across all samples. PCR-enriched samples were amplified using a N-PCR protocol with a degenerate and ARG primer pool, targeting the ARGs *aph(3), aph(4), aph(6), bla-$_{CTX}$, bla-$_{TEM}$, dfrA14, erm(B), rmtB*, sul2 and *tet(A)*.Metagenomic DNA was extracted using two methods, Zymobiomics miniprep kit (Z) or Qiagen DNeasy Powersoil kit (Q). Samples were sequenced using the RBK114.96 rapid barcoding kit on an R10.4.1 P2 flowcell. Samples were basecalled and demultiplexed using Guppy, and reads were mapped to the Resfinder AMR database with minimap2. The genomic context was determined by cross-referencing reads mapping to the metagenomic samples and the ResFinder AMR database to find reads with nucleotides extended 25bps or more up or downstream of target ARGs. The percentage was calculated by dividing the number of reads proving a genomic context by the number of reads mapping to the target ARG.

Chapter 5: Discussion

5.1 Genomic context

PCR paired with ONT effectively profiles ARGs in single-strain colonies (Zhang et al., 2021 & Zhao et al., 2022). Here, we have further increased the power of PCR paired with ONT sequencing by developing a method that implements a novel multiplexed nested PCR protocol to increase sensitivity to target ARGs compared to metagenomic sequencing. We can also determine the genomic context of each target ARG using degenerate primers. This provides information on the specific locations and arrangements, either chromosomal or plasmid bound, of these genes within the genome. This method could, in future developments, also determine the regulation of these genes (Botas et al., 2022) by understanding the flanking regions down and upstream of ARGs, as these regions could be part of MGEs transferred through HGT. Very recent research from Shaw & Neher (2023, preprint) shows that understanding the flanking regions of MGEs can help understand the structural diversity around MGEs. We could also use the extended region from target ARGs to identify the species of bacteria in a sample. However, 25 bp is likely to be a lower limit for accurate species determination to achieve this. Our method is also appealing from a temporal perspective: We have developed a method to detect ARGs in single-strain bacteria and metagenomic samples while providing a genomic context within 5-6 hours (**Fig. 2.3**).

5.2 Rapidly detecting ARGs in single colonies

We first tested our method on *E. coli* L3Cip3, a highly AMR strain with nine different ARGs, both chromosomal and plasmid bound (**Table 2.1**). We have shown that we can enrich all ARG targets within five hours using our method (**Fig 2.3**). Moreover, we were able to provide a genomic context for each target at an average frequency of 38%, demonstrating that this method is efficient for the use on single-strains. The primers designed for this protocol (**Supp. Table 6.1**) can easily be interchanged to target ARGs in different strains of *E. coli* or different species of bacteria, and with additional combinatorial experimentation, it is likely that the degenerate primer sets could be improved, either for efficiency of amplification or to optimise amplification of adjacent genomic or plasmid sequence. One area that we left relatively untested was the optimisation of DNA purification steps to increase the fraction of long molecule fragments that we sequenced; such fragments are much more likely to provide genomic context, and enrichment of long molecules can be relatively simple and fast, for example using bead purification.

5.3 Rapid detection of ARGs in metagenomic samples

Finally, we have demonstrated that enriching target ARGs in metagenomic samples with our novel N-PCR protocol is possible. We compared our method to our metagenomic sequencing and found we could enrich target ARGs up to 1000-fold (**Table 4.3**) while remaining able to determine the genomic context of target ARGs (**Table 4.4 & Fig. 4.4**). In our metagenomic analysis of samples from farms across New Zealand, we found a very high abundance of genes that encode resistance to tetracycline. This interesting result provides fodder for future research but is not entirely unexpected. Pattis et al. (2022) noted that tetracycline resistance is highly prevalent in New Zealand for cattle veterinary use. Moreover, tetracycline resistance is highly prevalent in clinical settings (Gasparrini et al., 2020).

During our single-strain tests, we attempted to increase the amplification and the frequency of reads that provide a genomic context for *tet(A).* We had some success in our single strain tests; however, in applying our method to metagenomic samples, we did not enrich this gene to high levels or could not provide a genomic context within any samples. Applying this method to a metagenomic sample has several limitations. We can only enrich target ARGs within our ARG primer pool, limiting its power to detect full resistant profiles of the bacteria within the samples. However, we did not test the full extent to which this protocol can be multiplexed, and there are a number of highly multiplexed PCR protocols that have been successfully employed (even in relatively complex metagenomic samples) (Khodakov et al., 2021, Li et al., 2022 & Xie et al., 2022).

5.4 An active tool to profile ARGs in bacteria

When designing a diagnostic test, the World Health Organization recommends that a method/test should be ASSURED: affordable, sensitive, specific, easy to use, without large equipment and delivered to the user (Kosack et al., 2017). Our N-PCR method is affordable due to the number of times each MinION or P2 flowcell can be reused. It is sensitive and specific due to using a novel N-PCR protocol. The relative simplicity of this method is clear: only PCR and nanopore sequencing training is needed. The biggest hurdle may be a thermocycler. Despite this, this method offers a reasonable compromise between accessibility and accuracy, such that it could effectively address New Zealand's antimicrobial resistance action plan released in 2017. Under objective two of their proposed plan, they want to increase surveillance and research to develop a list of crucial resistance genes and antimicrobials for national reporting (Ministry of Health and Ministry for Primary Industries, 2017).

5.5 Oxford nanopore as a cheap and reliable sequencing platform

This work firmly establishes the relative economy of the ONT platform compared to other sequencing platforms when flowcells are washed and reused (Beckley et al., 2023). We were often able to wash and reuse flowcells up to 10 times while still collecting more than sufficient data for our assays. For example, we found that 50-100 Mbp provided more than enough data to detect and profile target ARGs while providing genomic context in single colonies. This highlights the ability of the ONT platform to be reusable and cost-efficient, making this method accessible to institutes with low funding. To decrease the time to complete this protocol further, we tested the capabilities of the PromethION R10.4.1 flowcell. We found we could produce enough data to detect and profile target ARGs while providing genomic context to each within 30 minutes and have an estimated 30 uses when washing between sequencing runs. Currently, Promethion flowcells are cheaper than MinION flowcells (USD 900 for MinION; USD 3450 for a 4-pack of PromethION, and cost decreases as more flowcells are purchased). As for hardware, the MinION cost is USD 1000, and the P2 solo cost is USD 10,455. We did not analyse the exact cost per run, but this does give insight into the cost of using ONT as a sequencing platform. As the P2 platform becomes more available to other researchers, we expect that the additional sequencing capability will result in entirely new workflows dedicated to flowcell reuse, for example, by adding barcodes to each run to ensure no crosstalk between runs from re-used flowcells. Finally, compared to other NGS platforms, such as Illumina or PacBio, ONT has the advantage that the sample does not need to be sent away to be sequenced (Beckley et al., 2023 & Stevens et al., 2023).

5.6 Limitations

Our method has several advantages over other molecular methods: it is sensitive, rapid and highly accessible to users. However, it also has several limitations. As we are using degenerate primers that anneal to random regions of a genome, there is little guarantee that there will be amplification of a region of the genome down or upstream from the target ARG, therefore not providing any genomic context. This problem is evident in **Figure 4.4,** as the genomic context was found for ARGs only when a relatively high number of reads mapped to target ARGs. Our method is also limited in detecting novel ARGs as we design primers that will anneal to known ARGs. An essential factor to consider when comparing methods to detect, profile or find new ARGs is the question being asked. Is sensitivity or specificity more important to the research at hand?

5.7 Conclusion and future perspectives.

Antibiotic resistance is a significant burden for society, and its spread through healthcare, agriculture and environment-related paths is cause for concern. Many bacteria are now multidrug-resistant, with some strains resistant to nearly all commercially available antibiotics. Efficient methods that can rapidly and accurately profile multiple antibiotic resistance genes in bacteria are crucial to understanding resistance profiles of environments. Further, a method that can rapidly detect multiple resistance genes within highly pathogenic bacteria in clinical settings is vital to reducing the time to prescribe an effective therapy. Here, we have shown we can enrich target ARGs within a single-strain *E. coli* and within faecal samples that have target ARGs corresponding to our optimised ARG primer pool with a novel N-PCR protocol paired with Oxford Nanopore Technology. In future work, we will develop larger primer pools to target substantially more resistance genes in metagenomic samples and use the extended region of those flanking regions to identify bacteria down to the species level.

References

Abbo, A., Carmeli, Y., Navon-Venezia, S., Siegman-Igra, Y. & Schwaber, M. J. (2007). Impact of multi-drug resistant *Acinetobacter baumannii* on clinical outcomes. *European Journal of Clinical Microbiology & Infectious Diseases.* 26, 793-800. https://doi.org/10.1007/s10096-007-0371-8

Adekanmbi, A. O., Adejoba, A. T., Banjo, O. A., & Saki, M. (2020). Detection of sul1 and sul2 genes in sulfonamide-resistant bacteria (SRB) from sewage, aquaculture sources, animal wastes and hospital wastewater in South-West Nigeria. *Gene Reports*, *20*, 100742. https://doi.org/10.1016/j.genrep.2020.100742

Agyeman, W. Y., Bisht, A., Gopinath, A., Cheema, A. H., Chaludiya, K., Khalid, M., Nwosu, M., Konka, S., & Khan, S. (2022). A Systematic Review of Antibiotic Resistance Trends and Treatment Options for Hospital-Acquired Multidrug-Resistant Infections. *Cureus*, *14*(10). https://doi.org/10.7759/cureus.29956

Ahmad, M., & Khan, A. U. (2019). Global economic impact of antibiotic resistance: A review. *Journal of Global Antimicrobial Resistance*, *19*, 313-316. https://doi.org/10.1016/j.jgar.2019.05.024

Amarasinghe, S.L., Su, S., Dong, X., Zappia, L., Ritchie, M. E. & Gouil, Q. (2020). Opportunities and challenges in long-read sequencing data analysis. *Genome Biology, 21*(30). https://doi.org/10.1186/s13059-020-1935-5

Antimicrobial resistance collaborators. (2022). Global burden of bacterial antimicrobial resistance in 2019: a systematic analysis. *The Lancet. 399(10325)*, 629-655. DOI: https://doi.org/10.1016/S0140-6736(21)02724-0

Årdal, C., Outterson, K., Hoffman, S. J., Ghafur, A., Sharland, M., Ranganathan, N., Smith, R., Zorzet, A., Cohn, J., Pittet, D., Daulaire, N., Morel, C., Rizvi, Z., Balasegaram, M., Dar, O. A., Heymann, D. L., Holmes, A. H., Moore, L. S. P., Laxminarayan, R., Mendelssohn, D. L. & Røttingen, J. (2016). International cooperation to improve access to and sustain effectiveness of antimicrobials. *The Lancet*, *387*(10015), 296-307. https://doi.org/10.1016/S0140-6736(15)00470-5

Ashton, P. M., Nair, S., Dallman, T., Rubino, S., Rabsch, W., Mwaigwisya, S., & Wain, J. (2015). MinION nanopore sequencing identifies the position and structure of a bacterial antibiotic resistance island. *Nature Biotechnology*, *33*(3), 296-300. https://doi.org/10.1038/nbt.3103

Aslam, B., Khurshid, M., Arshad, M. I., Muzammil, S., Rasool, M., Yasmeen, N., Shah, T., Chaudhry, T. H., Rasool, M. H., Shahid, A., Xueshan, X., & Baloch, Z. (2021). Antibiotic Resistance: One Health One World Outlook. *Frontiers in Cellular and Infection Microbiology*, *11*, 771510. https://doi.org/10.3389/fcimb.2021.771510

Aminov, R. I. (2010). A Brief History of the Antibiotic Era: Lessons Learned and Challenges for the Future. *Frontiers in Microbiology*, *1*, 8040. https://doi.org/10.3389/fmicb.2010.00134

Ayukekbong, J.A., Ntemgwa, M. & Atabe, A.N. (2017) The threat of antimicrobial resistance in developing countries: causes and control strategies. *Antimicrobial Resistance & Infection Control*, *6*(47) https://doi.org/10.1186/s13756-017-0208-x

Bassetti, M., & Garau, J. (2021). Current and future perspectives in the treatment of multidrug-resistant Gram-negative infections. *Journal of Antimicrobial Chemotherapy*, *76*(Supplement_4), iv23-iv37. https://doi.org/10.1093/jac/dkab352

Beckley, L. E., Olivar, M. P., & Jeffs, A. G. (2023). Nanopore short-read sequencing: A quick, cost-effective and accurate method for DNA metabarcoding. *Environmental DNA*, *5*(2), 282-296. https://doi.org/10.1002/edn3.374

Berendonk, T. U., Manaia, C. M., Merlin, C., Cytryn, E., Walsh, F., Bürgmann, H., Sørum, H., Norström, M., Pons, M., Kreuzinger, N., Huovinen, P., Stefani, S., Schwartz, T., Kisand, V., Baquero, F., & Martinez, J. L. (2015). Tackling antibiotic resistance: The environmental framework. *Nature Reviews Microbiology*, *13*(5), 310-317. https://doi.org/10.1038/nrmicro3439

Botas, J., Giner-Lamia, J., & Huerta-Cepas, J. (2022). GeCoViz: Genomic context visualisation of prokaryotic genes from a functional and evolutionary perspective. *Nucleic Acids Research*, *50*(W1), W352. https://doi.org/10.1093/nar/gkac367

Brolund, A., Sundqvist, M., Kahlmeter, G., & Grape, M. (2010). Molecular Characterisation of Trimethoprim Resistance in Escherichia coli and Klebsiella pneumoniae during a Two Year Intervention on Trimethoprim Use. *PLoS ONE*, *5*(2). https://doi.org/10.1371/journal.pone.0009233

Bull, R. A., Adikari, T. N., Ferguson, J. M., Hammond, J. M., Stevanovski, I., Beukers, A. G., Naing, Z., Yeang, M., Verich, A., Gamaarachchi, H., Kim, K. W., Luciani, F., Eden, J., Rawlinson, W. D., van Hal, S. J., & Deveson, I. W. (2020). Analytical validity of nanopore sequencing for rapid SARS-CoV-2 genome analysis. *Nature Communications*, *11*(1), 1-8. https://doi.org/10.1038/s41467-020-20075-6

Burcham, Z. M., Schmidt, C. J., Pechal, J. L., Brooks, C. P., Rosch, J. W., Benbow, M. E., & Jordan, H. R. (2019). Detection of critical antibiotic resistance genes through routine microbiome surveillance. *PLOS ONE*, *14*(3), e0213280. https://doi.org/10.1371/journal.pone.0213280

Cadena, M., Durso, L. M., Miller, D. N., Waldrip, H. M., Castleberry, B. L., Drijber, R. A., & Wortmann, C. (2018). Tetracycline and Sulfonamide Antibiotic Resistance Genes in Soils From Nebraska Organic Farming Operations. *Frontiers in Microbiology*, *9*, 371278. https://doi.org/10.3389/fmicb.2018.01283

Canton, R., Maria, J., & Galán, J. C. (2012). CTX-M Enzymes: Origin and Diffusion. *Frontiers in Microbiology*, *3*. https://doi.org/10.3389/fmicb.2012.00110
Cao, B., Wang, H., Sun, H., Zhu, Y., & Chen, M. (2004). Risk factors and clinical outcomes of nosocomial multi-drug resistant Pseudomonas aeruginosa infections. *Journal of Hospital Infection*, *57*(2), 112-118. https://doi.org/10.1016/j.jhin.2004.03.021

Carattoli, A. (2013). Plasmids and the spread of resistance. *International Journal of Medical Microbiology*, *303*(6-7), 298-304. https://doi.org/10.1016/j.ijmm.2013.02.001

Cassini, A., Högberg, L. D., Plachouras, D., Quattrocchi, A., Hoxha, A., Simonsen, G. S., Colomb-Cotinat, M., Kretzschmar, M. E., Devleesschauwer, B., Cecchini, M., Ouakrim, D. A., Oliveira, T. C., Struelens, M. J., Suetens, C., & Monnet, D. L. (2018). Attributable deaths and disability-adjusted life-years caused by infections with antibiotic-resistant bacteria in the EU and

the European Economic Area in 2015: A population-level modelling analysis. *The Lancet Infectious Diseases*, *19*(1), 56-66. https://doi.org/10.1016/S1473-3099(18)30605-4

Centers for Disease Control and Prevention. (2019). Antibiotic resistance threats in the United States, 2019. Retrieved from https://www.cdc.gov/drugresistance/pdf/threats-report/2019-ar-threats-report-508.pdf

Cheng, W., Chen, H., Su, C. & Yan, S. (2013). Abundance and persistence of antibiotic resistance genes in livestock farms: A comprehensive investigation in eastern China. *Environmental International, 61*, 1-7. DOI: https://doi.org/10.1016/j.envint.2013.08.023

Chopra, I., & Roberts, M. (2001). Tetracycline Antibiotics: Mode of Action, Applications, Molecular Biology, and Epidemiology of Bacterial Resistance. *Microbiology and Molecular Biology Reviews*, *65*(2), 232-260. https://doi.org/10.1128/MMBR.65.2.232-260.2001

Dadgostar, P. (2019). Antimicrobial resistance: Implications and cost. *Infection and Drug Resistance, 12*, 3903-3910. DOI: 10.2147/IDR.S234610

Dancer, S. J. (2014). Controlling Hospital-Acquired Infection: Focus on the Role of the Environment and New Technologies for Decontamination. *Clinical Microbiology Reviews*, *27*(4), 665-690. https://doi.org/10.1128/CMR.00020-14

De, R. Metagenomics: aid to combat antimicrobial resistance in diarrhea. (2019). *Gut Pathogens, 11*, 47. https://doi.org/10.1186/s13099-019-0331-8

Dellinger, R. P., Levy, M. M., Rhodes, A., Annane, D., Gerlach, H., Opal, S. M., Sevransky, J. E., Sprung, C. L., Douglas, I. S., Jaeschke, R., Osborn, T. M., Nunnally, M. E., Townsend, S. R., Reinhart, K., Kleinpell, R. M., Angus, D. C., Deutschman, C. S., Machado, F. R., Rubenfeld, G. D., Webb, S. A., … Surviving Sepsis Campaign Guidelines Committee including the Pediatric Subgroup (2013). Surviving sepsis campaign: international guidelines for management of severe sepsis and septic shock: 2012. *Critical care medicine*, *41*(2), 580–637. https://doi.org/10.1097/CCM.0b013e31827e83af

Dhingra, S., Rahman, N. A. A., Peile, E., Rahman, M., Sartelli, M., Hassali, M. A., Islam, T., Islam, S. & Haque, M. (2020). Microbial resistance movements: An overview of global public health threats posed by antimicrobial resistance, and how best to counter. *Frontiers in Public Health, 8*(535668). DOI: 10.3389/fpubh.2020.535668

Diao, Z., Han, D., Zhang, R., & Li, J. (2022). Metagenomics next-generation sequencing tests take the stage in the diagnosis of lower respiratory tract infections. *Journal of Advanced Research*, *38*, 201-212. https://doi.org/10.1016/j.jare.2021.09.012

Doi, Y., & Arakawa, Y. (2016). Aminoglycoside Resistance: The Emergence of Acquired 16S Ribosomal RNA Methyltransferases. *Infectious Disease Clinics of North America*, *30*(2), 523. https://doi.org/10.1016/j.idc.2016.02.011

Eliopoulos, G. M., Cosgrove, S. E., & Carmeli, Y. (2003). The Impact of Antimicrobial Resistance on Health and Economic Outcomes. *Clinical Infectious Diseases*, *36*(11), 1433-1437. https://doi.org/10.1086/375081

Ferreira, C., Otani, S., Aarestrup, F. M., & Manaia, C. M. (2023). Quantitative PCR versus metagenomics for monitoring antibiotic resistance genes: Balancing high sensitivity and broad coverage. *FEMS Microbes*, *4*. https://doi.org/10.1093/femsmc/xtad008

Fierke, C. A., Johnson, K. A., & Benkovic, S. J. (1987). Construction and evaluation of the kinetic scheme associated with dihydrofolate reductase from Escherichia coli. *Biochemistry*, *26*(13), 4085–4092. https://doi.org/10.1021/bi00387a052

Florio, W., Baldeschi, L., Rizzato, C., Tavanti, A., Ghelardi, E., & Lupetti, A. (2020). Detection of Antibiotic-Resistance by MALDI-TOF Mass Spectrometry: An Expanding Area. *Frontiers in Cellular and Infection Microbiology*, *10*. https://doi.org/10.3389/fcimb.2020.572909

Prestinaci, F., Pezzotti, P. & Pantosti, A. (2015). Antimicrobial resistance: a global, multifaceted phenomenon. *Pathogens and Global Health, 109*(7), 309-318, DOI: 10.1179/2047773215Y.0000000030

Freed, N. E., Bumann, D., & Silander, O. K. (2016). Combining Shigella Tn-seq data with gold-standard E. Coli gene deletion data suggests rare transitions between essential and non-essential gene functionality. *BMC Microbiology*, *16*(1). https://doi.org/10.1186/s12866-016-0818-0

Freed, N. E., Vlková, M., Faisal, M. B., & Silander, O. K. (2020). Rapid and inexpensive whole-genome sequencing of SARS-CoV-2 using 1200 bp tiled amplicons and Oxford Nanopore Rapid Barcoding. *Biology Methods and Protocols*, *5*(1). https://doi.org/10.1093/biomethods/bpaa014

Frost, L. S., Leplae, R., Summers, A. O., & Toussaint, A. (2005). Mobile genetic elements: The agents of open source evolution. *Nature Reviews Microbiology*, *3*(9), 722-732. https://doi.org/10.1038/nrmicro123

Forbes, J. D., Knox, N. C., Ronholm, J., Pagotto, F. & Reimer, A. (2017). Metagenomics: The next culture-independent game changer. *Frontiers in Microbiology, 8*(1069). DOI: https://doi.org/10.3389/fmicb.2017.01069

Furuya, E. Y., & Lowy, F. D. (2006). Antimicrobial-resistant bacteria in the community setting. *Nature Reviews Microbiology*, *4*(1), 36-45. https://doi.org/10.1038/nrmicro1325

Garneau-Tsodikova, S., & Labby, K. J. (2016). Mechanisms of Resistance to Aminoglycoside Antibiotics: Overview and Perspectives. *MedChemComm*, *7*(1), 11. https://doi.org/10.1039/C5MD00344J

Gasparrini, A. J., Markley, J. L., Kumar, H., Wang, B., Fang, L., Irum, S., Symister, C. T., Wallace, M., Burnham, C., Andleeb, S., Tolia, N. H., Wencewicz, T. A., & Dantas, G. (2020). Tetracycline-inactivating enzymes from environmental, human commensal, and pathogenic bacteria cause broad-spectrum tetracycline resistance. *Communications Biology*, *3*(1), 1-12. https://doi.org/10.1038/s42003-020-0966-5

Gleckman, R., Blagg, N., & Joubert, D. W. (1981). Trimethoprim: Mechanisms of Action, Antimicrobial Activity, Bacterial Resistance, Pharmacokinetics, Adverse Reactions, and Therapeutic Indications. *Pharmacotherapy: The Journal of Human Pharmacology and Drug Therapy*, *1*(1), 14-19. https://doi.org/10.1002/j.1875-9114.1981.tb03548.x

Grant, J. R., Enns, E., Marinier, E., Mandal, A., Herman, E. K., Chen, C., Graham, M., Van Domselaar, G., & Stothard, P. (2023). Proksee: In-depth characterisation and visualisation of bacterial genomes. *Nucleic Acids Research*, *51*(W1), W484-W492. https://doi.org/10.1093/nar/gkad326

Guo, T., Lou, C., Zhai, W., Tang, X., Hashmi, M. Z., Murtaza, R., Li, Y., Liu, X., & Xu, J. (2018). Increased occurrence of heavy metals, antibiotics and resistance genes in surface soil after long-term application of manure. *Science of The Total Environment*, *635*, 995-1003. https://doi.org/10.1016/j.scitotenv.2018.04.194

Hoenen, T., Groseth, A., Rosenke, K., Fischer, R. J., Hoenen, A., Judson, S. D., Martellaro, C., Falzarano, D., Marzi, A., Squires, R. B., Wollenberg, K. R., Prescott, J., Safronetz, D., Bushmaker, T., Feldmann, F., McNally, K., Bolay, F. K., Fields, B., Sealy, T., Rayfield, M., Nichol, S. T., Zoon, K. C., Massaquoi, M., Munster, V. J. & Feldmann, H. (2016). Nanopore Sequencing as a Rapidly Deployable Ebola Outbreak Tool. *Emerging Infectious Diseases*, *22*(2), 331-334. https://doi.org/10.3201/eid2202.151796

Hofer, U. (2019). The cost of antimicrobial resistance. *Nature Reviews Microbiology*, *17*(1), 3. https://doi.org/10.1038/s41579-018-0125-x

Hu, Y., Yang, X., Li, J., Lv, N., Lui, F., Wu, J., Lin, I. Y. C., Wu, N., Weimer, B., Gao, G. F., Lui, Y. & Zhu, B. (2016). The bacteria mobile resistome transfer network connecting the animal and human microbiomes. *Applied and Environmental Microbiology, 82*(22). https://doi.org/10.1128/AEM.01802-16

Jahantigh, M., Samadi, K., Dizaji, R.E. & Salari, S. (2020). Antimicrobial resistance and prevalence of tetracycline resistance genes in *Escherichia coli* isolated from lesions of colibacillosis in broiler chickens in Sistan, Iran. *BMC Veterinary Research, 16*, 267. https://doi.org/10.1186/s12917-020-02488-z

Jain, M., Olsen, H.E., Paten, B. & Akeson, M. (2016). The Oxford Nanopore MinION: delivery of nanopore sequencing to the genomics community. *Genome Biology, 17*(239). https://doi.org/10.1186/s13059-016-1103-0

Khodakov, D., Li, J., Zhang, J. X., & Zhang, D. Y. (2021). Highly multiplexed rapid DNA detection with single-nucleotide specificity via convective PCR in a portable device. *Nature Biomedical Engineering*, *5*(7), 702-712. https://doi.org/10.1038/s41551-021-00755-4

Klemm, E. J., Wong, V. K., & Dougan, G. (2018). Emergence of dominant multidrug-resistant bacterial clades: Lessons from history and whole-genome sequencing. *Proceedings of the National Academy of Sciences of the United States of America*, *115*(51), 12872-12877. https://doi.org/10.1073/pnas.1717162115

Koch, A., Cox, H., & Mizrahi, V. (2018). Drug-resistant tuberculosis: Challenges and opportunities for diagnosis and treatment. *Current Opinion in Pharmacology*, *42*, 7-15. https://doi.org/10.1016/j.coph.2018.05.013

Kollef, M. H., Shorr, A. F., Bassetti, M., Timsit, J., Micek, S. T., Michelson, A. P. & Garnocho-Montero, J. (2021). Timing of antibiotic therapy in the ICU. *Critical Care, 25*, 360. https://doi.org/10.1186/s13054-021-03787-z

Kosack, C. S., Page, L., & Klatser, P. R. (2017). A guide to aid the selection of diagnostic tests. *Bulletin of the World Health Organization*, *95*(9), 639-645. https://doi.org/10.2471/BLT.16.187468

Kumar, A., Roberts, D., Wood, K. E., Light, B., Parrillo, J., Sharma, S., Suppes, R., Feinstein, D., Zanotti, S., Taiberg, L., Gurkha, D., Aseem, K. & Cheang, M. (2006). Duration of hypotension before initiation of effective antimicrobial therapy is the critical determinant of survival in human septic shock. *Critical Care Medicine, 34(*6), 1589-1596. DOI: 10.1097/01.CCM.0000217961.75225.E9

Lanza, V. F., Baquero, F., Martínez, J. L., Ramos-Ruíz, R., González-Zorn, B., Andremont, A., Sánchez-Valenzuela, A., Ehrlich, S. D., Kennedy, S., Ruppé, E., Willems, R. J., & Coque, T. M. (2018). In-depth resistome analysis by targeted metagenomics. *Microbiome*, *6*. https://doi.org/10.1186/s40168-017-0387-y

Larsson, D. G., & Flach, C. (2022). Antibiotic resistance in the environment. *Nature Reviews Microbiology*, *20*(5), 257-269. https://doi.org/10.1038/s41579-021-00649-x

Leclercq, R., & Courvalin, P. (1991). Bacterial resistance to macrolide, lincosamide, and streptogramin antibiotics by target modification. *Antimicrobial Agents and Chemotherapy*, *35*(7), 1267-1272. https://doi.org/10.1128/aac.35.7.1267

Levy, S. B., McMurry, L. M., Barbosa, T. M., Burdett, V., Courvalin, P., Hillen, W., Roberts, M. C., Rood, J. I., & Taylor, D. E. (1999). Nomenclature for New Tetracycline Resistance Determinants. *Antimicrobial Agents and Chemotherapy*, *43*(6), 1523-1524. https://doi.org/10.1128/aac.43.6.1523

Li, S., Zhang, R., Hu, J., Shi, W., Kuang, Y., Guo, X., & Sun, W. (2019). Occurrence and removal of antibiotics and antibiotic resistance genes in natural and constructed riverine wetlands in Beijing, China. *Science of The Total Environment*, *664*, 546-553. https://doi.org/10.1016/j.scitotenv.2019.02.043

Li, Y., Shi, X., Zuo, Y., Li, T., Liu, L., Shen, Z., Shen, J., Zhang, R., & Wang, S. (2022). Multiplexed Target Enrichment Enables Efficient and In-Depth Analysis of Antimicrobial Resistome in Metagenomes. *Microbiology Spectrum*, *10*(6). https://doi.org/10.1128/spectrum.02297-22

Linde, J., Brangsch, H., Hölzer, M., Thomas, C., Elschner, M. C., Melzer, F. & Herbert, T. (2023). Comparison of Illumina and Oxford Nanopore Technology for genome analysis of *Francisella tularensis, Bacillus anthracis*, and *Brucella suis*. *BMC Genomics, 24*(258). https://doi.org/10.1186/s12864-023-09343-z

Liu, C. T., Hanoian, P., French, J. B., Pringle, T. H., & Benkovic, S. J. (2013). Functional significance of evolving protein sequence in dihydrofolate reductase from bacteria to humans. *Proceedings of the National Academy of Sciences*, *110*(25), 10159-10164. https://doi.org/10.1073/pnas.1307130110

Lobanovska, M., & Pilla, G. (2017). Focus: Drug Development: Penicillin's Discovery and Antibiotic Resistance: Lessons for the Future? *The Yale Journal of Biology and Medicine*, *90*(1), 135-145. https://www.ncbi.nlm.nih.gov/pmc/articles/PMC5369031/

Lu, H., Ma, L., Zhang, H., Feng, L., Yu, Y., Li, L., Zhou, Y., Song, L., Li, W., Zhao, J. & Liu, L. (2022). The comparison of metagenomic next-generation sequencing with conventional

microbiological tests for identification of pathogens and antibiotic resistance genes in infectious diseases. *Infection and Drug Resistance*, *15*(2022), 6115-6128. DOI: 10.2147/IDR.S370964

Magiorakos, A., Srinivasan, A., Carey, R., Carmeli, Y., Falagas, M., Giske, C., Harbarth, S., Hindler, J., Kahlmeter, G., Olsson-Liljequist, B., Paterson, D., Rice, L., Stelling, J., Struelens, M., Vatopoulos, A., Weber, J., & Monnet, D. (2012). Multidrug-resistant, extensively drug-resistant and pan drug-resistant bacteria: An international expert proposal for interim standard definitions for acquired resistance. *Clinical Microbiology and Infection*, *18*(3), 268-281. https://doi.org/10.1111/j.1469-0691.2011.03570.x

Magnet, S. & Blanchard, J. S. (2005) Molecular insights into Aminoglycoside Action and Resistance. *Chemical Reviews, 105*(2), 477-498. https://pubs.acs.org/doi/epdf/10.1021/cr0301088

Majumder, M. A. A., Rahman, S., Cohall, D., Bharatha, A., Singh, K., Haque, M. & Hilaire, M. G. (2020). Antimicrobial stewardship: Fighting antimicrobial resistance and protecting global public health. *Infection and Drug Resistance*, *13*, 4713-4738. DOI: 10.2147/IDR.S290835

Manoil, C. (1999). [3] Tagging exported proteins using Escherichia coli alkaline phosphatase gene fusions. *Methods in Enzymology*, *326*, 35-47. https://doi.org/10.1016/S0076-6879(00)26045-X

Manyi-Loh, C., Mamphweli, S., Meyer, E., & Okoh, A. (2018). Antibiotic Use in Agriculture and Its Consequential Resistance in Environmental Sources: Potential Public Health Implications. *Molecules: A Journal of Synthetic Chemistry and Natural Product Chemistry*, *23*(4). https://doi.org/10.3390/molecules23040795

Marti, R., Scott, A., Tein, Y., Murray, R., Sabourin, L., Zhang, Y. & Topp, E. (2013). Impact of Manure Fertilization on the Abundance of Antibiotic-Resistant Bacteria and Frequency of Detection of Antibiotic Resistance Genes in Soil and on Vegetables at Harvest. *Applied and Environmental Microbiology, 79*(18). https://doi.org/10.1128/AEM.01682-13

Masterton, R. G., Galloway, A., French, G., Street, M., Armstrong, J., Brown, E., Cleverley, J., Dilworth, P., Fry, C., Gascoigne, A. D., Knox, A., Nathwani, D., Spencer, R., & Wilcox, M. (2008). Guidelines for the management of hospital-acquired pneumonia in the UK: Report of the Working Party on Hospital-Acquired Pneumonia of the British Society for Antimicrobial Chemotherapy. *Journal of Antimicrobial Chemotherapy*, *62*(1), 5-34. https://doi.org/10.1093/jac/dkn162

Mate, S. E., Kugelman, J. R., Nyenswah, T. G., Ladner, J. T., Wiley, M. R., Cordier-Lassalle, T., Christie, A., Schroth, G. P., Gross, S. M., Davies-Wayne, G. J., Shinde, S. A., Murugan, R., Sieh, S. B., Badio, M., Fakoli, L., Taweh, F., Munster, V. J., Pettitt, J., Prieto, K., . . . Palacios, G. (2015). Molecular Evidence of Sexual Transmission of Ebola Virus. *The New England Journal of Medicine*, *373*(25), 2448. https://doi.org/10.1056/NEJMoa1509773

Maugeri, G., Lychko, I., Sobral, P. R., & A. Roque, A. C. (2019). Identification and Antibiotic-Susceptibility Profiling of Infectious Bacterial Agents: A Review of Current and Future Trends. *Biotechnology journal*, *14*(1), e1700750. https://doi.org/10.1002/biot.201700750

Medugu, N., Aworh, M. K., Iregbu, K., Abdulraheem, K., Hull, D. M., Harden, L., Singh, P., Obaro, S., Egwuenu, A., & Thakur, S. (2022). Molecular characterisation of multi-drug resistant

Escherichia coli isolates at a tertiary hospital in Abuja, Nigeria. *Scientific Reports*, *12*(1), 1-10. https://doi.org/10.1038/s41598-022-19289-z

Ministry of Health and Ministry for Primary Industries. 2017. New Zealand Antimicrobial Resistance Action Plan. Wellington: Ministry of Health. ISBN 978-1-98-850276-2

Miranda, A., Ávila, B., Díaz, P., Rivas, L., Bravo, K., Astudillo, J., Bueno, C., Ulloa, M. T., Hermosilla, G., Del Canto, F., Salazar, J. C., & Toro, C. S. (2016). Emergence of Plasmid-Borne dfrA14 Trimethoprim Resistance Gene in Shigella sonnei. *Frontiers in Cellular and Infection Microbiology*, *6*. https://doi.org/10.3389/fcimb.2016.00077

Mokni-Tlili, S., Hechmi, S., Ouzari, H., Mechergui, N., Ghorbel, M., Jedidi, N., Hassen, A. & Hamdi, H. (2022). Co-occurance of antibiotic and metal resistance in long-term sewage sludge-amended soils: influence of application rates and pedo-climatic condition. *Environmental Science and Pollution Research, 30*, 26596-26612. https://doi.org/10.1007/s11356-022-23802-2

Mora-Ochomogo, M., & Lohans, C. T. (2021). β-Lactam antibiotic targets and resistance mechanisms: From covalent inhibitors to substrates. *RSC Medicinal Chemistry*, *12*(10), 1623-1639. https://doi.org/10.1039/d1md00200g

Moragues-Solanas, L., Scotti, R. & O'Grady, J. (2021). Rapid metagenomics for diagnosis of bloodstream and respiratory tract nosocomial infections: current status and future prospects. *Expert Review of Molecular Diagnostics, 21*(4), 371-380. DOI: https://doi.org/10.1080/14737159.2021.1906652

Morel, C.M., Alm, R.A., Årdal, C. Bandera, A., Bruno, G. M., Carrara, E., Colombo, G. L., de Kraker, M. E. A., Essack, S., Frost, I., Gonzalez-Zorn, B., Gossens, H., Guardabassi, L., Harbarth, S., Jorgensen, P. S., Kanj, S. S., Kostyanev, T., Laxminarayan, R., Leonard, F., Hara, G. L., Mendelson, M., Mikulska, M., Mutters, N. T. & Outterson, K. (2020). A one health framework to estimate the cost of antimicrobial resistance. *Antimicrobial Resistance & Infection Control*, *9,* 187. https://doi.org/10.1186/s13756-020-00822-6

Motta, S. S., Cluzel, P., & Aldana, M. (2015). Adaptive Resistance in Bacteria Requires Epigenetic Inheritance, Genetic Noise, and Cost of Efflux Pumps. *PLoS ONE*, *10*(3). https://doi.org/10.1371/journal.pone.0118464

Munk, P., Andersen, V. D., de Knegt, L., Jensen, M. S., Knudsen, B. E., Lukjancenko, O., Mordhorst, H., Clasen, J., Agersø, Y., Folkesson, A., Pamp, S. J., Vigre, H., & Aarestrup, F. M. (2017). A sampling and metagenomic sequencing-based methodology for monitoring antimicrobial resistance in swine herds. *Journal of Antimicrobial Chemotherapy*, *72*(2), 385-392. https://doi.org/10.1093/jac/dkw415

Nikaido, H. (2009). Multidrug Resistance in Bacteria. *Annual review of biochemistry*, *78*, 119. https://doi.org/10.1146/annurev.biochem.78.082907.145923

O'Neill, J. (2016). Tackling drug-resistant infections globally: final report and recommendations. https://apo.org.au/node/63983

O'Neill, J. I. M. (2014). Antimicrobial resistance: tackling a crisis for the health and wealth of nations. *Rev. Antimicrob. Resist.*

Ochman, H., Lawrence, J. G., & Groisman, E. A. (2000). Lateral gene transfer and the nature of bacterial innovation. *Nature*, *405*(6784), 299-304. https://doi.org/10.1038/35012500

Ovung, A., & Bhattacharyya, J. (2021). Sulfonamide drugs: Structure, antibacterial property, toxicity, and biophysical interactions. *Biophysical Reviews*, *13*(2), 259-272. https://doi.org/10.1007/s12551-021-00795-9

Pagès-Gallego, M., de Ridder, J. (2023). Comprehensive benchmark and architectural analysis of deep learning models for nanopore sequencing basecalling. *Genome Biology, 24*(71). https://doi.org/10.1186/s13059-023-02903-2

Pattis, I., Weaver, L., Burgess, S., Ussher, J. E., & Dyet, K. (2022). Antimicrobial Resistance in New Zealand—A One Health Perspective. *Antibiotics*, *11*(6). https://doi.org/10.3390/antibiotics11060778

Payne, A., Holmes, N., Rakyan, V., & Loose, M. (2019). BulkVis: A graphical viewer for Oxford nanopore bulk FAST5 files. *Bioinformatics*, *35*(13), 2193-2198. https://doi.org/10.1093/bioinformatics/bty841

Peter, S., Bosio, M., Gross, C., Bezdan, D., Gutierrez, J., Oberhettinger, P., Liese, J., Vogel, W., Dörfel, D., Berger, L., Marschal, M., Willmann, M., Gut, I., Gut, M., Autenrieth, I., & Ossowski, S. (2020). Tracking of Antibiotic Resistance Transfer and Rapid Plasmid Evolution in a Hospital Setting by Nanopore Sequencing. *MSphere*, *5*(4). https://doi.org/10.1128/mSphere.00525-20

Phuong Hoa, P. T., Nonaka, L., Hung Viet, P., & Suzuki, S. (2008). Detection of the sul1, sul2, and sul3 genes in sulfonamide-resistant bacteria from wastewater and shrimp ponds of north Vietnam. *Science of The Total Environment*, *405*(1-3), 377-384. https://doi.org/10.1016/j.scitotenv.2008.06.023

Prevention, C. (2013). Antibiotic resistance threats in the United States, 2013. *Threat Report*, 50-52.

Pulido, M. R., Garcia-Quintanilla, M., Martin-Pena, R., Cisneros, J. M. & McConnell, M. J. (2013). Progress on the development of rapid methods for antimicrobial susceptibility testing. *Journal of Antimicrobial Chemotherapy, 68*(12), 2710-2717. DOI: https://doi.org/10.1093/jac/dkt253

Quick, J., Grubaugh, N. D., Pullan, S. T., Claro, I. M., Smith, A. D., Gangavarapu, K., Oliveira, G., Rogers, T. F., Beutler, N. A., Burton, D. R., Laura, L., de Jesus, J. G., Giovanetti, M., Hill, S. C., Black, A., Bedford, T., Carroll, M. W., Nunes, M., Alcantara, L. C., Sabino, C. E., Baylis, S. A., Faria, N. R., Loose, M., Simpson, J. T., Pybus, O. G., Andersen, K. G. & Loman, N. J. (2017). Multiplex PCR method for MinION and Illumina sequencing of Zika and other virus genomes directly from clinical samples. *Nature Protocols*, *12*(6), 1261-1276. https://doi.org/10.1038/nprot.2017.066

Ramirez, M. S., Traglia, G. M., Lin, D. L., Tran, T., Tolmasky, M. E. (2014). Plasmid-mediated antibiotic resistance and virulence in gram-negatives: the *Klebsiella pneumoniae* paradigm. *Microbiology Spectrum*, *2*(5). https://doi.org/10.1128/microbiolspec.plas-0016-2013

Rasheed, A., Gill, R. A., Hassan, M. U., Mahmood, A., Qari, S., Zaman, Q. U., Ilyas, M., Aamer, M., Batool, M., Li, H., & Wu, Z. (2021). A Critical Review: Recent Advancements in the Use of

CRISPR/Cas9 Technology to Enhance Crops and Alleviate Global Food Crises. *Current Issues in Molecular Biology*, *43*(3), 1950-1976. https://doi.org/10.3390/cimb43030135

Read, A. F., & Woods, R. J. (2014). Antibiotic resistance management. *Evolution, Medicine, and Public Health*, *2014*(1), 147. https://doi.org/10.1093/emph/eou024

Review on Antimicrobial Resistance. (2014). Antimicrobial resistance: Tackling a crisis for the health and wealth of nations. Retrieved from https://amr-review.org/sites/default/files/AMR%20Review%20Paper%20-%20Tackling%20a%20crisis%20for%20the%20health%20and%20wealth%20of%20nations_1.pdf

Rice, L. B. (2012). Mechanisms of Resistance and Clinical Relevance of Resistance to β-Lactams, Glycopeptides, and Fluoroquinolones. *Mayo Clinic Proceedings*, *87*(2), 198-208. https://doi.org/10.1016/j.mayocp.2011.12.003

Roberts, M. C. (1996). Tetracycline resistance determinants: Mechanisms of action, regulation of expression, genetic mobility, and distribution. *FEMS Microbiology Reviews*, *19*(1), 1-24. https://doi.org/10.1111/j.1574-6976.1996.tb00251.x

Roca, I., Akova, M., Baquero, F., Carlet, J., Cavaleri, M., Coenen, S., Cohen, J., Findlay, D., Gyssens, I., Heure, O. E., Kahlmeter, G., Kruse, H., Laxminarayan, R., Liébana, E., López-Cerero, L., MacGowan, A., Martins, M., Rodríguez-Baño, J., Rolain, M., Segovia, C., Siguaque, B., Tacconelli, E., Wellington, E. & Vila, J. (2015). The global threat of antimicrobial resistance: Science for intervention. *New Microbes and New Infections*, *6*, 22-29. https://doi.org/10.1016/j.nmni.2015.02.007

Sajuthi, A., White, J., Ferguson, G., Freed, N. E. & Silander, O. K. (2020). Bac-PULCE: Bacterial strain and AMR profiling using long reads via CRISPR enrichment. bioRxiv: the preprint server for biology. https://doi.org/10.1101/2020.09.30.320226

Sarmah, A. K., Meyer, M. T., & Boxall, A. B. (2006). A global perspective on the use, sales, exposure pathways, occurrence, fate and effects of veterinary antibiotics (VAs) in the environment. *Chemosphere*, *65*(5), 725-759. https://doi.org/10.1016/j.chemosphere.2006.03.026

Schwaber, M. J., & Carmeli, Y. (2007). Mortality and delay in effective therapy associated with extended-spectrum β-lactamase production in Enterobacteriaceae bacteraemia: A systematic review and meta-analysis. *Journal of Antimicrobial Chemotherapy*, *60*(5), 913-920. https://doi.org/10.1093/jac/dkm318

Sengupta, S., Chattopadhyay, M. K., & Grossart, P. (2013). The multifaceted roles of antibiotics and antibiotic resistance in nature. *Frontiers in Microbiology*, *4*. https://doi.org/10.3389/fmicb.2013.00047

Sereika, M., Kirkegaard, R. H., Karst, S. M., Michaelsen, T. Y., Sørensen, E. A., Wollenberg, R. D., & Albertsen, M. (2022). Oxford Nanopore R10.4 long-read sequencing enables the generation of near-finished bacterial genomes from pure cultures and metagenomes without short-read or reference polishing. *Nature Methods*, *19*(7), 823-826. https://doi.org/10.1038/s41592-022-01539-7

Serra-Burriel, M., Keys, M., Campillo-Artero, C., Agodi, A., Barchitta, M., Gikas, A., Palos, C., & López-Casasnovas, G. (2020). Impact of multi-drug resistant bacteria on economic and clinical outcomes of healthcare-associated infections in adults: Systematic review and meta-analysis. *PLOS ONE*, *15*(1), e0227139. https://doi.org/10.1371/journal.pone.0227139

Shelburne, S. A., Kim, J., Munita, J. M., Sahasrabhojane, P., Shields, R. K., Press, E. G., Li, X., Arias, C. A., Cantarel, B., Jiang, Y., Kim, M. S., Aitken, S. L., & Greenberg, D. E. (2017). Whole-Genome Sequencing Accurately Identifies Resistance to Extended-Spectrum β-Lactams for Major Gram-Negative Bacterial Pathogens. *Clinical Infectious Diseases: An Official Publication of the Infectious Diseases Society of America*, *65*(5), 738-745. https://doi.org/10.1093/cid/cix417

Shen, W., Le, S., Li, Y., & Hu, F. (2016). SeqKit: A Cross-Platform and Ultrafast Toolkit for FASTA/Q File Manipulation. *PLoS ONE*, *11*(10). https://doi.org/10.1371/journal.pone.0163962

Shi, K., Caldwell, S. J., Fong, D. H., & Berghuis, A. M. (2013). Prospects for circumventing aminoglycoside kinase mediated antibiotic resistance. *Frontiers in Cellular and Infection Microbiology*, *3*. https://doi.org/10.3389/fcimb.2013.00022

Sköld, O. (2000). Sulfonamide resistance: Mechanisms and trends. *Drug Resistance Updates*, *3*(3), 155-160. https://doi.org/10.1054/drup.2000.0146

Smith, C., Halse, T. A., Shea, J., Modestil, H., Fowler, R. C., Musser, K. A., Escuyer, V., & Lapierre, P. (2021). Assessing Nanopore Sequencing for Clinical Diagnostics: A Comparison of Next-Generation Sequencing (NGS) Methods for Mycobacterium tuberculosis. *Journal of Clinical Microbiology*, *59*(1). https://doi.org/10.1128/JCM.00583-20

Smillie, C. S., Smith, M. B., Friedman, J., Cordero, O. X., David, L. A., & Alm, E. J. (2011). Ecology drives a global network of gene exchange connecting the human microbiome. *Nature*, *480*(7376), 241-244. https://doi.org/10.1038/nature10571

Sohier, D., Pavan, S., Riou, A., Combrisson, J. & Postollec, F. (2014). Evolution of microbiological analytical methods for dairy industry needs. *Frontiers in Microbiology, 5*(16). DOI: DOI: 10.3389/fmicb.2014.00016

Speer, B. S., Bedzyk, L., & Salyers, A. A. (1991). Evidence that a novel tetracycline resistance gene found on two Bacteroides transposons encodes an NADP-requiring oxidoreductase. *Journal of Bacteriology*, *173*(1), 176-183. https://doi.org/10.1128/jb.173.1.176-183.1991

Spellberg, B., & Gilbert, D. N. (2014). The Future of Antibiotics and Resistance: A Tribute to a Career of Leadership by John Bartlett. *Clinical Infectious Diseases: An Official Publication of the Infectious Diseases Society of America*, *59*(Suppl 2), S71. https://doi.org/10.1093/cid/ciu392
Stevens, B. M., Creed, T. B., Reardon, C. L., & Manter, D. K. (2023). Comparison of Oxford Nanopore Technologies and Illumina MiSeq sequencing with mock communities and agricultural soil. *Scientific Reports*, *13*(1), 1-11. https://doi.org/10.1038/s41598-023-36101-8

Stogios, P. J., Shakya, T., Evdokimova, E., Savchenko, A., & Wright, G. D. (2011). Structure and Function of APH(4)-Ia, a Hygromycin B Resistance Enzyme. *The Journal of Biological Chemistry*, *286*(3), 1966-1975. https://doi.org/10.1074/jbc.M110.194266

Svara, F., Rankin, D.J. (2011). The evolution of plasmid-carried antibiotic resistance. *BMC Evol Biol* 11, 130. https://doi.org/10.1186/1471-2148-11-130

Svetlov, M. S., Syroegin, E. A., Aleksandrova, E. V., Atkinson, G. C., Gregory, S. T., Mankin, A. S., & Polikanov, Y. S. (2021). Structure of Erm-modified 70S ribosome reveals the mechanism of macrolide resistance. *Nature chemical biology*, *17*(4), 412. https://doi.org/10.1038/s41589-020-00715-0

Tenover, F. C., McDougal, L. K., Goering, R. V., Killgore, G., Projan, S. J., Patel, J. B., & Dunman, P. M. (2006). Characterization of a Strain of Community-Associated Methicillin-Resistant Staphylococcus aureus Widely Disseminated in the United States. *Journal of Clinical Microbiology*, *44*(1), 108-118. https://doi.org/10.1128/JCM.44.1.108-118.2006

Thrash, A., Hoffmann, F. & Perkins, A. (2020). Toward a more holistic method of genome assembly assessment. *BMC Bioinformatics*, *249*(21). https://doi.org/10.1186/s12859-020-3382-4

Tsui, W. H., Yim, G., Wang, H. H., McClure, J. E., Surette, M. G., & Davies, J. (2004). Dual Effects of MLS Antibiotics: Transcriptional Modulation and Interactions on the Ribosome. *Chemistry & Biology*, *11*(9), 1307-1316. https://doi.org/10.1016/j.chembiol.2004.07.010

Vale, F. F., Lehours, P., & Yamaoka, Y. (2022). Editorial: The Role of Mobile Genetic Elements in Bacterial Evolution and Their Adaptability. *Frontiers in Microbiology*, *13*. https://doi.org/10.3389/fmicb.2022.849667

Ventola, C. L. (2015). The Antibiotic Resistance Crisis: Part 1: Causes and Threats. *Pharmacy and Therapeutics*, *40*(4), 277-283. https://www.ncbi.nlm.nih.gov/pmc/articles/PMC4378521/

Wang, J., Wang, Y., Wang, Y., Sun, F., Li, W., Wu, H., Shen, C., Pan, M., & Jiao, X. (2020). Emergence of 16S rRNA Methylase Gene rmtB in Salmonella Enterica Serovar London and Evolution of RmtB-Producing Plasmid Mediated by IS26. *Frontiers in Microbiology*, *11*. https://doi.org/10.3389/fmicb.2020.604278

Wang, J., Xiong, K., Zhao, S., Zhang, C., Zhang, J., Xu, L., & Ma, A. (2020). Long-Term Effects of Multi-Drug-Resistant Tuberculosis Treatment on Gut Microbiota and Its Health Consequences. *Frontiers in Microbiology*, *11*, 500124. https://doi.org/10.3389/fmicb.2020.00053

Wang, Y., Zhao, Y., Bollas, A., Wang, Y., & Au, K. F. (2021). Nanopore sequencing technology, bioinformatics and applications. *Nature Biotechnology*, *39*(11), 1348-1365. https://doi.org/10.1038/s41587-021-01108-x

Waseem, H., Jameel, S., Ali, J., Tauseef, I., Farooq, U., Jamal, A., & Ali, M. I. (2019). Contributions and Challenges of High Throughput qPCR for Determining Antimicrobial Resistance in the Environment: A Critical Review. *Molecules*, *24*(1), 163. https://doi.org/10.3390/molecules24010163

Wick, R.R., Judd, L.M. & Holt, K.E. (2019). Performance of neural network basecalling tools for Oxford Nanopore sequencing. *Genome Biology,* 20(129). https://doi.org/10.1186/s13059-019-1727-y

Wilson, D. N. (2014). Ribosome-targeting antibiotics and mechanisms of bacterial resistance. *Nature Reviews Microbiology*, *12*(1), 35-48. https://doi.org/10.1038/nrmicro3155

World Health Organization, WHO report on surveillance of antibiotic consumption: 2016–2018 early implementation,
https://www.who.int/publications/i/item/who-report-on-surveillance-of-antibiotic-consumption

Worthington, R. J., & Melander, C. (2013). Overcoming Resistance to β-Lactam Antibiotics. *The Journal of Organic Chemistry*, *78*(9), 4207. https://doi.org/10.1021/jo400236f

Xiao, K., Li, B., Ma, L., Bao, P., Zhou, X., Zhang, T., & Zhu, Y. (2016). Metagenomic profiles of antibiotic resistance genes in paddy soils from South China. *FEMS Microbiology Ecology*, *92*(3). https://doi.org/10.1093/femsec/fiw023

Xie, N. G., Wang, M. X., Song, P., Mao, S., Wang, Y., Yang, Y., Luo, J., Ren, S., & Zhang, D. Y. (2022). Designing highly multiplex PCR primer sets with Simulated Annealing Design using Dimer Likelihood Estimation (SADDLE). *Nature Communications*, *13*(1), 1-10. https://doi.org/10.1038/s41467-022-29500-4

Yao, W., Xu, G., Li, D., Bai, B., Wang, H., Cheng, H., Zheng, J., Sun, X., Lin, Z., Deng, Q., & Yu, Z. (2019). Staphylococcus aureus with an erm-mediated constitutive macrolide-lincosamide-streptogramin B resistance phenotype has reduced susceptibility to the new ketolide, solithromycin. *BMC Infectious Diseases*, *19*. https://doi.org/10.1186/s12879-019-3779-8

Yoon, E. & Jeong, S. H. (2021). MALDI-TOF mass spectrometry technology as a tool for the rapid diagnosis of antimicrobial resistance in bacteria. *Antibiotics, 10*(8), 982. https://doi.org/10.3390/antibiotics10080982

Zhang, C., Xiu, L., Li, Y., Sun, L., Li, Y., Zeng, Y., Wang, F., & Peng, J. (2021). Multiplex PCR and Nanopore Sequencing of Genes Associated with Antimicrobial Resistance in *Neisseria Gonorrhoeae* Directly from Clinical Samples. *Clinical Chemistry*, *67*(4), 610-620. https://doi.org/10.1093/clinchem/hvaa306

Zhang, S., Li, X., Wu, J., Coin, L., O'Brien, J., Hai, F. & Jiang, G. (2021). Molecular methods for pathogenic bacteria detection and recent advances in wastewater analysis. *Water, 13*, 3551. DOI: https://doi.org/10.3390/w13243551

Zhao, K., Tu, C., Chen, W., Liang, H., Zhang, W., Wang, Y., Jin, Y., Hu, J., Sun, Y., Xu, J. & Yu, Y. (2022). Rapid identification of drug-resistant tuberculosis genes using direct PCR amplification and Oxford nanopore technology sequencing. *Canadian Journal of Infectious Disease and Medical Microbiology, 2022*(7588033), 8. DOI: https://doi.org/10.1155/2022/7588033

Zhao, W., Zeng, W., Pang, B., Luo, M., Peng, Y., Xu, J., Kan, B., Li, Z., & Lu, X. (2023). Oxford nanopore long-read sequencing enables the generation of complete bacterial and plasmid genomes without short-read sequencing. *Frontiers in Microbiology*, *14*. https://doi.org/10.3389/fmicb.2023.1179966

zur Wiesch, P. A., Kouyos, R., Engelstädter, J., Regoes, R. R., & Bonhoeffer, S. (2011). Population biological principles of drug-resistance evolution in infectious diseases. *The Lancet Infectious Diseases*, *11*(3), 236-247. https://doi.org/10.1016/S1473-3099(10)70264-4

Chapter 6: Appendices

Supplementary Table 6.1. Panel of primers capable of multiplex qPCR. The list of primers was originally ordered and used for the initial test of amplification of target ARGs. Primers designed using Primalscheme v1.4.1 (Quick et al., 2017). Left (forward primer and right (reverse primer)

Name	Sequence	Length	Target
scheme_1_LEFT	TGGTGAATCGCATTCTGACTGG	22	aph(3'')-Ib_5_AF321551:+24
scheme_1_RIGHT	CATTGCGGGACACCACATCAA	21	aph(3'')-Ib_5_AF321551:-401
scheme_2_LEFT	CTGTTCACAGCCTATCGGTTGA	22	aph(3'')-Ib_5_AF321551:+332
scheme_2_RIGHT	ATTGAATAGGACAGCGAAGGCG	22	aph(3'')-Ib_5_AF321551:-708
scheme_3_LEFT	ACGTCTGTCGAGAAGTTTCTGA	22	aph(4)-Ia_1_V01499:+25
scheme_3_RIGHT	CGATTCCTTGCGGTCCGAAT	20	aph(4)-Ia_1_V01499:-405
scheme_4_LEFT	AAGACCTGCCTGAAACCGAAC	21	aph(4)-Ia_1_V01499:+302
scheme_4_RIGHT	GGCCTCCAGAAGAAGATGTTGG	22	aph(4)-Ia_1_V01499:-689
scheme_5_LEFT	CGGACAATGGCCGCATAACA	20	aph(4)-Ia_1_V01499:+617
scheme_5_RIGHT	CTATTCCTTTGCCCTCGGACGA	22	aph(4)-Ia_1_V01499:-1005
scheme_6_LEFT	CGCCTGTTTTTCCTGCTCATTG	22	aph(6)-Id_4_CP000971:+5
scheme_6_RIGHT	CCGCTGAAACAAAGCTGCAAA	21	aph(6)-Id_4_CP000971:-382
scheme_7_LEFT	GACTACCAGGCGACCGAAATTG	22	aph(6)-Id_4_CP000971:+283
scheme_7_RIGHT	AGAGAATGCGTCCGCCATCT	20	aph(6)-Id_4_CP000971:-662
scheme_8_LEFT	AACGCAGGTTGTCAAACTGACT	22	aph(6)-Id_4_CP000971:+418
scheme_8_RIGHT	TAGTATGACGTCTGTCGCACCT	22	aph(6)-Id_4_CP000971:-809
scheme_9_LEFT	AAAAATCACTGCGCCAGTTCAC	22	blaCTX-M-55_1_DQ810789:+8
scheme_9_RIGHT	GCCACGTTATCGCTGTACTGTA	22	blaCTX-M-114_1_GQ351346:-389
scheme_10_LEFT	ATTGCGGAAAAGCACGTCAATG	22	blaCTX-M-55_1_DQ810789:+331
scheme_10_RIGHT	GCCGGTTTTATCCCCCACAA	20	blaCTX-M-114_1_GQ351346:-698
scheme_11_LEFT	ACAGCTGGGAGACGAAACGTT	21	blaCTX-M-55_1_DQ810789:+468
scheme_11_RIGHT	GATTTTAGCCGCCGACGCTAA	21	blaCTX-M-114_1_GQ351346:-838
scheme_12_LEFT	AAAAATCACTGCGCCAGTTCAC	22	blaCTX-M-55_1_DQ810789:+8
scheme_12_RIGHT	GCCACGTTATCGCTGTACTGTA	22	blaCTX-M-114_1_GQ351346:-389
scheme_13_LEFT	ATTGCGGAAAAGCACGTCAATG	22	blaCTX-M-55_1_DQ810789:+331
scheme_13_RIGHT	GCCGGTTTTATCCCCCACAA	20	blaCTX-M-114_1_GQ351346:-698

scheme_14_LEFT	ACAGCTGGGAGACGAAACGTT	21	blaCTX-M-55_1_DQ810789:+468
scheme_14_RIGHT	GATTTTAGCCGCCGACGCTAA	21	blaCTX-M-114_1_GQ351346:-838
scheme_15_LEFT	TTTTCGTGTCGCCCTTATTCCC	22	blaTEM-1B_1_AY458016:+15
scheme_15_RIGHT	AGAAGTAAGTTGGCAGCAGTGT	22	blaTEM-30_1_AJ437107:-389
scheme_16_LEFT	AGCATCTTACGGATGGCATGAC	22	blaTEM-1B_1_AY458016:+326
scheme_16_RIGHT	CAATGATACCGCGAGACCCA	20	blaTEM-1B_1_AY458016:-714
scheme_17_LEFT	TTTGCACAACATGGGGGATCAT	22	blaTEM-1B_1_AY458016:+447
scheme_17_RIGHT	TCAGTGAGGCACCTATCTCAGC	22	blaTEM-30_1_AJ437107:-826
scheme_18_LEFT	TTTTCGTGTCGCCCTTATTCCC	22	blaTEM-1B_1_AY458016:+15
scheme_18_RIGHT	AGAAGTAAGTTGGCAGCAGTGT	22	blaTEM-30_1_AJ437107:-389
scheme_19_LEFT	AGCATCTTACGGATGGCATGAC	22	blaTEM-1B_1_AY458016:+326
scheme_19_RIGHT	CAATGATACCGCTAGACCCACG	22	blaTEM-30_1_AJ437107:-712
scheme_20_LEFT	TTTGCACAACATGGGGGATCAT	22	blaTEM-1B_1_AY458016:+447
scheme_20_RIGHT	TCAGTGAGGCACCTATCTCAGC	22	blaTEM-30_1_AJ437107:-826
scheme_21_LEFT	AGTATCATTGATGGCTGCGAAAG	23	dfrA14_1_KF921535:+6
scheme_21_RIGHT	TCGAAGGTATTTGGAATACTCGGG	24	dfrA14_1_KF921535:-384
scheme_22_LEFT	ACATACCCTGGTCCGCGAAA	20	dfrA14_1_KF921535:+59
scheme_22_RIGHT	ACCCTTTTTCCAAATTTGATAGCAATAGT	29	dfrA14_1_KF921535:-443
scheme_23_LEFT	ACGAGTGAAAAAGTACTCAACCAAA	25	erm(B)_1_JN899585:+37
scheme_23_RIGHT	GCAACCCTAGTGTTCGGTGAAT	22	erm(B)_1_JN899585:-409
scheme_24_LEFT	GGGAATATTCCTTACCATTTAAGCACA	27	erm(B)_1_JN899585:+295
scheme_24_RIGHT	AGACAATACTTGCTCATAAGTAACGG	26	erm(B)_1_JN899585:-674
scheme_25_LEFT	ACCTCCATCCTGGCCTCAAAAA	22	rmtB_1_AB103506:+22
scheme_25_RIGHT	TGATGACATCCCCCAATCCCTG	22	rmtB_1_AB103506:-400
scheme_26_LEFT	CTTAACCCCTTGGCGCTATACG	22	rmtB_1_AB103506:+340
scheme_26_RIGHT	ATAAGTTCTGTTCCGATGGTCTTTTT	26	rmtB_1_AB103506:-706
scheme_27_LEFT	ACATAACCTCGGACAGTTTCTCC	23	sul2_2_AY034138:+35
scheme_27_RIGHT	ATGTGATCCATGATGTCGCCAG	22	sul2_2_AY034138:-428
scheme_28_LEFT	GCGAAATCATCTGCCAAACTCG	22	sul2_2_AY034138:+355
scheme_28_RIGHT	TGTGTGCGGATGAAGTCAGC	20	sul2_2_AY034138:-727

scheme_29_LEFT	GAAACCCAACAGACCCCTGATC	22	tet(A)_4_AJ517790:+3
scheme_29_RIGHT	GAAACAGGCGCTCATGAAGC	20	tet(A)_4_AJ517790:-401
scheme_30_LEFT	TAGCCGGCGCTTATATTGCC	20	tet(A)_4_AJ517790:+344
scheme_30_RIGHT	GTCCCAGTGAAAGCGATCCT	20	tet(A)_4_AJ517790:-713
scheme_31_LEFT	CTGTTTCCTTTTGCCGGAGTCG	22	tet(A)_4_AJ517790:+531
scheme_31_RIGHT	CGAAGCAAGCAGGACCATGATC	22	tet(A)_4_AJ517790:-915

Supplementary Table 6.2. Testing of Freed degenerate primers at differing annealing temperatures 42℃+58℃ and 44℃+58℃. The first round of nested PCR was completed at 42℃ or 44℃ annealing and the second round of nested PCR at 58℃ annealing. Sequencing was completed using the RBK004 rapid barcoding kit from ONT and the library run on an R9.4.1 MinION flowcell. N50: The sequence length of the shortest contig at 50% of the total assembly length (Thrash et al., 2020). Num_seqs is the total number of reads produced from each sample. Max_len is the maximal sequence length, with gaps or spaces counted. Q1: First quartile of sequence length, with gaps or spaces counted. Q2: Median of sequence length, with gaps or spaces counted. Q3: Third quartile of sequence length, with gaps or spaces counted. Sum_gaps is the number of gaps within a sequence. Q20(%) is the percentage of bases with a quality score (phred score) greater than 20. Q30(%) Percentage of bases with a quality score (phred score) greater than 30. Sequencing statistics are produced using seqkit stats (Shen et al., 2016).

Sample	num_seqs	sum_len	avg_len	max_len	Q1	Q2	Q3	N50	Q20(%)	Q30(%)
F-NNN 42℃+58℃	7,637	2,476,372	324.3	15,310	211	256	338	324	44.47	7.96
F-ATG 42℃+58℃	14,497	4,827,754	333	2,930	251	319	401	358	57.41	13.31
F-TGA 42℃+58℃	19,534	7,165,846	366.8	3,983	228	296	451	421	56.72	15.34
F-TAA 42℃+58℃	21,207	9,226,487	435.1	2,157	257	366	544	508	57.89	15.87
F-NNN 44℃+58℃	21,902	9,022,475	411.9	2,775	249	346	505	470	57.64	16.33
F-ATG 44℃+58℃	20,737	9,580,754	462	2,340	269	389	579	544	59.66	16.86
F-TGA 44℃+58℃	9,945	3,512,687	353.2	15,746	222	280	411	391	53.73	14.07
F-TAA 44℃+58℃	8,712	2,790,263	320.3	2,984	218	275	378	344	54.55	14.36

Supplementary Table 6.3. Testing of Freed and Manoil degenerate primers at differing annealing temperatures 44℃+60℃, 46℃+60℃ and 42℃+60℃. The first round of nested PCR was completed at 42℃, 44℃ and 46℃ annealing and the second round of nested PCR at 60℃ annealing. Sequencing was completed using the RBK110.96 rapid barcoding kit from ONT and the library run on an R9.4.1 MinION flowcell. N50: The sequence length of the shortest contig at 50% of the total assembly length (Thrash et al., 2020). Num_seqs is the total number of reads produced from each sample. Max_len is the maximal sequence length, with gaps or spaces counted. Q1: First quartile of sequence length, with gaps or spaces counted. Q2: Median of sequence length, with gaps or spaces counted. Q3: Third quartile of sequence length, with gaps or spaces counted. Sum_gaps is the number of gaps within a sequence. Q20(%) Percentage of bases with a quality score (phred score) greater than 20. Q30(%) is the percentage of bases with a quality score (phred score) greater than 30. Sequencing statistics are produced using seqkit stats (Shen et al., 2016).

Sample	num_seqs	sum_len	avg_len	max_len	Q1	Q2	Q3	N50	Q20(%)	Q30(%)
F-NNN 44℃+60℃	1,672	529,984	317	1,847	234	278	348.5	313	34.35	5.67
F-TAA 44℃+60℃	19,523	8,206,458	420.3	3,375	273	362	498	454	55.23	14.61
F-ATG 44℃+60℃	14,253	5,879,408	412.5	4,576	256	337	484	446	53.87	13.83
F-TGA 44℃+60℃	20,659	8,386,430	405.9	3,708	261	336	471	430	53.49	13.56
M-NNN 44℃+60℃	15,213	6,500,404	427.3	3,791	267	350	502	464	53.47	14.34
M-TAA 44℃+60℃	17,942	7,925,394	441.7	3,608	264	350	514	483	54.32	14.41
M-ATG 44℃+60℃	12,399	4,923,221	397.1	3,835	246	311	444	415	54.48	14.52
M-TGA 44℃+60℃	3,616	1,385,953	383.3	2,126	253.5	322	448	401	51.3	13.02
F-NNN 46℃+60℃	11,779	5,360,117	455.1	3,423	263	354	533.5	508	57.02	15.39
F-TAA 46℃+60℃	5,716	2,489,444	435.5	3,454	257	335	495	470	55.84	14.82
F-ATG 46℃+60℃	19,225	8,496,589	442	5,477	264	357	523	488	57.39	15.73
F-TGA 46℃+60℃	7,225	3,098,940	428.9	1,851	274	382	538	489	54.58	14.8
M-NNN 46℃+60℃	5	2,991	598.2	1,136	426	525	532	532	13.54	2.01
M-TAA 46℃+60℃	5,324	2,409,672	452.6	3,215	256.5	343	527	509	57.65	16.07
M-ATG 46℃+60℃	204	59,128	289.8	877	204	227.5	310	276	44.88	10.24
M-TGA 46℃+60℃	7,838	2,935,528	374.5	2,732	242	304	431	390	55.82	15.19
F-TAA 42℃+60℃	9,634	4,777,022	495.9	2,540	285	411	604	569	57.34	15.99
F-ATG 42℃+60℃	5,817	2,789,340	479.5	2,452	283	402	586	542	57.17	15.41
F-TGA 42℃+60℃	15,434	7,358,281	476.8	2,979	283	406	587	544	57.51	15.4
M-NNN 42℃+60℃	7,086	3,123,597	440.8	3,407	264	360	533	495	57.61	16.06

Supplementary Table 6.4. Testing of Freed and Manoil degenerate primers at differing annealing temperatures 44℃+58℃ and 46℃+58℃. The first round of nested PCR was completed at 44℃ or 46℃ annealing, and the second round of nested PCR at 58℃ annealing. Sequencing was completed using the RBK110.96 rapid barcoding kit from ONT and the library run on an R9.4.1 MinION flowcell. N50: The sequence length of the shortest contig at 50% of the total assembly length (Thrash et al., 2020). Q1, Q2, and Q3 indicate the length of sequences (in bp) at the 25th, 50th, and 75th quartile, Q20(%) is the percentage of bases with a quality score (phred score) greater than 20. Q30(%) is the percentage of bases with a quality score greater than 30. Sequencing statistics were produced using seqkit stats (Shen et al., 2016).

Sample	num_seqs	sum_len	avg_len	max_len	Q1	Q2	Q3	N50	Q20(%)	Q30(%)
F-NNN 44℃+58℃	2,427	870,738	358.8	3,110	241	297	397	358	51.01	13.48
F-TAA 44℃+58℃	26,279	11,043,469	420.2	3,650	262	342	488	450	54.51	14.42
F-ATG 44℃+58℃	15,681	6,013,453	383.5	4,164	250	315	437	395	52.07	13.01
F-TGA 44℃+58℃	28,065	11,682,287	416.3	3,570	267	342	481	439	53.41	13.66
M-NNN 44℃+58℃	16,164	6,315,683	390.7	75,708	258	321	435	397	50.81	13.24
M-TAA 44℃+58℃	15,058	5,567,393	369.7	2,498	248	307	417	375	51.41	12.85
M-ATG 44℃+58℃	16,723	5,731,267	342.7	2,644	237	286	378	339	53.14	13.72
M-TGA 44℃+58℃	6,357	2,251,595	354.2	2,485	240	290	392	354	52.95	13.25
F-NNN 46℃+58℃	11,674	4,649,651	398.3	2,974	254	321	455	416	53.08	13.62
F-TAA 46℃+58℃	3,784	1,474,234	389.6	2,697	254	316	437.5	397	50.99	12.68
F-ATG 46℃+58℃	16,196	6,663,640	411.4	3,592	261	338	479	435	53.12	13.84
F-TGA 46℃+58℃	7,330	2,763,881	377.1	2,558	252	319	438	394	50.65	12.95
M-NNN 46℃+58℃	6,067	2,018,399	332.7	2,427	237	286	368	331	55.01	14.36
M-TAA 46℃+58℃	5,397	1,924,782	356.6	2,935	237	289	389	354	55.24	13.97
M-ATG 46℃+58℃	5,134	2,122,457	413.4	2,533	256	337	492	452	56.64	15.1
M-TGA 46℃+58℃	6,301	2,017,885	320.2	2,319	232	278	360	317	51.28	12.93

Supplementary Table 6.5. Testing of Freed and Manoil degenerate primers at differing annealing temperatures 44℃+62℃. The first round of nested PCR was completed at 44℃ annealing, and the second round of nested PCR at 62℃ annealing. Sequencing was completed using the RBK004 rapid barcoding kit from ONT and the library run on an R9.4.1 MinION flowcell. N50: The sequence length of the shortest contig at 50% of the total assembly length (Thrash et al., 2020). Q1, Q2, and Q3 indicate the length of sequences (in bp) at the 25th, 50th, and 75th quartile, Q20(%) is the percentage of bases with a quality score (phred score) greater than 20. Q30(%) is the percentage of bases with a quality score greater than 30. Sequencing statistics were produced using seqkit stats (Shen et al., 2016).

Sample	num_seqs	sum_len	avg_len	max_len	Q1	Q2	Q3	N50	Q20(%)	Q30(%)
F-NNN 44℃+62℃	1,543	565,641	366.6	3,352	193	249	425.5	443	48.59	12.76
F-TAA 44℃+62℃	17,653	5,975,357	338.5	2,624	226	286	400	356	56.54	15.65
F-ATG 44℃+62℃	17,974	5,723,756	318.4	3,826	208	249	342	314	57.21	16.5
F-TGA 44℃+62℃	10,438	3,118,528	298.8	3,240	213	254	334	296	55.06	14.66
M-NNN 44℃+62℃	2,597	874,239	336.6	5,418	188	231	359	374	49.86	12.77
M-TAA 44℃+62℃	486	235,740	485.1	2,439	274	392.5	586	556	46.26	11.53
M-ATG 44℃+62℃	28,366	9,032,585	318.4	3,752	212	258	349	317	57.36	16.24
M-TGA 44℃+62℃	14,466	5,191,740	358.9	5,743	226	281	409	377	54.75	15.27

Supplementary Table 6.6. Testing of Freed and Manoil degenerate primers at differing annealing temperatures 44℃+60℃ and 46℃+62℃. The first round of nested PCR was completed at 44℃ or 46℃ annealing, and the second round of nested PCR at 60℃ or 62℃ annealing. Sequencing was completed using the RBK110.96 rapid barcoding kit from ONT and the library run on an R9.4.1 MinION flowcell. N50: The sequence length of the shortest contig at 50% of the total assembly length (Thrash et al., 2020). Q1, Q2, and Q3 indicate the length of sequences (in bp) at the 25th, 50th, and 75th quartile, Q20(%) is the percentage of bases with a quality score (phred score) greater than 20. Q30(%) is the percentage of bases with a quality score greater than 30. Sequencing statistics were produced using seqkit stats (Shen et al., 2016).

Sample	num_seqs	sum_len	avg_len	max_len	Q1	Q2	Q3	N50	Q20(%)	Q30(%)
F-NNN 44℃+60℃	19,298	7,136,283	369.8	3,859	239	299	425	386	54.19	14.26
F-TAA 44℃+60℃	33,572	13,936,158	415.1	12,051	256	338	497	455	56.4	15.2
F-ATG 44℃+60℃	12,984	5,018,699	386.5	3,317	247	314	441	403	54.75	14
F-TGA 44℃+60℃	615	222,665	362.1	2,327	233	287	426	383	53.79	13.79
M-NNN 44℃+60℃	18,117	7,542,884	416.3	3,392	252	331	496	459	55.18	15.05
M-TAA 44℃+60℃	17,431	6,909,144	396.4	4,793	247	316	463	425	54.69	14.02
M-ATG 44℃+60℃	6,946	3,184,755	458.5	5,801	257	345	531	517	56.2	15.55
M-TGA 44℃+60℃	5	1,948	389.6	818	225	285	407	407	36.5	7.91
F-NNN 46℃+62℃	18,357	6,829,047	372	3,886	238	297	421	385	55.19	14.28
F-TAA 46℃+63℃	17,203	6,738,937	391.7	3,665	246	313	453	415	53.43	13.74
F-ATG 46℃+62℃	28,599	10,993,138	384.4	3,567	247	317	446	405	55.71	14.75
F-TGA 46℃+62℃	17,512	6,582,403	375.9	5,340	245	310	434	394	52.63	13.71
M-NNN 46℃+62℃	19,894	7,460,963	375	11,564	240	299	420	384	54.81	14.36
M-TAA 46℃+62℃	12,980	4,896,610	377.2	3,053	245	309	430	390	54.4	13.77
M-ATG 46℃+62℃	13,351	5,497,625	411.8	3,057	260	339	483	442	55.25	14.35
M-TGA 46℃+62℃	19,902	7,798,422	391.8	3,301	250	322	455	413	54.8	14.71

Supplementary Table 6.7. Testing of Freed and Manoil degenerate primers at differing annealing temperatures 46℃+60℃. The first round of nested PCR was completed at 46℃ annealing and the second round of nested PCR at 60℃ or 62℃ annealing. Sequencing was completed using the RBK004 rapid barcoding kit from ONT and the library run on an R9.4.1 MinION flowcell. N50: The sequence length of the shortest contig at 50% of the total assembly length (Thrash et al., 2020). Q1, Q2, and Q3 indicate the length of sequences (in bp) at the 25th, 50th, and 75th quartile, Q20(%) is the percentage of bases with a quality score (phred score) greater than 20. Q30(%) is the percentage of bases with a quality score greater than 30. Sequencing statistics were produced using seqkit stats (Shen et al., 2016).

Sample	num_seqs	sum_len	avg_len	max_len	Q1	Q2	Q3	N50	Q20(%)	Q30(%)
F-NNN 46℃+60℃	16,302	3,592,801	220.4	1,884	122	174	263	256	54.71	13.48
F-TAA 46℃+60℃	18,790	3,846,844	204.7	2,205	123	168	258	239	54.31	12.74
F-ATG 46℃+60℃	12,016	2,484,789	206.8	2,551	120	167	248	237	55.22	13.42
F-TGA 46℃+60℃	9,757	2,021,619	207.2	3,320	124	169	249	234	54.37	12.98
M-NNN 46℃+60℃	8,526	1,963,751	230.3	2,518	126	183	275	269	55.35	13.83
M-TAA 46℃+60℃	11,418	2,437,608	213.5	1,710	122	171	264	250	55.48	13.48
M-ATG 46℃+60℃	20,265	3,196,681	157.7	2,412	107	139	191	173	53.38	11.46
M-TGA 46℃+60℃	4,140	670,104	161.9	1,953	102	139	195	178	51.54	10.89

Supplementary Table 6.8. Testing of Freed and manoil degenerate primers at differing annealing temperatures 46℃+60℃ and a 0.7 bead clean. The first round of nested PCR was completed at 46℃ annealing and the second round of nested PCR at 60℃ or 62℃ annealing. Sequencing was completed using the RBK004 rapid barcoding kit from ONT and the library run on an R9.4.1 MinION flowcell. During the library preparation, we cleaned our produced with 0.7x AMPure beads to PCR product to reduce the number of small DNA fragments. N50: The sequence length of the shortest contig at 50% of the total assembly length (Thrash et al., 2020). Q1, Q2, and Q3 indicate the length of sequences (in bp) at the 25th, 50th, and 75th quartile, Q20(%) is the percentage of bases with a quality score (phred score) greater than 20. Q30(%) is the percentage of bases with a quality score greater than 30. Sequencing statistics were produced using seqkit stats (Shen et al., 2016).

Samples	num_seqs	sum_len	avg_len	max_len	Q1	Q2	Q3	N50	Q20(%)	Q30(%)
F-NNN 46℃+60℃	5,498	998,783	181.7	1,406	119	157	216	197	42.34	6.09
F-TAA 46℃+60℃	33,143	6,426,287	193.9	2,552	121	163	233	213	42.54	6.09
F-ATG 46℃+60℃	6,588	1,214,761	184.4	863	118	157	221	202	42.5	6.07
F-TGA 46℃+60℃	11,073	2,686,166	242.6	2,828	127	178	280	287	43.96	7.72
M-NNN 46℃+60℃	3,999	752,957	188.3	1,373	110	149	224	211	40.8	7.3
M-TAA 46℃+60℃	40,055	9,549,730	238.4	8,486	125	176	285	288	41.85	7.26
M-ATG 46℃+60℃	13,143	3,787,066	288.1	3,217	138	211	356	369	44.28	8.93
M-TGA 46℃+60℃	12,839	2,713,265	211.3	1,456	119	166	256	246	39.33	7.63

Supplementary Table 6.9. Statistics of testing the degenerate primer pool containing M-TAA, M-TGA, and F-TGA with individual ARG primers to provide genomic context to target ARGs. The first round of nested PCR was completed at 46°C annealing, and the second round of nested PCR at 58°C annealing. Sequencing was completed using the RBK004 rapid barcoding kit from ONT and the library run on an R9.4.1 MinION flowcell. N50: The sequence length of the shortest contig at 50% of the total assembly length (Thrash et al., 2020). Q1, Q2, and Q3 indicate the length of sequences (in bp) at the 25th, 50th, and 75th quartile, Q20(%) is the percentage of bases with a quality score (phred score) greater than 20. Q30(%) is the percentage of bases with a quality score greater than 30. Sequencing statistics were produced using seqkit stats (Shen et al., 2016).

Target ARG	num_seqs	sum_len	avg_len	max_len	Q1	Q2	Q3	N50	Q20(%)	Q30(%)
aph(3)	2,566	923,183	359.8	3,033	174	306	473	467	53.48	12.73
bla-$_{CTX}$	3,251	1,246,837	383.5	2,429	177	308	507	509	51.96	12.24
dfrA14	12,112	2,037,990	168.3	3,689	108	143	200	183	44.14	8.17
sul2	4,990	1,976,121	396	6,186	192	332	515	508	52.73	13.03

Supplementary Table 6.10. Testing individual degenerate primers with pooled ARG primers. ARG pool contains primers for the target ARGs *aph(3), aph(4), aph(6), bla-$_{CTX}$, bla-$_{TEM}$, dfrA14, erm(B), rmtB, sul2* and *tet(A)*. The first round of nested PCR was completed at 46℃ annealing, and the second round of nested PCR at 58℃ annealing. Sequencing was completed using the RBK004 rapid barcoding kit from ONT and the library run on an R9.4.1 MinION flowcell. N50: The sequence length of the shortest contig at 50% of the total assembly length (Thrash et al., 2020). Q1, Q2, and Q3 indicate the length of sequences (in bp) at the 25th, 50th, and 75th quartile, Q20(%) is the percentage of bases with a quality score (phred score) greater than 20. Q30(%) is the percentage of bases with a quality score greater than 30. Sequencing statistics were produced using seqkit stats (Shen et al., 2016).

Sample	num_seqs	sum_len	avg_len	max_len	Q1	Q2	Q3	N50	Q20(%)	Q30(%)
F-NNN + pooled ARG primers	26,280	9,115,998	346.9	1,261	280	344	417	370	28.43	3.35
F-TAA + pooled ARG primers	26,107	8,973,871	343.7	1,866	274	340	415	368	28.58	3.22
F-ATG + pooled ARG primers	11,910	4,067,999	341.6	1,652	274	336	411	365	28.33	3.19
F-TGA + pooled ARG primers	24,623	8,481,491	344.5	2,527	276	338	412	367	28.27	3.26
M-NNN + pooled ARG primers	21,785	7,649,116	351.1	1,511	283	348	421	377	28.44	3.35
M-TAA + pooled ARG primers	26,474	9,149,836	345.6	20,909	277	339	413	368	28.15	3.12
M-ATG + pooled ARG primers	34,864	11,850,695	339.9	1,916	273	331	408	361	28.48	3.52
M-TGA + pooled ARGprimers	13,568	4,869,309	358.9	965	283	347	424	380	28.23	3.11
Pooled degenerate+ pooled ARGprimers	10,840	3,777,823	348.5	1,277	282	347	419	373	28.68	3.54

Supplementary Table 6.11. Testing the degenerate primer pool containing M-TAA, M-TGA, and F-TGA with individual ARG primers to provide genomic context to target ARGs. The first round of nested PCR was completed at 46℃ annealing, and the second round of nested PCR at 58℃ annealing. Sequencing was completed using the RBK004 rapid barcoding kit from ONT and the library run on an R9.4.1 MinION flowcell. N50: The sequence length of the shortest contig at 50% of the total assembly length (Thrash et al., 2020). Q1, Q2, and Q3 indicate the length of sequences (in bp) at the 25th, 50th, and 75th quartile, Q20(%) is the percentage of bases with a quality score (phred score) greater than 20. Q30(%) is the percentage of bases with a quality score greater than 30. Sequencing statistics were produced using seqkit stats (Shen et al., 2016).

Target ARGs	num_seqs	sum_len	avg_len	max_len	Q1	Q2	Q3	N50	Q20(%)	Q30(%)
aph(3)	4,584	1,165,548	254.3	63,746	134	196	300	303	47.83	10.6
bla-$_{CTX}$	7,179	1,594,396	222.1	3,506	127	181	267	256	49.59	10.82
bla-$_{TEM}$	5,005	1,217,539	243.3	1,435	136	198	307	294	51.68	9.57
dfrA14	8,372	1,843,625	220.2	2,043	124	174	265	257	47.77	9.93
erm(B)	1,070	238,235	222.6	1,199	116	175	273	274	51.95	10.09
rmtB	3,436	1,171,760	341	3,524	144	247	462.5	485	49.71	11.75
sul2	12,689	4,617,608	363.9	3,208	183	290	468	464	49.33	10.82
tet(A)	12,102	3,814,889	315.2	3,690	150	239	386	400	50.43	10.26

Supplementary Table 6.12. Testing the degenerate primer pool containing M-TAA, M-TGA, and F-TGA with individual ARG primers to provide genomic context to target ARGs. The first round of nested PCR was completed at 46℃ annealing, and the second round of nested PCR at 58℃ annealing. Sequencing was completed using the RBK004 rapid barcoding kit from ONT and the library run on an R9.4.1 MinION flowcell. During the library preparation, we cleaned our produced with 0.7x AMPure beads to reduce the number of small DNA fragments. N50: The sequence length of the shortest contig at 50% of the total assembly length (Thrash et al., 2020). Q1, Q2, and Q3 indicate the length of sequences (in bp) at the 25th, 50th, and 75th quartile, Q20(%) is the percentage of bases with a quality score (phred score) greater than 20. Q30(%) is the percentage of bases with a quality score greater than 30. Sequencing statistics were produced using seqkit stats (Shen et al., 2016).

Target ARGs	num_seqs	sum_len	avg_len	max_len	Q1	Q2	Q3	N50	Q20(%)	Q30(%)
aph(3)	10,664	3,373,495	316.3	2,526	135	233	409	435	47.65	10.92
bla-$_{CTX}$	6,406	1,974,524	308.2	2,825	132	222	393	428	46.43	10.65
bla-$_{TEM}$	6,183	1,640,126	265.3	2,725	126	194	328	345	43.88	9.85
dfrA14	10,462	2,528,267	241.7	2,914	118	174	276	296	45.86	9.25
rmtB	3,270	630,298	192.8	1,527	108	158	242	231	43.98	8.44
sul2	2,439	805,831	330.4	3,044	135	247	457	480	47.84	11.33
tet(A)	8,184	1,871,295	228.7	3,408	101	155	271.5	308	46.52	9.63

Supplementary Table 6.13. Testing individual degenerate primers with primers targeting *aph(3)* and *tet(A)*. The first round of nested PCR was completed at 46℃ annealing, and the second round of nested PCR at 58℃ annealing. Sequencing was completed using the RBK110.96 rapid barcoding kit from ONT and the library run on an R9.4.1 MinION flowcell. N50: The sequence length of the shortest contig at 50% of the total assembly length (Thrash et al., 2020). Q1, Q2, and Q3 indicate the length of sequences (in bp) at the 25th, 50th, and 75th quartile, Q20(%) is the percentage of bases with a quality score (phred score) greater than 20. Q30(%) is the percentage of bases with a quality score greater than 30. Sequencing statistics were produced using seqkit stats (Shen et al., 2016).

Samples	num_seqs	sum_len	avg_len	max_len	Q1	Q2	Q3	N50	Q20(%)	Q30(%)
F-NNN + *tet(A)*	2,698	730,849	270.9	2,712	131	196.5	323	340	53.72	13.52
F-ATG + *tet(A)*	3,870	1,013,152	261.8	2,614	135	191	307	315	52.45	12.79
F-TAA + *tet(A)*	2,580	820,161	317.9	2,093	132	207	384	455	55.03	13.49
F-TGA + *tet(A)*	4,123	1,087,668	263.8	1,927	136	198	315.5	320	53.34	12.85
M-NNN + *tet(A)*	3,249	697,925	214.8	1,762	116	165	248	249	50.36	11.53
M-ATG + *tet(A)*	3,453	776,839	225	3,070	120	175	257	256	52.58	12.49
M-TAA + *tet(A)*	3,214	707,841	220.2	2,393	116	169	252	256	53.06	12.57
M-ATG + *tet(A)*	3,569	882,316	247.2	2,736	120	178	282	305	51.44	12.33
F-NNN + *aph(3)*	1,667	400,619	240.3	1,887	118	174	281.5	299	53.4	13.24
F-ATG + *aph(3)*	1,057	284,097	268.8	2,989	125	194	314	345	53.52	13.71
F-TAA + *aph(3)*	847	236,425	279.1	2,018	126	192	306.5	367	52.87	13.11
F-TGA + *aph(3)*	3,207	791,312	246.7	2,308	119	182	288	305	51.96	12.51
M-NNN + *aph(3)*	1,973	392,918	199.1	1,771	110	151	228	230	52.56	12.38
M-ATG + *aph(3)*	1,536	369,116	240.3	2,250	114.5	164	257	289	52.46	12.77
M-TAA + *aph(3)*	1,196	244,301	204.3	2,769	111	154	233	235	51.29	11.68
M-ATG + *aph(3)*	2,401	489,716	204	2,376	112	156	237	237	51.77	12.33

Supplementary Table 6.14. Testing individual degenerate primers with primers targeting *aph(4)* and *tet(A)*. The first round of nested PCR was completed at 46℃ annealing, and the second round of nested PCR at 58℃ annealing. Sequencing was completed using the RBK110.96 rapid barcoding kit from ONT and the library run on an R9.4.1 MinION flowcell. N50: The sequence length of the shortest contig at 50% of the total assembly length (Thrash et al., 2020). Q1, Q2, and Q3 indicate the length of sequences (in bp) at the 25th, 50th, and 75th quartile, Q20(%) is the percentage of bases with a quality score (phred score) greater than 20. Q30(%) is the percentage of bases with a quality score greater than 30. Sequencing statistics were produced using seqkit stats (Shen et al., 2016).

Sample	num_seqs	sum_len	avg_len	max_len	Q1	Q2	Q3	N50	Q20(%)	Q30(%)
F-NNN + *aph(4)*	6,482	2,152,022	332	3,162	152	246	426	443	49.93	11.92
F-ATG + *aph(4)*	6,885	2,486,860	361.2	5,144	162	267	457	482	49.25	11.65
F-TAA + *aph(4)*	5,092	1,773,537	348.3	3,694	161	265	462	468	51.68	12.24
M-ATG + *aph(4)*	7,790	2,321,732	298	2,612	150	238	391	385	48.58	10.66
M-NNN + *aph(4)*	6,567	2,091,791	318.5	3,056	143	216	372	425	50.33	12.01
M-ATG + *aph(4)*	4,807	1,825,655	379.8	3,763	157	264	488	537	49.64	11.93
M-TAA + *aph(4)*	7,034	1,857,635	264.1	2,204	129	189	301	325	49.97	11.45
M-TGA + *aph(4)*	8,585	2,555,517	297.7	3,422	133	199	336	397	49.92	11.68
F-NNN + *tet(A)*	4,174	1,086,014	260.2	3,142	134	190	300	311	50.87	11.99
F-ATG + *tet(A)*	2,231	695,758	311.9	2,521	142	210	369.5	415	51.23	12.44
F-TAA + *tet(A)*	5,853	1,811,097	309.4	3,450	141	208	368	417	50.36	12.01
F-TGA + *tet(A)*	8,086	2,348,728	290.5	3,112	140	208	343	366	49.74	11.65
M-NNN + *tet(A)*	4,788	1,429,038	298.5	3,253	135	204	344	391	50.29	11.78
M-ATG + *tet(A)*	7,526	2,116,020	281.2	3,602	131	192	323	364	49	11.26
M-TAA + *tet(A)*	4,269	1,100,336	257.8	2,522	128	188	296	317	48.79	11.2
M-ATG + *tet(A)*	5,515	1,575,558	285.7	3,219	134	201	335	367	50.5	11.86

Supplementary Table 6.15. Testing the degenerate primer pool containing M-TAA, M-TGA, F-TGA and F-TAA with individual ARG primers to provide genomic context to target ARGs. Pooled ARG primers contained primers for *aph(3), aph(4), aph(6), bla-$_{CTX}$, bla-$_{TEM}$, dfrA14, rmtB, sul2* and *tet(A).* The first round of nested PCR was completed at 46℃ annealing, and the second round of nested PCR at 58℃ annealing. Sequencing was completed using the RBK004 rapid barcoding kit from ONT and the library run on an R9.4.1 MinION flowcell. During the library preparation, we cleaned our produced with 0.7x AMPure beads to PCR product to reduce the number of small DNA fragments. N50: The sequence length of the shortest contig at 50% of the total assembly length (Thrash et al., 2020). Q1, Q2, and Q3 indicate the length of sequences (in bp) at the 25th, 50th, and 75th quartile, Q20(%) is the percentage of bases with a quality score (phred score) greater than 20. Q30(%) is the percentage of bases with a quality score greater than 30. Sequencing statistics were produced using seqkit stats (Shen et al., 2016).

Target ARGs/Sample	num_seqs	sum_len	avg_len	max_len	Q1	Q2	Q3	N50	Q20(%)	Q30(%)
aph(3)	11,952	2,142,339	179.2	1,314	106	149	221	207	38.3	6.58
bla-$_{CTX}$	6,728	1,130,987	168.1	1,869	96	137	200.5	193	36.59	6.31
bla-$_{TEM}$	3,054	556,726	182.3	2,074	100	149	230	221	40.58	5.49
dfrA14	6,686	1,613,898	241.4	2,224	112	170	286	316	37.88	7.01
rmtB	2,412	455,935	189	1,526	92.5	141	232	239	39.3	7.28
sul2	8,438	2,897,368	343.4	2,756	135	248	472	507	40.8	8.36
tet(A)	9,081	2,318,569	255.3	2,602	116	186	313	336	39	7.02
Pooled ARG primers + Pooled degenerate primers	4,085	1,119,726	274.1	2,533	107	163	299	418	40.53	7.38

Supplementary Table 6.16. Testing the degenerate and ARG primer pools on faecal samples. Pooled ARG primers contained primers for *aph(3), aph(4), aph(6), bla-$_{CTX}$, bla-$_{TEM}$, dfrA14, rmtB, sul2* and *tet(A).* Pooled degenerate primers contain M-TAA, M-TGA, F-TGA and F-TAA. The first round of nested PCR was completed at 46℃ annealing, and the second round of nested PCR at 58℃ annealing. Sequencing was completed using the RBK004 rapid barcoding kit from ONT and the library run on an R9.4.1 MinION flowcell. During the library preparation, we cleaned our produced with 0.7x AMPure beads to PCR product to reduce the number of small DNA fragments. N50: The sequence length of the shortest contig at 50% of the total assembly length (Thrash et al., 2020). Q1, Q2, and Q3 indicate the length of sequences (in bp) at the 25th, 50th, and 75th quartile, Q20(%) is the percentage of bases with a quality score (phred score) greater than 20. Q30(%) is the percentage of bases with a quality score greater than 30. Sequencing statistics were produced using seqkit stats (Shen et al., 2016).

Sample	num_seqs	sum_len	avg_len	max_len	Q1	Q2	Q3	N50	Q20(%)	Q30(%)
Positive control (*E. coli* L3CIp3)	6,109	1,217,683	199.3	2,831	114	154	221	217	45.41	7.62
Faecal sample 04-zymo	1,788	269,178	150.5	730	97	129	177	163	44.56	6.88
Faecal sample 04-zymo (1:10 dilution)	351	43,698	124.5	375	85	113	148	136	44.66	8.09

Supplementary Table 6.17. Testing the developed degenerate and ARG primer pools on faecal samples. Pooled ARG primers contained primers for *aph(3), aph(4), aph(6), bla-$_{CTX}$, bla-$_{TEM}$, dfrA14, rmtB, sul2* and *tet(A)*. Pooled degenerate primers contain M-TAA, M-TGA, F-TGA and F-TAA. The first round of nested PCR was completed at 46°C annealing, and the second round of nested PCR at 58°C annealing. Sequencing was completed using the RBK004 rapid barcoding kit from ONT and the library run on an R9.4.1 MinION flowcell. During the library preparation, we cleaned our produced with 0.7x AMPure beads to PCR product to reduce the number of small DNA fragments. N50: The sequence length of the shortest contig at 50% of the total assembly length (Thrash et al., 2020). Q1, Q2, and Q3 indicate the length of sequences (in bp) at the 25th, 50th, and 75th quartile, Q20(%) is the percentage of bases with a quality score (phred score) greater than 20. Q30 (%) is the percentage of bases with a quality score greater than 30. Sequencing statistics were produced using seqkit stats (Shen et al., 2016).

Samples	num_seqs	sum_len	avg_len	max_len	Q1	Q2	Q3	N50	Q20(%)	Q30(%)
Faecal sample 04-zymo	12,117	3,068,589	253.2	381,418	105	144	218	339	39.53	7.22
Faecal sample 04-zymo + *E. coli* L3Clp3	7,721	2,165,165	280.4	2,889	120	162	252	397	47.64	8.91

Supplementary Table 6.18. Testing the degenerate and ARGprimer pools on faecal samples using two DNA extraction methods. Pooled ARG primers contained primers for *aph(3), aph(4), aph(6), bla-$_{CTX}$, bla-$_{TEM}$, dfrA14, rmtB, sul2* and *tet(A)*. Pooled degenerate primers contain M-TAA, M-TGA, F-TGA and F-TAA. The first round of nested PCR was completed at 46°C annealing, and the second round of nested PCR at 58°C annealing. Sequencing was completed using the RBK004 rapid barcoding kit from ONT and the library run on an R9.4.1 MinION flowcell. During the library preparation, we cleaned our produced with 0.7x AMPure beads to PCR product to reduce the number of small DNA fragments. N50: The sequence length of the shortest contig at 50% of the total assembly length (Thrash et al., 2020). Q1, Q2, and Q3 indicate the length of sequences (in bp) at the 25th, 50th, and 75th quartile, Q20(%) is the percentage of bases with a quality score (phred score) greater than 20. Q30(%) is the percentage of bases with a quality score greater than 30. Sequencing statistics were produced using seqkit stats (Shen et al., 2016).

Samples	num_seqs	sum_len	avg_len	max_len	Q1	Q2	Q3	N50	Q20(%)	Q30(%)
04-zymo	49,821	10,107,360	202.9	2,526	122	173	254	235	37.34	5.8
10-zymo	65,923	13,076,602	198.4	102,112	120	169	245	227	38.05	5.67
77-zymo	51,831	11,574,058	223.3	17,661	123	176	260	256	41.04	6.66
13-zymo	78,307	16,135,373	206.1	3,570	126	179	257	236	37.3	5.64
69-zymo	35,359	7,704,510	217.9	386,034	119	167	243	243	39.68	6.48
04-qiagen	53,671	10,818,795	201.6	4,166	121	170	249	231	39.72	6.36
10-qiagen	88,616	17,056,219	192.5	42,653	116	161	231	216	40.86	6.32
77-qiagen	33,296	6,664,737	200.2	41,160	120	169	246	228	41.35	6.38
13-qiagen	46,945	8,755,601	186.5	1,205	117	163	232	212	41.49	6.21
69-qiagen	8,903	1,711,612	192.3	2,528	117	159	224	211	41.87	6.27
Positive control (*E. coli* L3Clp3)	14,743	1,921,909	130.4	1,073	87	115	154	142	40.22	5.15

Supplementary Table 6.19. Testing the degenerate and ARG primer pools on faecal samples using two DNA extraction methods with new ONT chemistry. Pooled ARG primers contained primers for *aph(3), aph(4), aph(6), bla-$_{CTX}$, bla-$_{TEM}$, dfrA14, rmtB, sul2* and *tet(A)*. Pooled degenerate primers contain M-TAA, M-TGA, F-TGA and F-TAA. The first round of nested PCR was completed at 46℃ annealing, and the second round of nested PCR at 58℃ annealing. Sequencing was completed using the RBK114.96 rapid barcoding kit from ONT and the library run on an R10.4.1 PromethION P2 solo flowcell. During the library preparation, we cleaned our produced with 0.7x AMPure beads to PCR product to reduce the number of small DNA fragments. N50: The sequence length of the shortest contig at 50% of the total assembly length (Thrash et al., 2020). Q1, Q2, and Q3 indicate the length of sequences (in bp) at the 25th, 50th, and 75th quartile, Q20(%) is the percentage of bases with a quality score (phred score) greater than 20. Q30(%) is the percentage of bases with a quality score greater than 30. Sequencing statistics were produced using seqkit stats (Shen et al., 2016).

Sample	num_seqs	sum_len	avg_len	max_len	Q1	Q2	Q3	N50	Q20(%)	Q30(%)
04-zymo	2,729	657,285	240.9	1,908	172	220	289	262	48.46	23.54
10-zymo	5,930	1,428,630	240.9	4,990	174	220	283	255	50.64	25.27
77-zymo	2,530	840,556	332.2	4,145	187	252	369	377	56.21	30.63
13-zymo	6,205	1,618,770	260.9	4,960	186	234	305	274	49.24	24.49
69-zymo	3,834	1,237,184	322.7	2,516	193	253	365	353	54.94	29.69
04-qiagen	3,636	917,201	252.3	1,556	179	225	296	270	50.91	26.01
10-qiagen	14,800	4,091,026	276.4	2,764	179	229	311	294	55.8	29.65
77-qiagen	1,322	342,921	259.4	2,598	176	225	300	276	55.53	29.49
13-qiagen	4,304	976,673	226.9	1,161	168	214	273	245	52.53	26.35
69-qiagen	1,238	354,711	286.5	1,891	175	226.5	318	307	55.19	29.23

Supplementary Table 6.20. Testing the degenerate and ARG primer pools on metagenomic faecal samples using two DNA extraction methods with new ONT chemistry (Repeat). Pooled ARG primers contained primers for *aph(3), aph(4), aph(6), bla-$_{CTX}$, bla-$_{TEM}$, dfrA14, rmtB, sul2* and *tet(A).* Pooled degenerate primers contain M-TAA, M-TGA, F-TGA and F-TAA. The first round of nested PCR was completed at 46℃ annealing, and the second round of nested PCR at 58℃ annealing. Sequencing was completed using the RBK114.96 rapid barcoding kit from ONT and the library run on an R10.4.1 PromethION P2 solo flowcell. During the library preparation, we cleaned our produced with 0.7x AMPure beads to PCR product to reduce the number of small DNA fragments. N50: The sequence length of the shortest contig at 50% of the total assembly length (Thrash et al., 2020). Q1, Q2, and Q3 indicate the length of sequences (in bp) at the 25th, 50th, and 75th quartile, Q20(%) is the percentage of bases with a quality score (phred score) greater than 20. Q30(%) is the percentage of bases with a quality score greater than 30. Sequencing statistics were produced using seqkit stats (Shen et al., 2016).

Sample	num_seqs	sum_len	avg_len	max_len	Q1	Q2	Q3	N50	Q20(%)	Q30(%)
04-zymo	5,083	1,238,685	243.7	2,126	164	213	290	265	60.58	33.47
10-zymo	5,259	1,490,322	283.4	3,423	175	233	336	316	62.81	36.03
77-zymo	11,729	3,268,468	278.7	23,484	172	229	328	311	61.21	34.64
13-zymo	6,337	1,933,054	305	3,057	176	238	364	357	63.08	36.02
69-zymo	1,313	371,524	283	11,880	146	213	356	380	60.22	35.13
04-qiagen	7,375	1,931,037	261.8	1,683	181	235	320	287	57.31	29.79
10-qiagen	8,196	2,163,127	263.9	1,747	178	234	322.5	292	59.19	31.93
77-qiagen	6,964	2,331,765	334.8	3,587	183	253	392	392	62.13	35.91
13-qiagen	7,428	2,095,858	282.2	2,578	179	237	332	309	58.34	31.48
69-qiagen	7,792	2,175,002	279.1	2,995	179	234	328	304	58.5	32.06
Positive control (*E. coli* L3CIp3)	21,702	9,458,150	435.8	216,522	189	280	551	659	63.82	38.69